DEVELOPMENT AND CHARACTERIZATION OF SURFACE-MODIFIED EMULSION TEMPLATED SCAFFOLDS FOR TISSUE ENGINEERING APPLICATIONS

A Thesis Submitted to
the Graduate School of Engineering and Sciences of
İzmir Institute of Technology
in Partial Fulfillment of the Requirements for the Degree of

MASTER OF SCIENCE

in Bioengineering

by
Mehmet KOCAGÖZ

July 2024
İZMİR

We approve the thesis of **Mehmet KOCAGÖZ**
Examining Committee Members

Asst. Prof. Dr. Betül ALDEMİR DİKİCİ
Department of Bioengineering, İzmir Institute of Technology

Assoc. Prof. Dr. Nermin Seda KEHR
Department of Chemistry, İzmir Institute of Technology

Asst. Prof. Dr. Ecem SAYGILI
Department of Biomedical Engineering, İzmir Democracy University

16 July 2024

Asst. Prof. Dr. Betül ALDEMİR DİKİCİ

Supervisor
Department of Bioengineering,
İzmir Institute of Technology

Prof. Dr. Volga BULMUŞ ZAREIE
Co-Supervisor
Department of Bioengineering,
İzmir Institute of Technology

Assoc. Prof. Dr. Ceyda ÖKSEL KARAKUŞ
Head of the Department of Bioengineering

Prof. Dr. Mehtap EANES
Dean of the Graduate School
of Engineering and Sciences

ACKNOWLEDGMENTS

I would like to thank Dr. Betül ALDEMİR DİKİCİ for being my advisor during my graduate studies. She opened the doors of her laboratory to me, providing me with a great opportunity to expand my research experience. Her encouragement and support throughout every step of this study have been invaluable, and I am truly grateful for her advice and patience. My sincerest thanks go to my co-advisor, Prof. Dr. Volga BULMUŞ.

I especially thank the Baldemir Group and Dikici Group members for their support and patience.

I acknowledge the Scientific and Research Council of Turkey (TUBITAK) for financially supporting me under the 2210/C National MSc/MA Scholarship Program in the Priority Fields in Science and Technology and the İzmir Institute of Technology (IYTE) Scientific Research Council (BAP) for financially supporting the study with the project number of IYTE BAP, 2021-IYTE-1-0110.

I would like to thank the IYTE Center for Material Research for allowing me to use the scanning electron microscope and Brunauer-Emmett-Teller device, and the IYTE Biotechnology and Bioengineering Research and Application Center for allowing me to use the lyophilizer, Fourier-transform infrared spectrometer, rotary evaporator, spectrophotometer and fluorescence microscope. I would like to thank Dr. Hüseyin ÖZGEZENER for his assistance on the proton nuclear magnetic resonance spectroscopy.

I would like to thank Prof. Dr. Metin TANOĞLU for opening his laboratory for me and Dr. Ceren TÜRKDOĞAN for support during contact angle experiments. I would like to thank Prof. Dr. Funda TIHMINLIOĞLU for providing the bicinchoninic acid (BCA) protein assay kit and Dr. Sedef TAMBURACI for providing the protocol of protein adsorption and supporting me with her experience during the experiment. I would like to thank Assoc. Prof. Dr. Ceyda ÖKSEL KARAKUŞ for providing Saos-2 cells.

I would like to express my deep gratitude to my family, Adile KOCAGÖZ, Bekir KOCAGÖZ, and Muhammet Tevfik KOCAGÖZ, for their trust, patience, support and encouragement. They have been my rock throughout this journey, and I am truly grateful for their love and support.

I would like to thank all my friends for their endless support and friendship. They have been a constant source of inspiration and encouragement throughout this journey.

I would like to express my gratitude to Fatma KURUL for being there on my side and making me happy throughout this journey. Her support and friendship have been invaluable, and I am truly grateful for her unwavering support.

ABSTRACT

DEVELOPMENT AND CHARACTERIZATION OF SURFACE-MODIFIED EMULSION TEMPLATED SCAFFOLDS FOR TISSUE ENGINEERING APPLICATIONS

Emulsion templating is an advantageous scaffold fabrication method that provides high and open porosity. In this method, water-in-oil emulsions are obtained by mixing hydrophobic polymers and water. Polymerized emulsions with an internal phase greater than 74% are named high internal phase emulsions (PolyHIPEs). Polycaprolactone is a synthetic, biodegradable and biocompatible polymer widely used in tissue engineering, but its hydrophobicity limits cell-material interactions. Accordingly, this study aims to develop and characterize the NaOH-treated emulsion templated polycaprolactone tetramethacrylate (4PCLMA)-based scaffolds to improve its biological performance. Firstly, 4PCLMA pre-polymer was synthesized by ring-opening polymerization and functionalized with methacrylate groups. 4PCLMA was successfully synthesized with ~97% degree of methacrylation. 4PCLMA PolyHIPEs were fabricated by emulsion templating and post-treated with sodium hydroxide (NaOH) at three different concentrations and incubation times. The effects of NaOH treatment on mass loss, water absorption capacity, mechanical characteristics, surface area, hydrophilicity and biological performance of the scaffolds were investigated. The morphologies of the scaffolds were investigated using SEM. NaOH treatment reduced the weight and mechanical strength of the scaffolds, but it also increased the water absorption capacity, hydrophilicity, surface area and protein adsorption of the scaffolds. Chemical changes in PolyHIPEs after NaOH treatment were confirmed via spectroscopy. *In vitro* results showed that NaOH treatment did not cause cytotoxicity on L929 cells and positively affected the cell attachment and proliferation behaviour of Saos-2 cells. As a result of this study, NaOH treatment was investigated as an alternative surface modification technique to improve the hydrophilicity and biological performance of emulsion-templated scaffolds.

ÖZET

DOKU MÜHENDİSLİĞİ UYGULAMALARI İÇİN YÜZEY MODİFİKASYONU UYGULANMIŞ, EMÜLSİYON ŞABLONLAMA YÖNTEMİ İLE ÜRETİLMİŞ İSKELELERİN GELİŞTİRİLMESİ VE KARAKTERİZASYONU

Emülsiyon şablonlama, yüksek ve açık gözeneklilik sağlayan avantajlı bir iskele üretim yöntemidir. Bu yöntemde hidrofobik polimerlerin su ile karıştırılmasıyla yağ içerisinde su (w/o) emülsiyonları elde edilir. İç faz hacmi %74'ün üzerinde olan polimerize emülsiyonlar, yüksek iç fazlı emülsiyonlar (PolyHIPE'ler) olarak adlandırılır. Polikaprolakton, doku mühendisliğinde yaygın olarak kullanılan sentetik, biyolojik olarak bozunabilen ve biyouyumlu bir polimerdir, ancak malzemenin hidrofobik karakteri hücre-materyal etkileşimlerini sınırlamaktadır. Bu nedenle, bu çalışma kapsamında, emülsiyon şablonlama yöntemi ile üretilmiş, polikaprolakton tetrametakrilat (4PCLMA) esaslı iskelelerin biyolojik performanslarını artırmak için iskelelerin alkali muamelesi ve elde edilen iskelelerin karakterize edilmesi amaçlanmıştır. İlk olarak halka açma polimerizasyonu ile 4PCLMA pre-polimeri sentezlenmiş ve metakrilat grupları ile fonksiyon kazandırılmıştır. 4PCLMA ~%97 metakrilasyon derecesi ile başarıyla sentezlenmiş, 4PCLMA esaslı PolyHIPE'ler emülsiyon şablonlama yöntemi ile üretilmiş, üç farklı konsantrasyonda ve inkübasyon süresinde sodyum hidroksit (NaOH) ile muamele edilmiştir. NaOH işleminin iskelelerin morfolojileri, kütle kaybı, su tutma kapasitesi, mekanik özellikleri, yüzey alanı, hidrofilisitesi ve biyolojik performansı üzerindeki etkileri araştırılmıştır. NaOH uygulamasının iskelelerin ağırlığını ve mekanik mukavemetini azalttığı ancak aynı zamanda iskelelerin su tutma kapasitesini, hidrofilisitesini, yüzey alanını ve protein adsorpsiyon kapasitesini artırdığı görülmüştür. NaOH işleminden sonra PolyHIPE'lerdeki kimyasal değişiklikler spektroskopi ile doğrulanmıştır. *In vitro* sonuçlar, NaOH uygulamasının L929 hücreleri üzerinde sitotoksisiteye neden olmadığını ve Saos-2 hücrelerinin tutunma ve çoğalma davranışını olumlu yönde etkilediğini göstermiştir. Bu çalışma sonucunda NaOH muamelesinin, emülsiyon şablonlama ile üretilmiş doku iskelelerinin hidrofilisitesini ve biyolojik performansını artırmak adına alternatif bir yüzey modifikasyon yöntemi olarak kullanılabileceği gösterilmiştir.

TABLE OF CONTENTS

LIST OF FIGURES

Figure **Page**

Figure **Page**

Figure **Page**

LIST OF TABLES

Table **Page**

LIST OF ABBREVIATIONS

ΔL	: Displacement of Sample
E	: Strain
Σ	: Applied Compressive Stress
3D	: Three-dimensional
°C	: Degree Celsius
ε	: Compression Modulus
μm	: Micrometer
4PCL	: 4 arm Polycaprolactone
4PCLMA	: 4 arm Polycaprolactone Tetramethacrylate
A	: Surface area
Å	: Angstrom
Alg	: Alginate
AX	: Arabinoxylan
BCA	: Bicinchoninic Acid
BET	: Brunauer–Emmett–Teller
BSA	: Bovine Serum Albumin
BTE	: Bone Tissue Engineering
C_2H_5OH	: Ethanol
$C_6H_5CH_3$	: Toluene
$CaCl_2$	: Calcium Chloride
$CDCl_3$	: Deuterated Chloroform
$CHCl_3$	: Chloroform
CHT	: Chitosan
CO_2	: Carbon Dioxide
COL I	: Collagen I
d	: Average Window Size
D	: Average Pore Size
DBTDL	: Dibutyltin Dilaurate
DCE	: Dichloroethane
DCM	: Dichloromethane

Dex : Dexamethasone

DI : Dispersion Index

DM : Degree of Methacrylation

DMEM : Dulbecco's Modified Eagle's Medium

dH_2O : Distilled Water

DOI : Degree of Interconnectivity

DOO : Degree of Openness

ECM : Extracellular Matrix

E. Coli : Escherichia Coli

F : Force

Fe^{2+} : Iron(II)

FBS : Fetal Bovine Serum

FTIR : Fourier Transform Infrared Spectroscopy

g : Gram

GO : Graphene Oxide

GPC : Gel Permeation Chromatography

GS : Gentamicin Sulfate

H : Hydrogen

HAP : Hydroxyapatite

HCl : Hydrochloric Acid

HDMS : Hexamethyldisilane

HIPE : High Internal Phase Emulsion

K : Kelvin

KCl : Potassium Chloride

kV : Kilovolt

L929 : Mouse Fibroblast Cell Line

L_0 : Initial Length of Sample

M : Molar Concentration

m_1 : Before the NaOH treatment

m_2 : After the NaOH treatment

m^2 : Square Meter

m^3 : Cubic Meter

MAAn : Methacrylic Anhydride

$MgCl_2.6H_2O$: Magnesium Chloride Hexahydrate

MHz : Megahertz

min : Minute

mL : Milliliter

mM : Millimolar

M_n : Number of Average Molecular Weight

MPa : Megapascal

M_w : Weight Average Molecular Weight

N0 : Control Group

N0.1M3h : Scaffold treated with 0.1 Molar NaOH for 3 hours

N0.1M6h : Scaffold treated with 0.1 Molar NaOH for 6 hours

N0.1M24h : Scaffold treated with 0.1 Molar NaOH for 24 hours

N1M3h : Scaffold treated with 1 Molar NaOH for 3 hours

N1M6h : Scaffold treated with 1 Molar NaOH for 6 hours

N1M24h : Scaffold treated with 1 Molar NaOH for 24 hours

N5M3h : Scaffold treated with 5 Molar NaOH for 3 hours

N5M6h : Scaffold treated with 5 Molar NaOH for 6 hours

N5M24h : Scaffold treated with 5 Molar NaOH for 24 hours

N : Newton

NaCl : Sodium Chloride

$NaHCO_3$: Sodium Bicarbonate

NaH_2PO_4 : Monosodium Phosphate

NaOH : Sodium Hydroxide

NIPS : Nonsolvent-induced Phase Separation

NMR : Nuclear Magnetic Resonance

nm : Nanometer

PAAm : Polyacrylamide

P. Aeruginosa : Pseudomonas Aeruginosa

PBS : Phosphate Buffer Saline

PCL : Polycaprolactone

PDMS : Polydimethylsiloxane

PDX : Patient-derived Xenograft

PGA : Polyglycolic Acid

PGPR : Polyglycerol polyricinoleate

PI : Propidium Iodide

PLA : Polylactic Acid

PLGA : Poly(lactic-co-glycolic acid)

PLLA : Poly-L-lactic acid

PolyHIPE : Polymerised High Internal Phase Emulsion

PolyK : Poly(L-lysine)

PS : Penicillin/streptomycin

PU : Polyurethane

PVA : Polyvinyl Alcohol

rpm : Rotation Per Minute

RR : Resazurin Reduction Assay

RGD : Arginylglycylaspartic Acid

RGDC : Arginine–glycine–aspartic acid–cysteine

SA : Sodium Alginate

S. Aureus : Staphylococcus aureus

Saos-2 : Human Osteosarcoma Cell Line

SEM : Scanning Electron Microscopy

$SnOct_2$: tin(II) 2-ethyl hexanoate

TEA : Triethylamine

TCP : Tissue Culture Plate

THF : Tetrahydrofuran

T_g : Glass Transition Temperature

TIPS : Thermally Induced Phase Separation

UATR : Universal Attenuated Total Reflectance Accessory

UV : Ultraviolet

VIPS : Vapor-Induced Phase Separation

w/w : Weight in Weight

w/o : Water-in-oil emulsion

W_d : Dry Weights

W_w : Wet Weights

mg : Milligram

μL : Microliter

CHAPTER 1

INTRODUCTION

1.1. Bone Physiology and Hierarchy

Bones are complex structures with vascular and neural networks, consisting of components such as bone tissue, bone marrow and bone membrane (periosteum) (Wentao Zhang et al. 2022). The primary function of bones is protecting vital organs and providing the required rigidity for skeletal movement (Lijun Wang et al. 2022; Blumer 2021). Additionally, bones play a crucial role in the production and storage of blood cells (haematopoiesis). They also serve as a reservoir for minerals (such as calcium and phosphorus), growth factors, and cytokines (Su et al. 2019). Bones are specialized connective tissue consisting of four major cell types: osteoblasts, osteocytes, bone lining cells, and osteoclasts (Fuchs, Thompson, and Warden 2018). It is additionally a dynamic organ, with osteoclasts constantly resorbing and osteoblasts continually neo-forming (Rinaldo et al. 2015). They have a complex and functional structure that includes both organic (more than 30 proteins including type I collagen) and inorganic substances (primarily crystalline hydroxyapatite (HA)) in terms of their biochemical structure (K. Zhu and Prince 2015; Feng 2009). Bone tissue is a composite structure that provides the body protection and structural support. Bone tissue is a complicated and hierarchical structure that exists on multiple scales, ranging from macroscale to sub-nanoscale. The hierarchical structure of bone is shown in Figure 1.

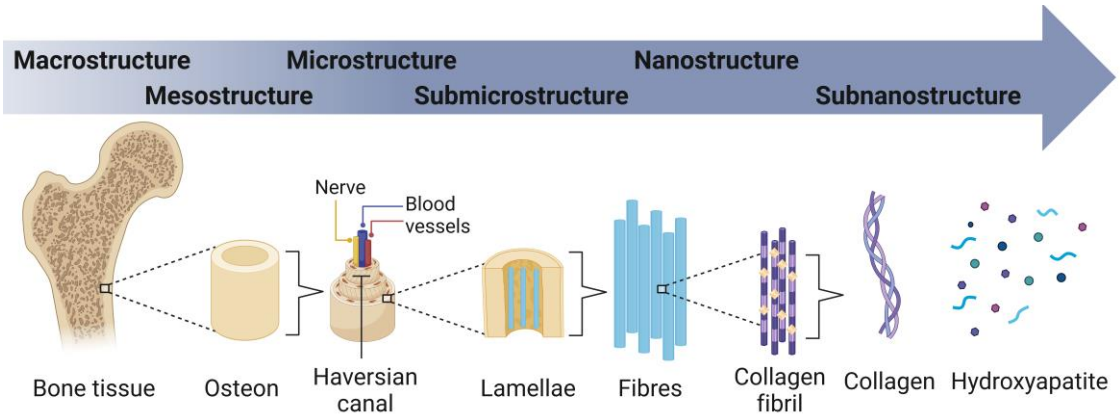

Figure 1. The hierarchical structure of bone from macrostructure to subnanostructure.

The bone is composed of an organic matrix, primarily collagen, and a mineral phase (HA) at the macroscopic level. Depending on the combination of these components, the properties of bone, such as hardness, durability and toughness, may vary (Fratzl et al. 2004). When the bone is examined on a microscale, it is seen that it consists of Haversian canals, which are approximately 100 μm in diameter and have a cylindrical structure. The Haversian canal is a structure containing blood vessels and nerves, and osteons consist of layers surrounding the Haversian canal. Osteons contain lamellae, which display different fiber patterns and consist of layers of collagen fibers. Thanks to its structure, it provides resistance against crack propagation and increases the strength of the bone (D. Zhang, Chippada, and Jordan 2007). The characteristic structure of these layers is important for the mechanical flexibility of bone tissue (Zuo and Wei 2007). Bone consists of nanoscale collagen fibers with a diameter of approximately 5 μm. These collagen fibers form the organic phase of bone and ensure mineral accumulation. In this way, it contributes significantly to the tensile strength and flexibility of bone (Fratzl et al. 2004). We see that bone consists of mineralized collagen fibrils at the subnanoscale, approximately 500 nm in diameter. These fibrils consist of HA nanocrystals and collagen molecules. The mineral phase strengthens the collagen matrix and increases the compressive strength and hardness of the bone. At the subnanoscale, the structure of bone consists of collagen and HA molecules (Duchstein and Zahn 2011). Collagen molecules form a triple helix structure, with HA crystals forming on the collagen molecules (Nikolov and Raabe 2008). Understanding this hierarchical organization of bone is necessary to develop biomaterials suitable for bone tissue.

1.2. Bone Tissue Engineering

People may suffer tissue and organ loss or damage because of genetic disorders, accidents, or diseases. Such losses can seriously reduce the quality of life of individuals by making it difficult for them to continue their daily lives. Bone fractures are an important worldwide health problem that has significant financial costs. According to the report from the Global Burden of Disease Study 2019, the total number of new fracture cases worldwide was estimated to be 178 million, highlighting the substantial and widespread impact of bone deformations and fractures as a major health concern worldwide (A. M. Wu et al. 2021). Every year, 4 million people worldwide need bone transplantation or bone replacement surgery. Studies predict that by 2025, there will be 3 million age-related bone problems in the US, up from 2.1 million elderly people in 2005 (Amin et al. 2014). In parallel, fracture cases in Europe are expected to increase by approximately 28% from 2010 to 2025 due to the increasing population. Large bone defects are the leading cause of disability worldwide, and the condition affects the lives of approximately 1.71 billion people. Therefore, the clinically effective treatment of bone diseases has critical importance (Bauso et al. 2024).

Bones have a structure that is constantly restructuring, responds to stimuli, and can heal damage caused by trauma. Bone tissue can renew itself; however, when the extent of damage reaches critical levels, this natural healing process may not be sufficient. Complex fractures in bones and conditions such as cancer can cause damage beyond their ability to heal. Such severe damage can usually be healed by surgical intervention (Su et al. 2019). Available surgical procedures often include methods such as ceramic fillings, titanium nails, or total joint replacements. In these methods, materials that remain permanently in the body and cannot be broken down may cause biological problems such as infection or mechanical problems in the body (Szczęsny et al. 2022). Bone grafts are currently frequently used in the clinic to treat bone tissue damage.

Bone grafts are classified based on the sources from which they are obtained (Figure 2). In general, bone graft materials are examined in three groups: autografts, allografts, and xenografts (Wickramasinghe, Dias, and Premadasa 2022). Autografts are obtained from the same body from a different unaffected site (Archunan and Petronis 2021). The iliac crest, mandibular symphysis (chin region), external oblique ridge, and

proximal ulna are possible sources of autografts (Zhao et al. 2021). However, it might lead to complications related to harvesting.

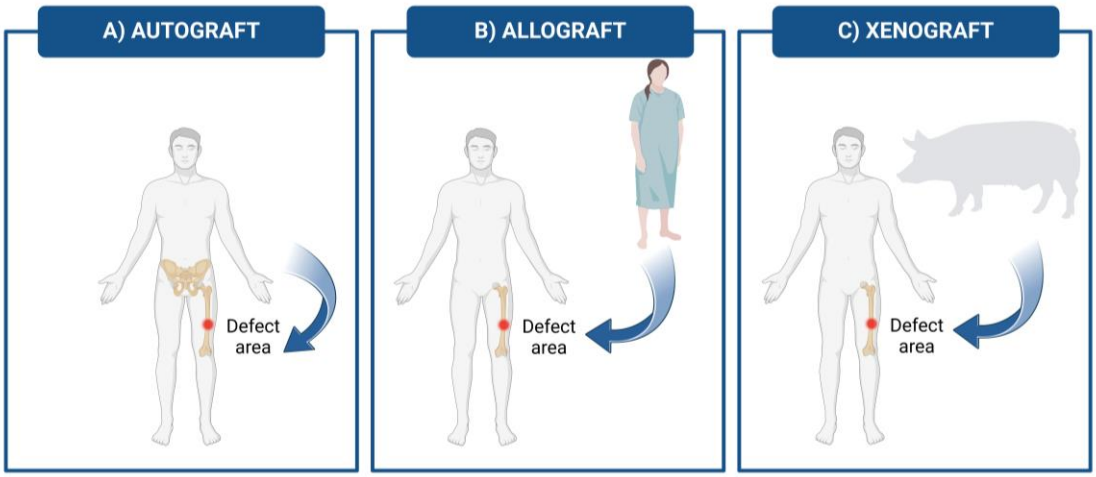

Figure 2. Types of bone grafts include allograft, autograft, and xenograft.

Allograft involves transplanting tissue from one individual to another of the same species. Allografts are extensively employed in medical fields to repair or replace damaged tissues, with applications ranging from bone reconstruction to the restoration of tendons, ligaments, skin, and heart valves (Kohnken, Porcu, and Mishra 2017). A xenograft is used primarily in medical and biological research, where tissues or cells from one species (commonly mice, rats and bovine) are transplanted into another species (usually human). This model is widely used in cancer biology, pharmacology, and tissue engineering. In clinical trials, patient-derived xenograft (PDX) models provide a fundamental and effective approach to studying cancer biology. (Koga and Ochiai 2019; Kohnken, Porcu, and Mishra 2017). The advantages and disadvantages of all types of grafts are shown in Table 1.

Table 1. Advantages and disadvantages of types of grafts.

Types of grafts	Advantages	Disadvantages	References
Autograft	• No risk of immune rejection • Best integration with host tissue • No risk of disease transmission • Cost-effective • Shortest healing time • High osteogenic potential	• The additional surgical site increases the risk of infection and morbidity • Amount limitations • Pain in the donor site	(Sungsoo S. Lee et al. 2013; Kim, Seon, and Jo 2013; Sheikh, Sima, and Glogauer 2015)
Allograft	• Unlimited amount • No need for a second surgery • Can be processed to reduce immune response	• Risk of immune rejection • Potential disease transmission • May require immunosuppressive therapy	(Mankin, Hornicek, and Raskin 2005; Marrale, Morrissey, and Haddad 2007)
Xenograft	• Abundant supply • Can be obtained in large quantities	• High risk of immune rejection • Ethical concerns • Potential zoonotic infections	(H. S. Lee et al. 2019; Cabezas-s et al. 2020; Simons and Brayton 2017)

There are several disadvantages of bone grafts, including the possibility of disease transmission, donor-site morbidity, and restricted donor availability, depending on the type, as presented in Table 1 (Roberts and Rosenbaum 2012). At this point, tissue engineering offers new approaches for bone tissue damage. One of the main purposes of tissue engineering is to repair or regenerate damaged tissues and organs.

Tissue engineering consists of three main components. There are cells, signal molecules and scaffolds (Vacanti 2006). New tissue matrices are synthesized by the cells at the damage site, while scaffolds offer temporary 3D frameworks to promote cell proliferation and differentiation. The signal molecules promote the division of cells and the growth of new tissue at the defect site (Hutmacher et al. 2007). The ability of the scaffold to promote specific cellular responses and direct tissue regeneration can be enhanced by using growth factors or bioactive molecules. By using growth factors or bioactive molecules in scaffold production, biomaterials that support the regeneration of different tissues can be created (Ozkendir et al. 2024). The goal of bone tissue engineering is to gradually integrate into the patient to replace the damaged bone with functional live

tissue. Since bone is constantly remodelling, a biodegradable scaffold will disintegrate if the timing is correct, replacing the biomaterial as the native tissue at the implanted place remodels and grows again. By combining the scaffold with the patient's own cells, regeneration can occur not only at the material interface but throughout the scaffold (Amini, Laurencin, and Nukavarapu 2012). Therefore, the development of bioactive, biocompatible and biodegradable 3D porous scaffolds that can provide a suitable environment for cellular activity is a critical issue for bone tissue engineering.

Scaffolds provide many advantages in the regeneration of bone tissue (Seunghun S. Lee et al. 2022). These 3D scaffolds can be used as filling material for the defective area, as structural support or as temporary extracellular matrix (ECM) and provide support until the bone cells form their own ECM environment. A scaffold to be used as an ideal bone graft should be biocompatible, biodegradable, mechanically compatible, and have osteoconductive and osteoinductive properties (Qu et al. 2019).

Scaffolds used in tissue engineering are structures that provide support for cell attachment, proliferation and differentiation. The design and architecture of scaffolds significantly affect their effectiveness in promoting tissue regeneration (Chan and Leong 2008). One of the important things to consider in scaffolding design is porosity. Porous structure plays a crucial role in scaffold design because it significantly affects cell infiltration, nutrient and oxygen diffusion, and waste removal (Loh and Choong 2013). Additionally, high porous structure is also important for vascularization, which is necessary for tissue regeneration (Chiu et al. 2011). Porous structure can be examined in two groups: open porous structure and closed porous structure. An open porous structure allows cells, nutrients, and metabolic waste to move freely (Figure 3). An open porous structure is necessary to promote cell migration and cell proliferation and for better integration of the material with the host tissue. Closed porous structure, on the other hand, consists of pores that are not connected and limit the movement of cells, tissues and metabolic wastes (Loh and Choong 2013). Although closed pore structures increase the mechanical strength of the scaffold, they are insufficient to support tissue integration and vascularization (Chan and Leong 2008).

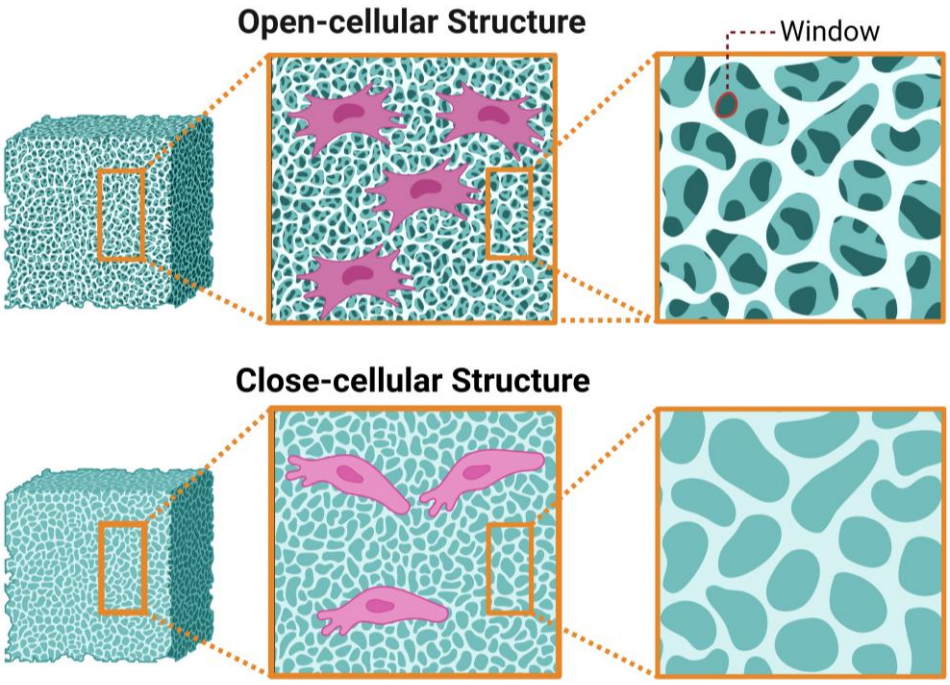

Figure 3. Representation of the open and close porous structures.

Porosity can not only be achieved by conventional methods but porous fiber structures can also be obtained using techniques such as electrospinning. These structures can more closely mimic the ECM (Bhardwaj and Kundu 2010).

1.2.1. Biomaterials

1.2.1.1. Ceramics

There are four main types of biomaterials: ceramics, polymers, composites and metals. The former three types of biomaterials are more widely used as tissue engineering scaffold material. Ceramics such as HA, bioactive glass and tricalcium phosphate are important materials used as bone substitutes due to their biocompatibility and osteoconductive properties. The most important feature of these materials is that they

mimic the mineral component of bone well, promoting bone cell attachment and proliferation. In contrast, ceramics have serious disadvantages, such as fragility. Considering this disadvantage, the use of materials in non-load-bearing applications gives better results. In addition, processing techniques used on ceramic materials expand their application areas by improving their mechanical properties (Rezwan et al. 2006).

1.2.1.2. Polymers

Polymers are examined in two groups, natural and synthetic, depending on whether their origin and production processes are natural or not. Natural polymers such as collagen, fibrin, gelatin, chitosan, and silk are extracted from organic sources, including plants, microorganisms, and algae or animals. On the other hand, synthetic polymers, also known as manufactured polymers, including polylactic acid (PLA), polycaprolactone (PCL), poly(lactic-co-glycolic acid) (PLGA), polyglycolic acid (PGA), and polyvinyl alcohol (PVA) that are artificially produced in laboratories (Satchanska, Davidova, and Petrov 2024). These synthetic polymers are currently used to produce biodegradable scaffolds (Place et al. 2009).

Synthetic polymers have several advantages over natural polymers, including tunable properties and established structures. Controlling the molecular weights of synthetic polymers offers an advantage that allows the polymerization process, interconnection of chains, and functionality to be directed as desired (McDonald et al. 2023; Gunatillake, Adhikari, and Gadegaard 2003; Javid-Naderi et al. 2023). Furthermore, due to well-defined chemical manufacturing processes, synthetic polymers are reproducible, offering performance reliability that is essential for clinical applications (Thang, Chien, and Cuong 2023). Also, natural polymers can have significant batch-to-batch variation and slower production rates compared to synthetic polymers (N. Zhang and Kohn 2012). Synthetic polymers also allow for easy modification with functional groups, enabling the integration of bioactive molecules, growth factors, or cell adhesion peptides to enhance cell attachment, proliferation, and differentiation (Tessmar, Mikos, and Göpferich 2003; Bolívar-Monsalve et al. 2021). Conversely, natural polymers, such as collagen and fibrin, have complex structures and can be expensive to make and purify, even though they are biocompatible and biodegradable. In addition, synthetic polymers

are also advantageous due to ethical considerations as they do not require the procurement of resources from humans or animals, hence avoiding related ethical issues.

The advantages and disadvantages of natural and manufactured polymers are compared in Table 2.

Table 2. Advantages and disadvantages of natural and synthetic polymers.

Source	Examples	Advantages	Disadvantages	References
Natural	• Collagen • Fibrin • Gelatin • Chitosan • Silk	• Biocompatible • Biodegradable • Hydrophilic • Ease of processing	• Low mechanical strength • Batch-to-batch variation • The slow rate of production	(Phutane et al. 2023; Maghsoudi et al. 2020; Sundaramurthi, Krishnan, and Sethuraman 2014)
Synthetic	• PLA • PCL • PLGA • PGA • PVA	• Controllable mechanical properties • Controllable degradation rate • Long shelf life	• Limited cell-material interaction • Limited solubility in water • Mostly hydrophobic • Lack of bioactivity • Low protein adsorption	(Phutane et al. 2023; Niu, Chen, and Wu 2023; Arabpour et al. 2024)

Synthetic polymers can be classified as thermoplastics and thermosets based on their behaviour when they are exposed to heat (Oladele et al. 2023). Thermoplastic polymers can soften and change shape when heated and return to their original shape when cooled again. Due to this property, they can be melted and shaped repeatedly, making them ideal for recycling. These materials are generally soluble in organic solvents. They exhibit properties such as being soft, weak, and less brittle compared to thermoset polymers (Bîrcă et al. 2019; Radlmaier et al. 2017). On the other hand, thermoset polymers form network-shaped bonds, which provide thermosets with superior resistance to heat and chemicals (Massy 2017). These materials are insoluble in organic

solvents. They are characterized by their hardness, strength, and brittleness. (Ahmad, Razali, and Razelan 2017).

PCL is a widely used synthetic polymer that is biocompatible, non-toxic and has favourable properties. PCL is a hydrophobic and semi-crystalline polymer. Its melting point ranges around 60 °C. The average molecular weight of the commercially available linear PCL vary between 3,000 and 90,000 g/mol, and they are graded based on the molecular weight (Woodruff and Hutmacher 2010). A chemical drawing of commercially available linear thermoplastic PCL is shown in Figure 4.

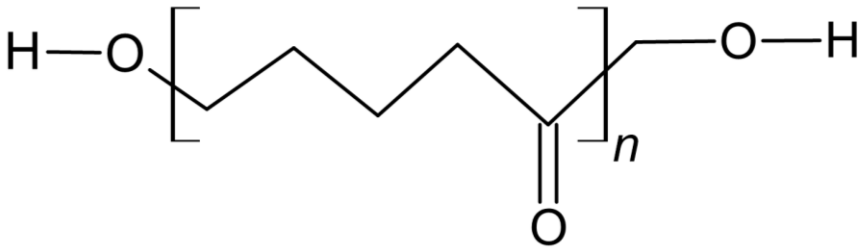

Figure 4. Chemical structure of commercially available linear PCL.

As the molecular weight of PCL increases, its crystallinity decreases. PCL is an advantageous polymer for potential applications in the biomedical industry due to its compatibility, low melting point, and variety of solubility (Malikmammadov et al. 2018). PCL and PCL-based materials can be used as promising materials in areas such as controlled drug release, scaffold production, artificial organs, and nerve regeneration. PCL can be prepared by ring-opening polymerization of ε-caprolactone, a cyclic monomer, using different catalysts (such as anionic, cationic and coordination). The molecular weight, molecular weight distribution, and end group composition obtained in both methods affect the chemical structure of the polymer (Woodruff and Hutmacher 2010). PCL can be dissolved at room temperature in various solvents such as chloroform, dichloromethane (DCM), benzene and toluene (Temtem et al. 2008). Additionally, the biodegradation period of PCL is limited to a few years (Murray et al. 2015). Due to its high biocompatibility and thermoplasticity, PCL has been used in various biomedical applications and has had many successful commercial applications. PCL has been used in many applications for bone and cartilage tissue engineering (C. S. Wu and Liao 2012).

1.2.1.3. Composites

Composite biomaterials are produced by combining two or more materials with dissimilar physical or chemical properties. A composite material is produced when the properties of two or more separate materials combine. This composite material has distinctive features from the individual components. Composite biomaterials are advantageous as they can be tailored to specific applications, offering improved mechanical, biological, and chemical properties over traditional biomaterials (Aslam Khan et al. 2021).

Composite biomaterials are generally categorized based on their matrix materials, which are polymers or ceramics (Aslam Khan et al. 2021). Polymer matrix composites are generally reinforced with bioactive ceramics to increase their mechanical properties and bioactivity (J.L. Robinson, Brudnicki, and Lu 2017). Ceramic matrix composites combine with other materials, such as polymers, to increase their durability and reduce their brittleness. HA and calcium phosphate are commonly utilized in bone tissue engineering because of their osteoconductivity and biocompatibility (Ielo et al. 2022). In bone tissue engineering applications, composite scaffolds are often designed to mimic the hierarchical structure of bone, provide mechanical support to bone, and promote osteogenesis. For example, polymer-ceramic composites such as PLA combined with HA are being extensively investigated for bone regeneration. Bernardo *et al*. created bioactive PLA scaffolds with a high HA content. The mechanical characteristics of these 3D composite scaffolds were comparable with those of trabecular bone. Additionally, *in vitro* tests performed with mesenchymal stem cells showed that it was highly biocompatible. (Bernardo et al. 2022).

1.2.2. Scaffold Fabrication Techniques

Various methods are used to fabricate the scaffolds in bone tissue engineering. Solvent casting, freeze-drying, phase separation, gas foaming, electrospinning, porogen leaching, 3D printing and emulsion templating are some of the commonly used methods

in scaffold fabrication. A general comparison of the pros and cons of the scaffold fabrication techniques is shown in Table 3. All scaffold fabrication techniques will be explained in detail in the following section.

Table 3. Advantages and disadvantages of the widely used scaffold fabrication techniques.

Fabrication Method	Advantages	Disadvantages	References
Solvent Casting	• Controlled porosity	• Can be hazardous to the environment due to residual solvents • Limited mechanical strength	(Rohani Shirvan et al. 2022; Annabi et al. 2010)
Freeze-drying	• Highly porous structure • Easy of processing • Large-scale production	• Lengthy procedure • High energy consumption	(Murphy, Haugh, and O'Brien 2010; Bajaj et al. 2014; Ho et al. 2004; Meeremans et al. 2021)
Phase Separation	• Homogenous porosity • Low-cost process	• Solvent residual • Shrinkage issues • Small-scale production	(Ghalia and Dahman 2016; Meeremans et al. 2021)
Gas Foaming	• Solvent-free • Highly porous structures • Scalable	• Possibility of closed pore structure • High utilization of heat • Limited mechanical strength	(Kumar and Jacob 2022; Eltom, Zhong, and Muhammad 2019)
Electrospinning	• Porosity with high interconnectivity • High surface area/volume ratio	• Possibility of solvent residual • Limitation of thickness	(L. Li and Hsieh 2005; Rahmati et al. 2021)
Porogen Leaching	• Homogenous pore distribution • Ease of process	• Can cause limited pore interconnectivity • Weak mechanical properties	(Owen et al. 2020; Y. Wu et al. 2015)
3D Printing	• Tailored design • Scalability • High precision	• May require technical expertise • Costly	(Q. Zhang et al. 2023)
Emulsion Templating	• Tunable porosity, pore size and interconnectivity • High interconnectivity • Reproducibility	• Requirement for the development of a stable emulsion • Generally, hazardous surfactants and solvents are needed • Surface skin formation • Having a high number of process parameters that affect the final morphology requires expertise	(Mudassir et al. 2021)

1.2.2.1. Solvent Casting

Solvent casting is a traditional method used in the production of polymeric films consisting of porous networks (Deliormanlı and Atmaca 2020). This method involves dissolving the polymer in an organic solvent, dispersing the components by mechanical mixing, casting this mixture onto the supporting surface, and finally evaporating the solvent. The schematic of the solvent casting method is given in Figure 5A.

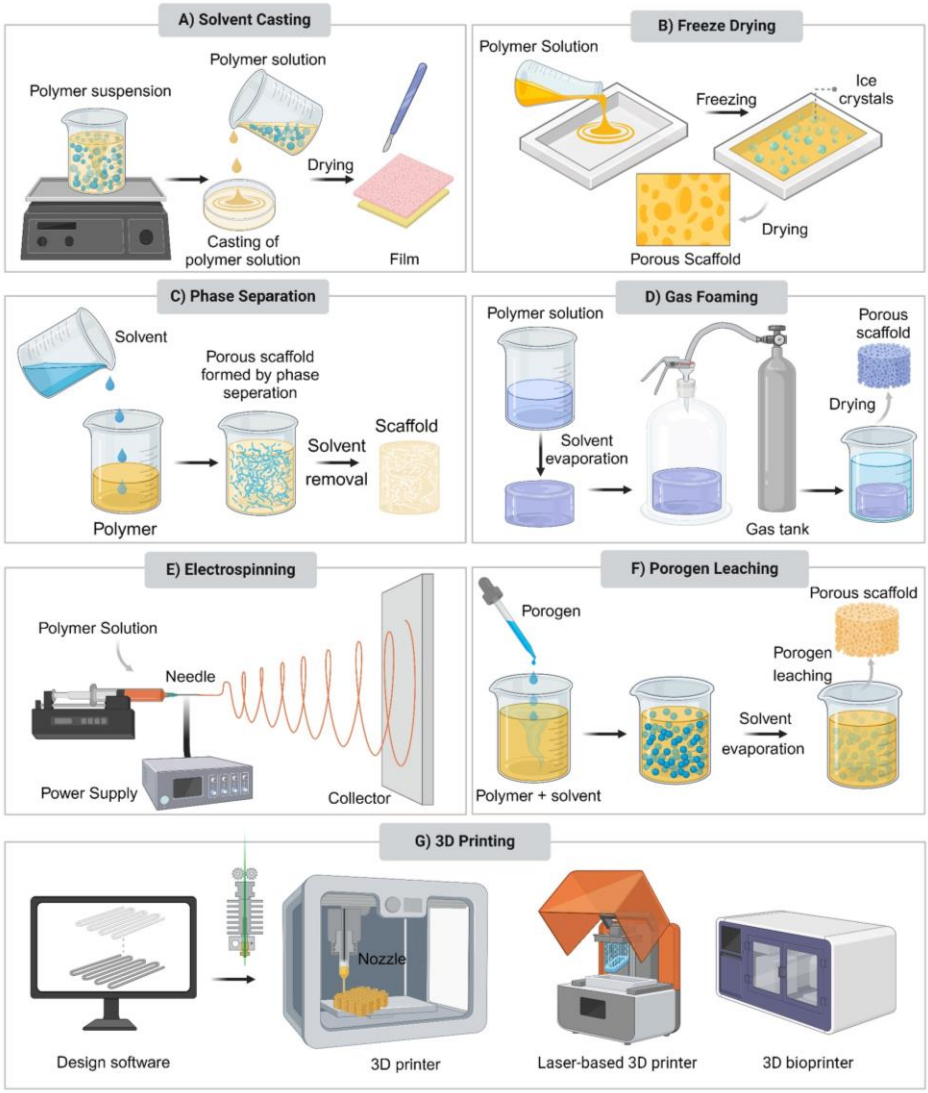

Figure 5. Schematic illustration of the most widely used scaffold fabrication set-ups.

As the solvent inside evaporates during the drying phase, a solid layer forms on the surface. Chloroform, tetrahydrofuran and DCM are the three main solvents frequently used in this method (Turnbull et al. 2018; Cheerarot and Saikrasun 2023). This method is used in many fields, including biomedical applications, pharmaceutical applications, and materials science. The main drawback of this method is that it may result in low interconnected structures.

Gümüşderelioğlu et al. developed a double-layer barrier membrane using chitosan and PCL by solvent casting and electrospinning method. The chitosan-based layer was formed using the solvent-casting method. In this method, silica particles were added to the mixture as a porogen after chitosan was dissolved in aqueous acetic acid. The solvent was allowed to evaporate at room temperature after dissolving the silica particles and producing a porous matrix. Interconnected and homogeneous morphology was observed on the resulting chitosan membrane, and the average pore size was measured as 170 ± 79 μm. In contrast, the surface of the scaffold in contact with the glass petri dish showed less porous and small pore structure (Mavis et al. 2009).

1.2.2.2. Freeze-drying

Freeze-drying (lyophilization) is a well-rounded method that enables the production of uniform pore morphology without the need for an additional pore-forming agent (Capuana et al. 2021; Bhushan et al. 2022). In this technique, a porous structure can be obtained while preserving the structural integrity of the material by evaporating water (X. Zhang vd., 2015). In detail, crystal formation is encouraged by freezing a water-based polymer solution at low temperatures (−70 to −80 °C). The polymer forms in the spaces around ice crystals. The remaining solvent is removed by applying a vacuum in the chamber. The schematic representation of the freeze-drying technique is given in Figure 5B. This process allows the development of the dry and interconnected porous structures by complete sublimation of the solvent. In addition, water residues that have not previously solidified are removed in the secondary drying stage by desorption.

The main advantage of this method is obtaining highly porous and interconnected structures. Jain *et al.* used the freeze-drying method to fabricate composite scaffolds

composed of chitosan, PCL, and HA. These scaffolds exhibited pore sizes between 50 and 200 μm. Also, the scaffolds were produced with 90% porosity (Jain et al. 2015). Yashaswini *et al*. fabricated dexamethasone-loaded sodium alginate-graphene oxide (Alg-GO-Dex) microspheres using air-dry followed by freeze-drying technique for bone tissue engineering. The porosity of Alg-GO-Dex was measured as 84% (Devi et al. 2021).

1.2.2.3. Phase Separation

Phase separation is another technique used for the creation of highly porous structures (Figure 5C). Different phase separation methods are nonsolvent-induced phase separation (NIPS), thermally induced phase separation (TIPS), and vapor-induced phase separation (VIPS). TIPS is dependent on a temperature shift, causing a homogenous polymer solution to combine and a multiphase system to develop. It allows the formation of monodisperse and high porosity particles (Conoscenti et al. 2017; Nogueira et al. 2020; Tanaka, Tsuchiya, Takahashi, Taniguchi, and Lloyd 2006; Tanaka, Tsuchiya, Takahashi, Taniguchi, Ohara, et al. 2006). NIPS involves immersing a polymer solution film in a solvent-free deposition bath. As a result, the film is divided into two phases: the membrane matrix, which is the polymer-rich phase, and the membrane pores, which are the polymer-poor phase. It allows the production of membranes with a dense surface with an asymmetric morphology (Jung et al. 2016; Basko et al. 2023; Garcia et al. 2020). The generated membrane in the VIPS method is first exposed to a vapour nonsolvent to cause phase separation, and then it is immersed in a nonsolvent coagulation bath to form the final membrane. It provides highly porous and isotropic membranes with rough surfaces (Venault et al. 2013; Menut et al. 2008).

1.2.2.4. Gas Foaming

The gas foaming technique is another porous scaffold fabrication technique. The general schematic of the gas foaming method is shown in Figure 5D. This technique

occurs in three steps. These are polymer/gas solution acquisition, gas bubble-induced pore formation, and pore volume expansion (Jiang et al. 2015; Moghadam et al. 2017). This method provides the production of microporous (<10 μm) in the scaffolds (P. Song et al. 2018).

Wang and coworkers fabricated PCL/PLA tissue engineering scaffolds using different ratios of PCL/PLA blends. They optimize the foaming process (temperature, pressure, and CO_2 dissolution time) for scaffold morphology and mechanical strength of the material. They successfully obtained the scaffolds with interconnected porous structures using a gas foaming technique (Lixia Wang et al. 2019).

1.2.2.5. Electrospinning

Electrospinning is a technique that produces continuous fibers from a polymer solution with the help of a high-voltage source in a high-voltage electric field, with a production capacity of fibers with diameters from nanometers to micrometres (Teo and Ramakrishna 2006).

Electrospinning consists of four main components (Figure 5E). These are a high-voltage power supply, a polymeric solution syringe, a spinneret, and a grounded collector (Y. Li et al. 2021). With the electrospinning technique, ECM structures can be mimicked by producing loosely connected 3D fiber structures (Agarwal, Wendorff, and Greiner 2008). Electrospinning is a commonly used technology in various fields, such as nanotechnology (Castillo-Henríquez et al. 2020), nanocatalysis (Y. Ma et al. 2019), drug delivery systems (S. Chen et al. 2018), environmental engineering (Wenshuo Zhang et al. 2020; J. Song et al. 2023) and tissue engineering scaffolds (Welle et al. 2007). Although electrospinning can provide fibers that mimic the native ECM structure, it has a critical drawback. Polymer solutions are created with toxic organic solvents that need lots of post-treatment to be used in medical applications. Recently, many approaches have been researched to find solutions to this problem (Avossa et al. 2022). In electrospinning, environmental conditions (temperature, humidity, etc.) must be optimized to obtain the desired morphology. Additionally, optimization can take time and require experience (Dahlin, Kasper, and Mikos 2011).

1.2.2.6. Porogen Leaching

Porogen leaching is a simple technique to fabricate a porous scaffold. In this technique, porogen materials are used to create porous structures, and they are incorporated with a polymer solution (Figure 5F). Porogens are insoluble in hydrophobic solvents such as crystals of sugar or salt, paraffin microspheres, fibers, beads and emulsion particles (Thadavirul, Pavasant, and Supaphol 2014). They were able to simply remove the negative replica pores from the scaffold following the solvent evaporation process. Porogen material structure design enables the modification of scaffold characteristics, including pore size, porosity, shape, and interconnectivity (Owen et al. 2020; Sin et al. 2010). To increase pore interconnectivity, porogen materials are bonded before mixing them with a polymer matrix.

Liang *et al.*, produced interconnected porous PLGA scaffolds using a leaching technique with a porosity of about 92%. Cubic salt particles in the range of 300-450 μm were used as a porogen (Liang et al. 2018).

1.2.2.7. 3D Printing

3D printing is a well-designed technique for developing functional scaffolds for damaged tissues (Liu and Yan 2018). 3D printing is an important technique used to produce scaffolds with complicated morphologies that are unable to be produced using conventional manufacturing methods (Yazdanpanah et al. 2022). 3D printing involves creating a workpiece by injecting material into a shape designed by a computer program. Then, this material is extruded from a nozzle (Figure 5G). The valuable advantage of this technique is reproducibility. It also stands out with its high control of pore morphology, interconnectivity, high resolution, and rapid prototyping (Pavan Kalyan and Kumar 2022). This technique can also be used in combination with other production techniques. An example of this is Dikici et al., who developed a scaffold by using emulsion templating and 3D printing together. PCL-based scaffolds with a hierarchical architecture have been developed for bone tissue engineering (Aldemir Dikici, Reilly, and Claeyssens 2020).

1.2.2.8. Emulsion Templating

1.2.2.8.1. Development of Emulsion Templated Matrices

Emulsion templating is a two-step technique. Initially, at least two immiscible liquids are combined to create an emulsion. This emulsion consists of two phases (*internal phase (dispersed phase) and continuous phase (external phase)*). Then, the continuous phase of the emulsion is solidified (T. Zhang et al. 2019). The droplets forming the internal phase act as templates during solidification. After solidification is achieved, the internal phase is removed, and porous matrices are obtained. The general schematic of Polymerised High Internal Phase Emulsions (PolyHIPE) production via the emulsion templating method is shown in Figure 6.

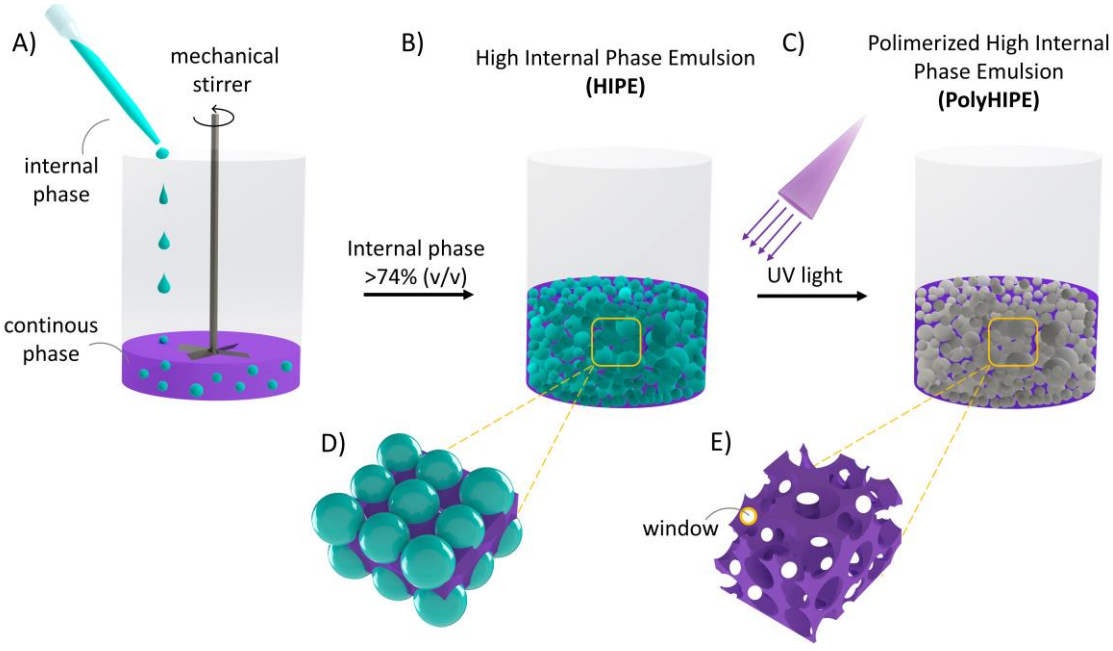

Figure 6. Fabrication steps of Polymerised High Internal Phase Emulsions (PolyHIPE) via emulsion templating.

These two-phase emulsions are called water-in-oil (w/o) or oil-in-water (o/w) emulsions, depending on where the hydrophilic (polar, water-loving) and lipophilic (non-polar, oil-loving) components are located (D. V. Johnson et al. 2024). The emulsion templating technique is a comparably new fabrication method compared to other widely used scaffold fabrication methods. Thus, when comparing emulsion templating with other widely utilized scaffold manufacturing methods, emulsion templating is the method with the least number of reported studies regarding tissue engineering applications. However, in recent years, the number of articles on emulsion templating has appeared to be increasing. The number of publications on different scaffold manufacturing methods between 1900 and 2024 is shown in Figure 7A. The number of articles published using the emulsion templating method in tissue engineering over the last 20 years is shown in Figure 7B.

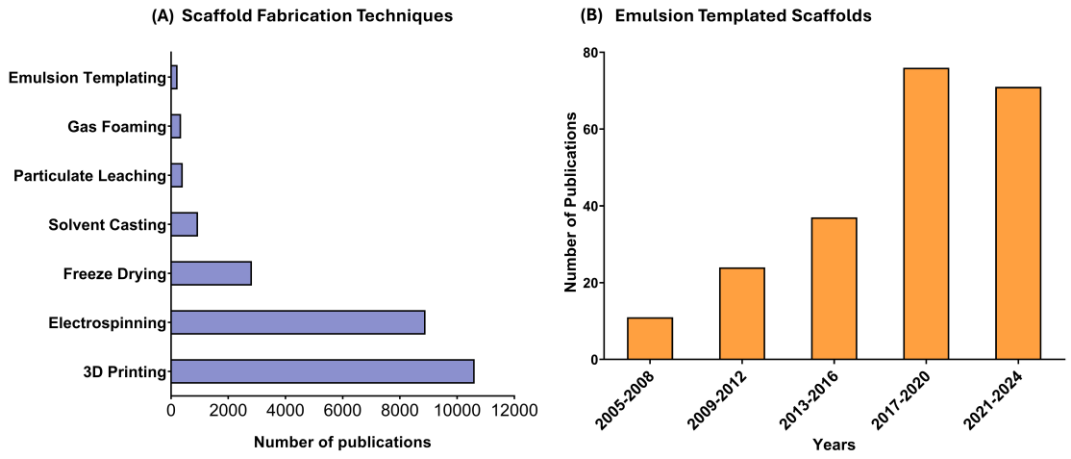

Figure 7. A) The number of publications on different scaffold manufacturing methods (1900-2024), B) The number of articles on the use of emulsion templating in tissue engineering over the last 20 years.

Scaffolds produced by the emulsion templating method stand out because their porosity can be easily adjusted by increasing the internal phase volume. Depending on the Kepler Conjecture, the densest achievable monodisperse sphere packing density is the value of 0.74048 ($\pi/\sqrt{18}$) (Hales 2005). This number is consistent with monodisperse, unharmed, hexagonally packed droplets, according to Oswald's phase volume theory

(Princen 1979). It is considered that unless the emulsion is heterodisperse, it will tend to break if its internal phase volume is above this value. In the case of heterodispersity, smaller-volume droplets fill the areas where larger-volume droplets intersect. In this way, the emulsion can have an internal phase volume of more than 74%.

Polymerized emulsions can be categorized into three different groups based on their internal phase volume. This classification includes Polymerized High Internal Phase Emulsions (PolyHIPE) (>74%), Polymerized Intermediate Internal Phase Emulsions (PolyMIPEs) (30–74%) and Polymerized Low Internal Phase Emulsions (PolyLIPEs) (<30%) (Aldemir Dikici and Claeyssens 2020). In generally reported studies, PolyHIPEs have varying average pore sizes between 1-150 μm, and the average window size varies between 2-50 μm (Moglia et al. 2014). The main factor affecting porosity in emulsion-templated scaffolds is the internal phase volume. The porosity of PolyHIPE scaffolds is not directly correlated with the internal phase volume. This results from the scaffolds shrinking throughout the cross-linking and following drying processes (Aldemir Dikici et al. 2019). The droplets are packed more closely because of an increase in internal phase volume, which may result in a decrease in pore size (Sušec et al. 2015).

Emulsion-templated scaffolds are fabricated for use in tissue engineering applications following several steps. These are (i) the preparation of HIPEs, (ii) the polymerization of HIPEs and (iii) post-processes.

1.2.2.8.2. Preparation of HIPEs

HIPEs consist of at least three key components. They consist of at least a stabilizer, an internal phase, and a continuous phase (polymer phase). In addition to these basic ingredients, additional ingredients (diluting solvent, photoinitiator) can be added to both phases of the emulsion. An appropriate monomeric or oligomeric pre-polymer is used for the continuous phase. The continuous phase may also contain additives (solvent, stabilizer, and initiator) to be added to the selected polymer. Pre-polymers can be in the solid state or a highly viscous liquid phase when mixing two immiscible states to form an emulsion. The components of HIPE are illustrated in Figure 8.

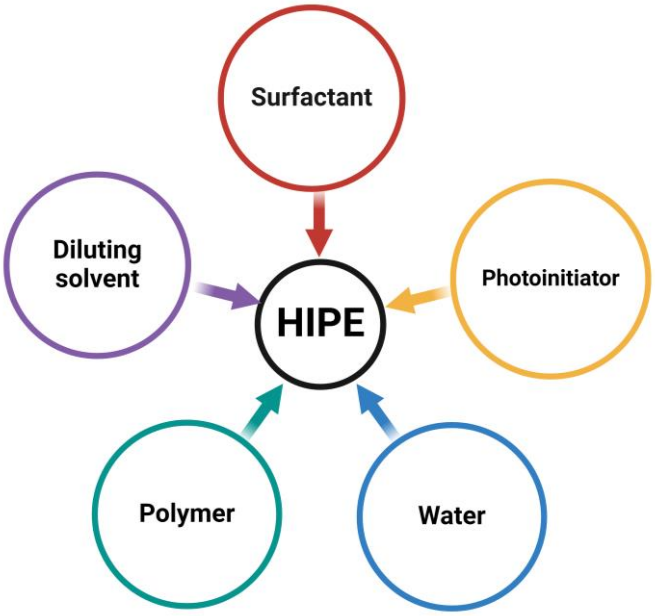

Figure 8. Schematic illustration of the components of HIPE used within this study.

In addition to improving the kinetic stability of the emulsion, the continuous phase viscosity should ensure efficient two-phase mixing. The viscosity of the continuous phase might be decreased by a variety of approaches. First, the viscosity can be reduced by increasing the system temperature. Second, polymers can be diluted with diluent or porogenic solvent. Nanoscale porosity in the walls of PolyHIPEs can be observed by adding dilution solvents to the continuous phase (Silverstein et al. 2005). Furthermore, the characteristics of HIPEs and PolyHIPEs are greatly impacted by the type and volume of the diluent utilized (Aldemir Dikici et al. 2019). Generally non-polar solvents are such as tetrahydrofuran (THF), toluene (W. Busby, Cameron, and Jahoda 2001; Aldemir Dikici et al. 2019), dichloroethane (DCE) (Johnson et al. 2015), chloroform (Aldemir Dikici et al. 2019), and DCM are included into w/o emulsions as diluents. The characteristics of HIPEs and PolyHIPEs are also greatly affected by the diluent volume. The maximum volume of the internal phase that can be incorporated into the emulsion increases as the diluent volume increases. HIPE stability decreases as the solvent volume increases further after a certain point (Aldemir Dikici et al. 2019). Because of this, a limited range of processing is required to form a stable emulsion

While water is mostly used in the internal phase of w/o emulsions, toluene (Krajnc, Štefanec, and Pulko 2005) is generally used in the internal phase of (o/w)

emulsions. The internal phase composition and volume utilized affect the properties of HIPEs and PolyHIPEs. To improve the stability of water-in-oil emulsions, some salts can be added to the internal phase, including potassium iodide, sodium sulfate (Na_2SO_4), calcium chloride ($CaCl_2$) (Márquez et al. 2010), sodium chloride (NaCl) (Shafiei et al. 2022) and sodium chloride (NaCl).

At the liquid interfaces, there is a strong surface tension when two liquids interact to create the structure of an emulsion without mixing. Droplets of the internal phase added to the continuous phase gradually coalesce, eventually reducing the surface area and inevitably causing phase separation. At this point, stabilizing the two liquid surfaces through the use of stabilizing agents decreases the interfacial tension. (Khan et al. 2011). The surfactant is an amphiphilic molecule, and its head dissolves in water, and its tail dissolves in oil. Surfactants form a film surrounding the internal phase, acting as a barrier between the surface and the oil phase. As a result, the emulsion becomes more stable, and the interfacial tension decreases. Surfactants can be categorized as cationic, anionic, non-ionic, and amphoteric, based on the charge of the hydrophilic head. The properties of PolyHIPE and the stability of emulsions are affected by the concentration and surfactant choice (Wendy Busby, Cameron, and Jahoda 2002; Aldemir Dikici et al. 2019).

The volume of the phases determines the sort of emulsion that forms when surfactant is not utilized. The continuous phase will have a greater volume phase. In fact, according to Bancroft's Rule (Parks 1982), when surfactants are used, the continuous phase is formed by the phase where the surfactant is more dissolved. In addition, water-soluble surfactants perform better in o/w emulsions, while oil-soluble surfactants perform better in w/o emulsions (Bancroft 1912). In w/o emulsions, oil-soluble non-ionic surfactants are often utilized to stabilize the emulsion (Silverstein 2014). The most commonly utilized surfactants for w/o emulsions are Hypermer 246, Span 80, and polyglycerol polyricinoleate (PGPR). During the preparation of HIPEs, the most used concentration of surfactants is in the range of 1-30% (w/w) (of monomer).

Solid particles (micro or nanoparticles) can be used to stabilize emulsions in addition to surfactants in liquid form. The emulsions obtained in this way are called Pickering emulsions (W. Li et al. 2022). The pore size of particle-stabilized emulsions can be modified by varying the concentration of the particles (S. Zhou, Bismarck, and Steinke 2012).

1.2.2.8.3. Polymerization of HIPEs

Polymers can be solidified through different routes. Free radical polymerization, step-growth (condensation) polymerization, solvent evaporation, cross-linking and ring-opening polymerization are commonly used approaches for emulsion solidification. The free radical polymerization method was used in this study. Free radical polymerization is a chain growth polymerization that occurs by sequential addition of free radical building blocks. It is widely used in solidifying emulsions. The main reason for its use is its simple applicability and effectiveness. Free radical polymerization can be achieved by heating the emulsion, exposing it to Ultraviolet (UV) light, or by redox initiation, depending on the type of initiator used (Awwad et al. 2020). When photoinitiators are exposed to light, they generate reactive species. They are incorporated into the composition of HIPEs through photoinitiation, allowing the emulsion to polymerize. Additionally, the polymerization is initiated in the continuous phase, allowing the emulsion to solidify into a porous structure. If the emulsion mixture contains the photoinitiator, an emulsion is exposed to UV light for a second to min for solidification of the polymer, depending on the sample thickness (Aldemir Dikici and Claeyssens 2020).

Initiators can be included in both phases of emulsions. The location where initiators initiate polymerization has a significant impact on porous structures (Benaddi et al. 2021). The absorption band of the photoinitiator and the emission spectrum of the light source used to polymerize the emulsion must intersect with each other. This parameter is the most critical parameter for photoinitiator selection (Dumur 2023). Diphenyl(2,4,6-trimethyl benzoyl)phosphine oxide/2-hydroxy-2-methylpropiophenone mixture (Sherborne et al. 2018; Dikici et al. 2019) and phenyl bis(2,4,6−trimethyl benzoyl)−phosphine oxide (BAPO) (Jennifer L. Robinson et al. 2016) are the most commonly used photoinitiators. Photoinitiators have been mostly used in studies at concentrations of 0.2 to 10% (w/w) by weight of the polymer contained in HIPE (Aldemir Dikici and Claeyssens 2020).

1.2.2.8.4. Post-processes of PolyHIPEs

Following the fabrication of the scaffolds using emulsion templates, a washing procedure is required to remove any remaining surfactant and uncured material. Failure to disinfect the scaffolds might be harmful to further cell culture tests (Caldwell et al. 2012). The washing procedure can be carried out with a Soxhlet extractor or by manual soaking in certain solvents.

The parameter to be considered when choosing the washing solvent is the solubility of the materials to be removed. The high solubility of various polymers in acetone makes it one of the most often utilized solvents for washing PolyHIPEs. (Caldwell et al. 2012). There have been studies in which methanol was preferred because it is less toxic than acetone and also causes less damage to cross-linked monoliths (Dikici et al. 2019; Aldemir Dikici et al. 2019). Additionally, various studies utilise isopropanol (Bokhari et al. 2005) and mixtures of many different solvents (Krajnc, Štefanec, and Pulko 2005).

An additional factor to take into account is that scaffolds designated for use in tissue engineering applications must be free of any living organism contamination, including bacteria and viruses, for both *in vitro* and *in vivo* testing, as well as human implantation. Many techniques have been utilized for sterilization. In clinics, ethylene oxide (Andrews, Hunt, and Black 2007), gamma irradiation (Fleith et al. 2005) and heat treatment (Fleith et al. 2005) are the most often utilized sterilization methods. The methods used vary in terms of removing microorganisms or reducing the degree of inactivation. It is important to understand the distinction between sterilization and disinfection. The process of removing or killing all microbiological life forms, such as viruses, fungi, and bacterial spores, is known as sterilization. Disinfection is the process of reducing or destroying pathogenic microorganisms on the surface of objects to a level that will not harm human health. Unlike sterilization, all microorganisms (especially resistant bacterial spores) may not be destroyed in the disinfection process (Rutala and Weber 2016). In the clinic, the use of both sterilization and disinfection is critical. The sterilization process is more commonly used for surgical instruments, implants, and other items that come into contact with sterile areas of the body, while the disinfection process

is generally used for surfaces, equipment, and tools that come into contact with non-critical body surfaces (Mohapatra 2017).

UV treatment and ethanol are frequently utilized in *in vitro* applications. Scaffold disinfection methods should be chosen by taking into account the test duration, material properties and application type. Ethanol is mostly used as a disinfection method for PolyHIPE scaffolds (Caldwell et al. 2012). 4PCLMA, a thermoset polymer, can withstand high temperatures without melting because it has a stable and cross-linked structure. In other words, sterilization methods such as autoclaving and dry heat that require high temperatures are applicable methods for 4PCLMA polymer. In addition, 4PCLMA is resistant to alcohols and other disinfectants, which allows the material to be re-disinfected without deterioration (Aldemir Dikici et al. 2019).

1.2.3. Surface Modification of Tissue Engineering Scaffolds

1.2.3.1. Motivation for Surface Modification

The chemical properties, hydrophilic properties, ionic groups, surface morphology and topography of biomaterials play an important role in the interaction of the biomaterial with the surrounding biological environment. These properties of the biomaterials determine their biocompatibility and biodegradability while also significantly affecting their interactions with cells (Rahmati et al. 2020). Surface properties of biomaterials, such as wettability, surface charge and topography, significantly affect cell adhesion to the biomaterial (Metwally and Stachewicz 2019). Surface modification methods are generally used to overcome properties such as the hydrophobicity of biomaterials. With these methods, hydrophilic and rough surfaces can be created on the biomaterial surface. In this way, it allows better organization of protein complexes that support the adhesion and growth of cells. Methods such as plasma treatment, chemical grafting, surface coating, and alkaline hydrolysis are some of the approaches utilized for the surface modification of the scaffolds and for improving their interaction with cells (Nemani et al. 2018).

In the following sections, each modification technique is summarized, and their pros and cons are compared in Table 4.

Table 4. General overview of surface modification techniques.

Surface Modification Type	Advantages	Disadvantages	References
Chemical Grafting	• Stable modification	• Requirement of a complex procedure • Specific conditions • Time-consuming • Can cause toxicity	(Teimouri et al. 2023)
Plasma Treatment	• No harsh chemical utilazition • Easy and fast modification	• Requires equipment • May be costly • Penetration restrictions	(Asadian et al. 2020; Recek 2019; Hesari et al. 2021)
Surface Coating	• Requirements for the coating material	• May reduce the diameter of the pore	(Pereira et al. 2020)
Alkaline Hydrolysis	• Easy to process • No equipment needed • Scalability	• May reduce mechanical strength	(Park et al. 2021)

1.2.3.2. Chemical Grafting

Functional groups are added to the surfaces of polymers via the chemical grafting technique (Figure 9A). This approach uses chemical bonding to attach biomolecules to polymer chains. Chemical grafting provides cells on polymer surfaces with an invasive biological ability. Polymers and reactive monomers are usually used in this technique (Drobota, Ursache, and Aflori 2022).

Ma and colleagues grafted polyacrylamide (PAAm) onto the surface of PLLA membranes to improve cytocompatibility for chondrocytes. The researchers performed photo-oxidation in hydrogen peroxide solution using UV light and then grafted PAAm onto the membrane surfaces by grafting polymerization under Iron(II) (Fe^{2+}). The polymerization duration and monomer concentration both affected the degree of grafting. Measurements of contact angles showed that surface modification decreased contact angles and enhanced the cytocompatibility of material (Z. Ma, Gao, and Shen 2003).

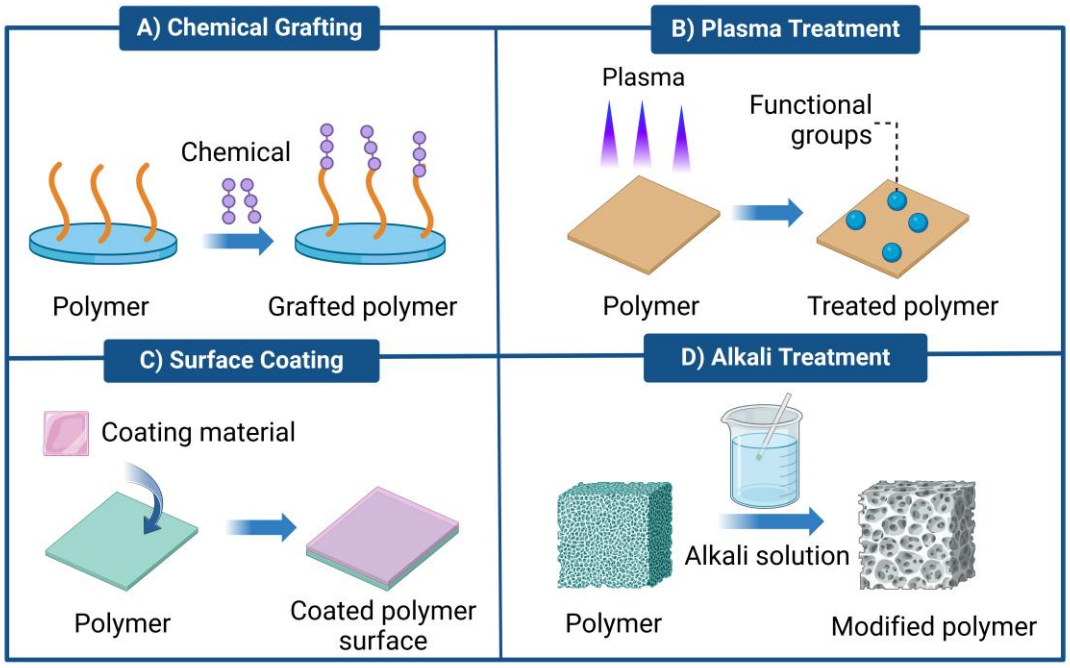

Figure 9. Schematic illustrations of commonly used scaffold surface modification techniques.

1.2.3.3. Plasma Treatment

Plasma treatment is a surface modification method used to change the physical and chemical properties of the polymer surfaces. High-energy plasma is used in this method. Plasma application is carried out using plasmas such as oxygen, nitrogen and ammonia. Through this process, the surface becomes more hydrophilic and produces

functional groups (Figure 9B). In addition, treating the surfaces of polymers with oxygen plasma increases cell adhesion as it creates hydrophilic surfaces on the polymer surfaces (Jacobs et al. 2012).

Pakeyangkoon and his colleagues applied air plasma to the poly(styrene/ethylene glycol dimethacrylate) (poly(S/EGDMA)) PolyHIPEs. They investigated the impact of surface modification on the behavior L929. They observed that the degree of water contact angle on the PolyHIPE porous foam surface decreased sharply after plasma modification. However, depending on the plasma treatment applied, damage was observed in the PolyHIPE samples after a certain time (30 min). Therefore, the plasma device must operate for the optimum time for scaffold surface modification. Cell adhesion also reached its highest level after 30 min of application. According to cell culture results, it was observed that the quantity of adherence and proliferation of cells on (S/EGDMA) PolyHIPEs was increased in atmospheric plasma-treated groups (Pakeyangkoon et al. 2012).

1.2.3.4. Surface Coating

Surface coating is the process of coating a thin layer on polymer surfaces, and this process is used to improve the surface properties of biomaterials (Figure 9C). The surfaces of polymers can be coated using different biomolecules (collagen and fibronectin) or bioceramics (HA, calcium phosphate).

Jongprateep and colleagues produced an aluminium/polymer composite scaffold using 3D printing technology. They designated this scaffold as having a cubic shape. Then, they coat the surface of the scaffold with HA to enhance its surface properties. They added HA to the scaffolds using the hydrothermal method. Consequently, the uncoated scaffolds exhibited a rough surface morphology with distinctive grains of aluminium. The average pore size and coating thickness of the scaffolds coated with 10, 15, and 20 vol% HA were observed to be 118.98–168.46 μm and 38.21–46.53 μm, respectively. The potential bioactivity of the covered scaffolds was then investigated. After being immersed in SBF for 28 days, the mass of the coated scaffolds improved by more than 10% (Jongprateep et al. 2022).

1.2.3.5. Alkali Hydrolysis

Alkaline hydrolysis is used to change the morphology and surface chemistry of polymers and initiates degradation on the surface of polymers (Baran and Erbil 2019). The rate of degradation of polymers through hydrolysis can be increased by using catalysts such as NaOH (Figure 9D). This degradation mechanism causes morphological changes on the surface and affects many properties of the material (such as hydrophilicity, biodegradability, and mechanical strength). In addition, the ester groups (-COO-) in the microstructure of PCL (Yaseri et al. 2023) are hydrolyzed by alkaline treatment to generate hydroxyl and carboxylic acid groups (Figure 10). Producing carboxylic acid groups on the PCL surface allows for more effective protein immobilization. In this way, it improves the activities of cells, such as cell adhesion and cell proliferation (Park JS et al. 2007; F. Chen, Lee, and Teoh 2007). Surface hydrolysis not only increases hydrophilicity but also increases surface roughness. Furthermore, *in vivo* investigations demonstrated that PCL-TCP scaffolds treated with NaOH showed a greater capability for bone formation compared to untreated groups (Yeo, Wong, and Teoh 2010).

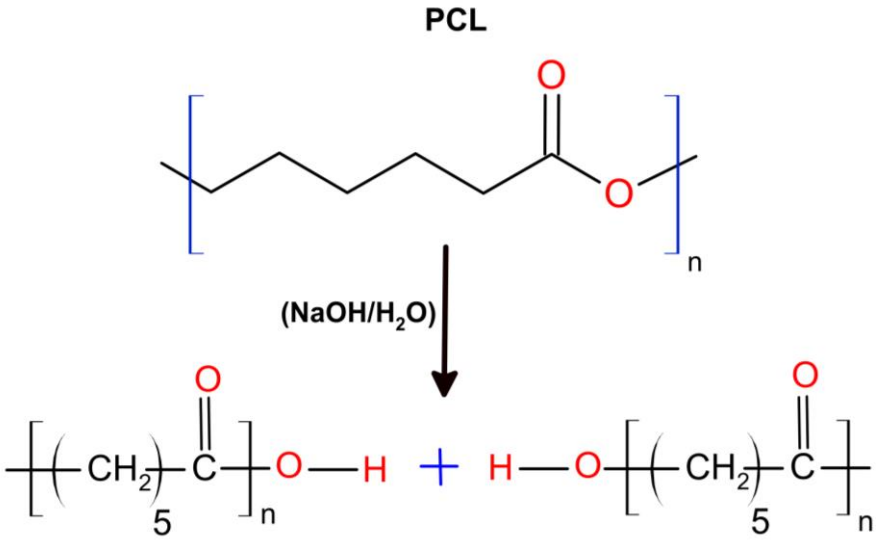

Figure 10. Chemical drawing of hydrolysis of PCL.

1.3. Thesis Outline, Aim and Objectives

In the scope of the thesis, it was aimed to develop and characterise the NaOH-treated emulsion templated 4PCLMA-based tissue engineering scaffolds. The main motivation for using NaOH hydrolysis as a surface modification technique is that it offers a practical, scalable, and cost-effective route without causing a significant change in the overall morphology. Accordingly, the objectives of the thesis are as follows:

- Synthesis of 4PCLMA with a high degree of methacrylation and characterization of 4PCLMA with nuclear magnetic resonance spectroscopy and gel permeation chromatography,
- Development of 4PCLMA-based PolyHIPEs with interconnected porosity,
- NaOH treatment of 4PCLMA PolyHIPE scaffolds and investigation of NaOH concentration and incubation time on the morphological characteristics of PolyHIPEs,
- NaOH treatment of 4PCLMA PolyHIPE scaffolds and investigation of NaOH concentration and incubation time on the surface chemistry and wettability of PolyHIPEs,
- NaOH treatment of 4PCLMA PolyHIPE scaffolds and investigation of NaOH concentration and incubation time on the mass change and mechanical characteristics of PolyHIPEs,
- Determination of the optimum NaOH concentration and incubation time with the criteria of resulting in hydrophilic material, causing less deteriorating effect on mass and mechanical strength,
- Investigation of surface area and protein adsorption capacity on selected groups in comparison with the control group (non-treated PolyHIPE),
- Investigation of cytotoxicity of developed matrices *in vitr*o with L929 cells,
- Investigation of cell attachment morphology, cell seeding efficiency and cell proliferation *in vitro* with Saos-2 cells on selected groups in comparison with the control group.

  The graphical abstract of the study is illustrated in Figure 11.

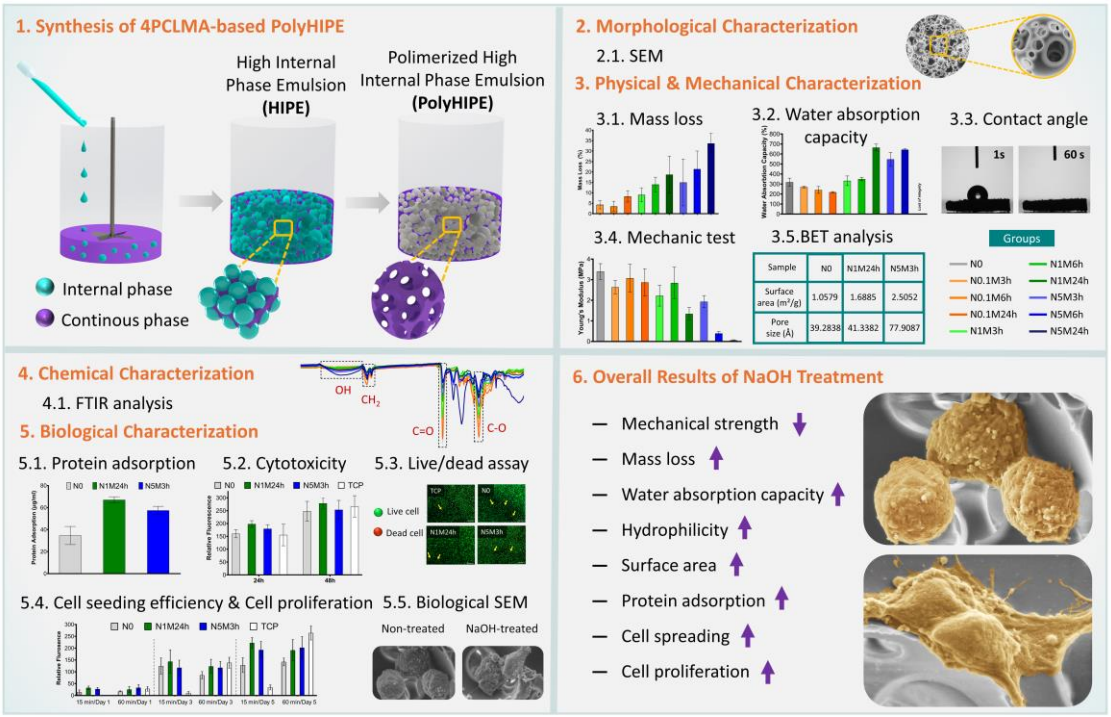

Figure 11. Graphical abstract of the thesis. Development and characterization of surface-modified 4PCLMA-based PolyHIPEs as tissue engineering scaffolds.

CHAPTER 2

MATERIALS AND METHODS

2.1. Materials

Pentaerythritol (98%), ε-caprolactone, trimethylamine (TEA), methacrylic anhydride (MAAn), tin(II) 2-ethyl hexanoate ($SnOct_2$), photoinitiator (diphenyl(2,4,6-trimethyl benzoyl)phosphine oxide/2-hydroxy-2-methylpropiophenone)) DCM, 37% hydrochloric acid (HCl), sodium chloride (NaCl), calcium chloride ($CaCl_2$), chloroform, toluene, sodium hydroxide (NaOH), potassium chloride (KCl), magnesium chloride hexahydrate ($MgCl_2.6H_2O$), monosodium phosphate (NaH_2PO_4), sodium bicarbonate ($NaHCO_3$), phosphate-buffered saline (PBS), trypsin, penicillin/streptomycin (PS), L-glutamine, glutaraldehyde, formaldehyde solution, resazurin salt, hexamethyldisilazane (HMDS) were all purchased from Sigma Aldrich. Dulbecco's Modified Eagle Media (DMEM) and fetal bovine serum (FBS) were purchased from Gibco™. Methanol, ethanol, and Pierce bicinchoninic acid (BCA) protein assay kits were obtained from Thermo Fisher Scientific. Calcein AM viability dyes and assay Kits (22002) were purchased from AAT Bioquest. Polydimethylsiloxane (PDMS) molds were produced using SYLGARD™ 184 Silicone Elastomer Kit. The surfactant Hypermer B246–SO-M was obtained as a sample from Croda. All ingredients were utilized without further purification unless otherwise indicated.

2.2. Methods

2.2.1. Synthesis and Characterization of 4PCLMA

2.2.1.1. 4PCL Synthesis

12 g pentaerythritol (0.088 mol) and 80.35 g caprolactone (0.705 mol) were added to a three-necked round-bottom flask. Then, the flask was heated to 160 °C using an oil bath. Nitrogen flow was introduced using one of the necks of the flask, and the system was mixed with the help of a magnetic stirrer (ISOLAB Laborgeräte GmbH) at 200 rpm. Then, 50 μL of tin (II) 2-ethylhexanoate (1.25 g/mL, 0.08 wt% monomer) was added from the middle neck of the round flask. Then, the pentaerythritol was let to dissolve completely in the system. Then, the system was left overnight to react to form the 4PCL. When the synthesis process was completed, after getting away from the oil bath, the system was left to cool at room temperature.

2.2.1.2. Methacrylation of 4PCL

300 mL of DCM was used to dissolve 4PCL. After that, 52.62 g TEA (0.52 mol) was added to the system. Then, 200 mL more of DCM was added, and all reactants were mixed using a magnetic stirrer. After mixing all reactants, the three-necked flask was submerged in an ice bath. 100 mL DCM was used to dissolve 80.22 g MAAn (0.52 mol). Subsequently, one drop of the resulting solution was added to the system each second using a dropping funnel. When the MAAn solution was introduced to the system completely, the system was taken out of the ice bath and left to react for 68 h at room temperature. 4PCL pre-polymer synthesis steps are illustrated in Figure 12A.

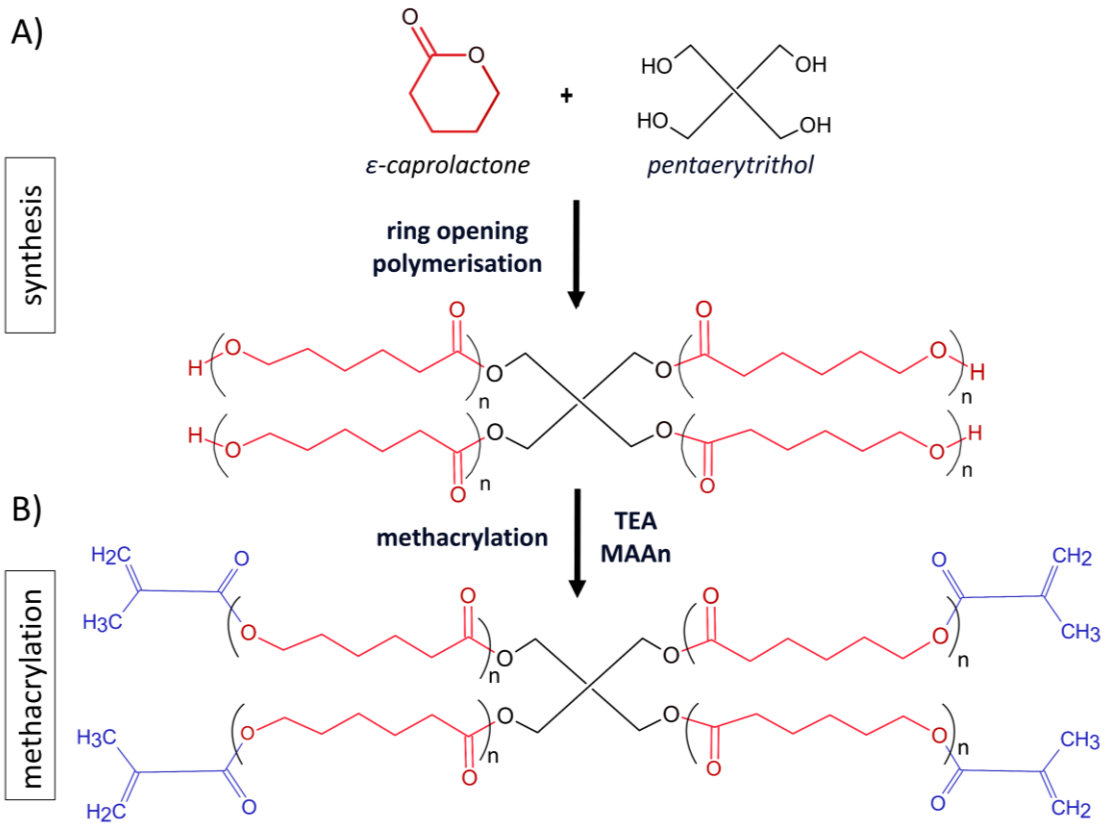

Figure 12. A) Synthesis of 4PCL pre-polymer via ring-opening polymerization, B) The methacrylate functionalization of hydroxyl end groups of PCL to form 4PCLMA pre-polymer.

Following the synthesis of the pre-polymer, the residual MAAn, TEA, and salts in the system were removed by washing with a concentrated hydrochloric acid (HCl) solution (1M, 1000 mL) prepared with deionized water (dH_2O). This process was repeated three times before washing with dH_2O three times. After the washing process, the remaining solvents were removed using a rotary evaporator (Heidolph Laborota 4000 Evaporator). The schematic of methacrylate functionalization of 4PCL pre-polymer and photos of pre-polymer synthesis steps are given in Figure 12B and Figure 13, respectively.

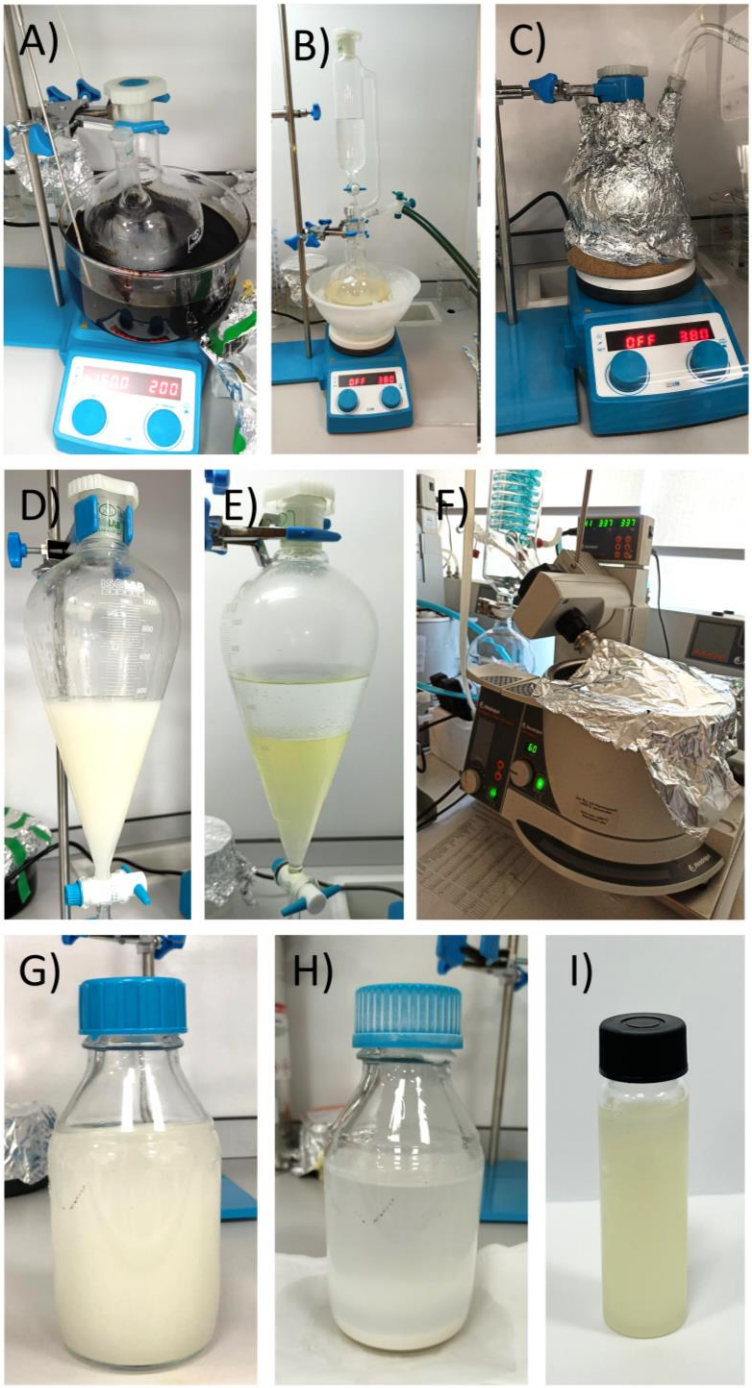

Figure 13. Synthesis steps of 4PCLMA pre-polymer.

The obtained 4PCLMA pre-polymer was transferred to the Duran bottle, and three methanol washes were applied, followed by the addition of approximately 500 mL of methanol. The bottle was kept at -80 °C until precipitation accumulated at the bottom. After that, the methanol was taken out and replaced by fresh methanol. This process was

repeated three times. After washing with methanol, the resulting pre-polymer was transferred to the one-neck flask. The remaining solvent was evaporated with the use of a rotating evaporator. At the end of these processes, the pre-polymer was obtained successfully and kept at -20 °C for use in future experiments.

2.2.1.3. Characterization of 4PCLMA

Proton (^{1}H) NMR spectroscopy analysis was carried out on a Varian INOVA NMR spectrometer at 400 MHz to verify the structure of the 4PCLMA pre-polymer. Deuterated chloroform ($CDCl_3$) was utilized as a diluent. MestReNova software was used to analyze the obtained spectra. The degree of methacrylation (DM) of 4PCLMA pre-polymer was calculated using the following equation.

$$DM = \frac{\int nonmethacrylated\ ends}{\int nonmethacrylated\ ends + \int methacrylated\ ends} * 100 \qquad (1)$$

Gel Permeation Chromatography (GPC) analysis was conducted at Sivas Cumhuriyet University to confirm the molecular weight and molecular weight distribution of the polymer. THF was utilized as a solvent. The solvent with 100 µL volume was injected with a flow rate of 1 mL/min. Both the detector and column temperatures were maintained at 35°C. Conventional calibration was used for the analysis (Malvern Viscotek GPCMax Model VE2001).

2.2.2. Preparation of HIPEs and Polymerization of HIPEs (PolyHIPEs)

The overall synthesis process of 4PCLMA-based PolyHIPE is shown in Figure 14.

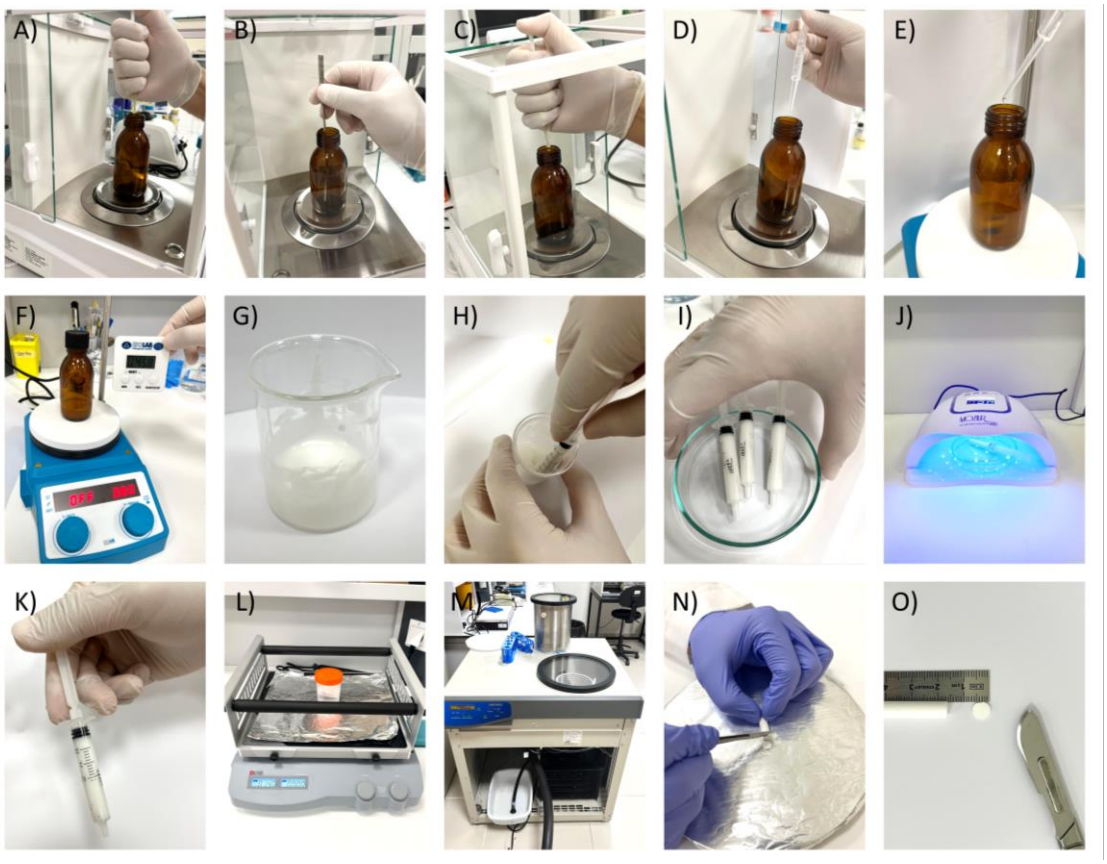

Figure 14. Synthesis process of 4PCLMA-based PolyHIPE via emulsion templating.

1.6 g of 4PCLMA pre-polymer and 0.16 g of surfactant (Hypermer B246) were added to a glass vial. Subsequently, the vial was heated to 40 °C to dissolve the surfactant and then allowed to cool. 2.4 g of the chloroform: toluene solvent mixture (80:20 (w/w)) was added to the vial. Photoinitiator (diphenyl (2,4,6-trimethyl benzoyl) phosphine oxide/2-hydroxy-2 methyl propiophenone) was added to the vial at a ratio of 10% of the polymer (w/w). Afterwards, the system was mixed at 375 rpm for 1 min at room temperature using a magnetic stirrer. After obtaining a homogeneous mixture, the emulsion (4PCLMA HIPE) was stirred for a further two minutes after 10 mL of water was added to the bottle drop by drop.

The resulting emulsion was put into syringes that have a 2.5 mL capacity and a 6 mm diameter, and all sides of the syringe were light polymerized for 1 min (4 min in total) using a light source (MOZIUR UV LED Nail Lamp M-10 MAX). A cylindrical monolith was isolated from the syringe. To remove the unpolymerized 4PCLMA, unused photoinitiator, chloroform, toluene, and surfactant, the resultant 4PCLMA PolyHIPE was

rinsed 100% methanol four times for a duration of 24 h each. After that, the samples were gradually switched from methanol to water (100% methanol, 75% methanol: 25% water, 50% methanol: 50% water, 25% methanol: 75% water, 100% water), and washed for 24 h in each solution. Following the washing procedure, samples were taken out of the water and stored at -20°C in the freezer. Subsequently, the porous structure of 4PCLMA PolyHIPE was dried under a vacuum for a day using a lyophilizer (LABCONCO FreeZone Console Freeze Dry System) to prevent any collapse. A scalpel was used to cut pieces of the dried cylindrical samples that were ~500 μm thick.

2.2.3. Determination of Porosity

The porosity of PolyHIPEs was determined using Equation 2. The volume and mass values of the samples were measured to calculate the densities of PolyHIPEs. The volume and mass value of the polymer were also measured to calculate its density. The porosity of the 4PCLMA-based PolyHIPE scaffolds was calculated. Three repeated measurements were carried out.

$$Porosity\ (\%) = \left(1 - \frac{\rho_{\text{PolyHIPE}}}{\rho_{\text{PCLMA}}}\right) x100 \quad (2)$$

2.2.4. Development of Alkali Treated 4PCLMA-based PolyHIPEs

2.2.4.1. NaOH Treatment of 4PCLMA-based PolyHIPEs

Freeze-dried samples were re-wetted by transferring them into 100% methanol, 75% methanol: 25% water, 50% methanol: 50% water, 25% methanol: 75% water and then 100% water, respectively, to completely immerse in water. NaOH (molecular weight

(M_w) 39.997 g/mol) solutions with various concentrations (0.1 M, 1 M, and 5 M) were prepared using dH_2O. PolyHIPE samples were taken out of the water and then immersed in NaOH solutions at three different concentrations for three different incubation periods (3 h, 6 h, and 24 h). For this process, Eppendorf tubes with a capacity of 1.5 mL were used, and 1 mL NaOH solution was placed in these containers. Samples were incubated at room temperature and under static conditions. After NaOH incubation, the scaffolds were removed from the containers, washed with dH_2O three times and placed for 1 h in a freezer (-20 °C). After that, they were transferred to the lyophilizer and dried under a vacuum for a day.

2.2.4.2. Nomenclature of 4PCLMA-based PolyHIPEs

Nine groups of scaffolds were fabricated to investigate the impact of NaOH concentration and incubation period on the characteristics of PolyHIPEs. Additionally, non-treated 4PCLMA PolyHIPE was used as a control group. Each group is designated using a nomenclature of the form NMh, where 'N' denotes the NaOH treatment, 'M' signifies the molarity of the NaOH, and 'h' represents the incubation time. The control group was identified as 'N0'. For example, the designation 'N0.1M3h' corresponds to a PolyHIPE sample that underwent treatment with 0.1 M NaOH for a period of 3 h.

2.2.5. SEM Analysis

SEM analysis was performed to examine the morphological structure and surface features of NaOH-treated and untreated 4PCLMA PolyHIPE scaffolds. Vertical sections were taken from NaOH-treated and untreated scaffolds using a scalpel. These sections were fixed to aluminium pins glued to carbon pads to examine the microstructure of 4PCLMA-based PolyHIPEs. The samples were coated with gold for 1 min at 15 kV to increase the conductivity. Then, the scaffolds were examined using an SEM (FEI QUANTA 250 FEG), and images were recorded at different magnifications.

ImageJ Software was used to analyze SEM images. Measurements were taken by randomly selecting 50 pores and 100 windows. The pore measurements were corrected for the underestimate of diameter using a statistical correction factor ($2/\sqrt{3}$). The average pore size (D) was divided by the average window size (d) to determine the degree of interconnectivity (DOI) value. The open surface area was divided by the total surface area to calculate the degree of openness (DOO) value (Carnachan et al. 2006). To display the pore and window size distribution of the scaffolds, histograms of the diameters of the pores and windows were created (Pulko et al. 2010).

2.2.6. Chemical Characterization of Scaffolds Using Fourier-transform Infrared Spectroscopy (FTIR) Analysis

The chemical structures of PolyHIPE scaffolds treated with NaOH were investigated using Fourier Transform Infrared (FTIR) spectroscopy. Samples were prepared for FTIR analysis, as explained in Section 2.2.2. Each sample was placed on a multi-bounce ZnSe crystal. FTIR spectra were carried out on a Spectrum Two FT-IR Spectrometer (PerkinElmer) combined with a Universal Attenuated Total Reflectance Accessory (UATR) internal reflection module. The transmittance was measured using 20 scans with a resolution of 4 cm^{-1} in the range of 4000 to 400 cm^{-1}. The experiment was carried out using PerkinElmer Spectrum Software (Version 10.5.2). The spectra of samples were processed using Origin 2024b software.

2.2.7. Determination of Mass Change

This work package aims to investigate the degradation ratio of scaffolds treated with different concentrations of NaOH and different incubation times. For this purpose, changes in the masses of the scaffolds after treatment with NaOH were determined. The scaffolds were weighed using a balance (Weightlab WSA-224) before (m_1) and after (m_2)

the NaOH treatment, and the mass change was calculated using Equation 3. Three scaffolds were used for each group. All measurements were performed in triplicate.

$$Mass\ change\ of\ scaffolds\ (\%) = \frac{m_1 - m_2}{m_1}\ x\ 100 \quad (3)$$

2.2.8. Water Absorption Capacity

Swelling tests were performed to determine the water absorption capacity of PolyHIPE scaffolds. Firstly, the dry weights (W_d) of the samples were measured and recorded. Then, the scaffolds were placed in dH_2O at room temperature for swelling testing. Samples were taken out at regular intervals, and filter paper was used to carefully remove excess liquid that was on the surface. The weights of the wet samples were measured and noted (W_w). Equation 4 was used to determine the degree of swelling (water absorption capacity). Three measurements were carried out from each sample group with three replicates.

$$Swelling\ Capacity\ (\%) = \frac{W_w - W_d}{W_d}\ x100 \quad (4)$$

2.2.9. Water Contact Angle

The contact angle experiment was carried out to evaluate the hydrophilicity of the scaffolds. For this purpose, 5 µL of a water droplet was dropped onto the surface of PolyHIPE scaffolds. Then, water contact angles were determined using a contact angle measuring device (KSV Attension brand Theta) under laboratory conditions. The images from 1 s to 60 s were recorded, and the contact angle of 4 time points (1 s, 10 s, 30 s and

60 s) was calculated. Three repeated measurements were performed from each group. The contact angle measurement set-up used in contact angle measurements of PolyHIPE scaffolds is shown in Figure 15.

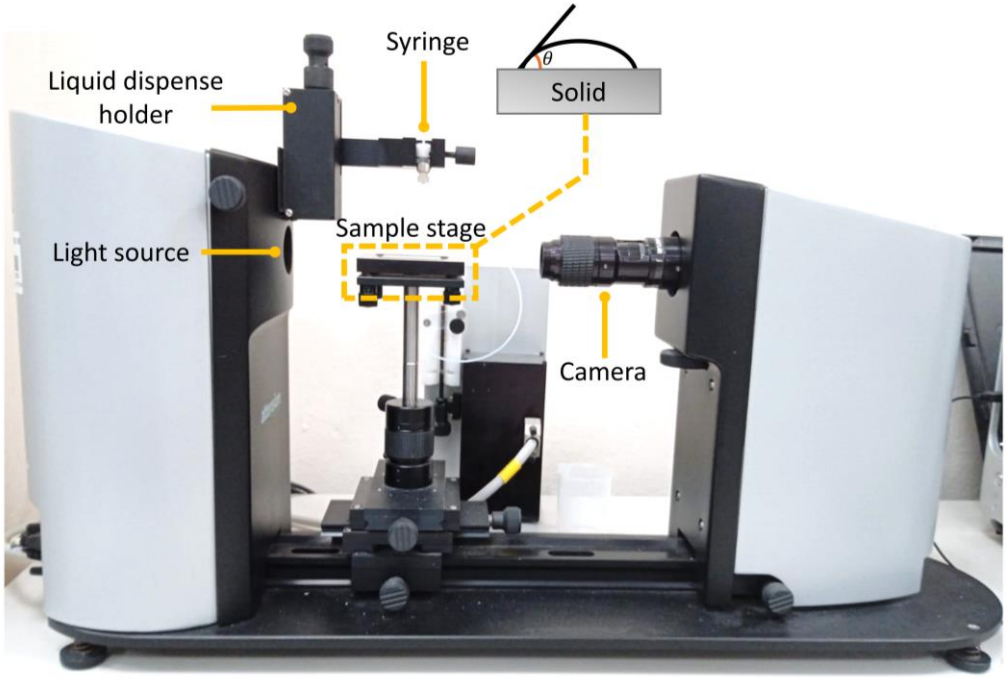

Figure 15. The contact angle measurement set-up.

2.2.10. Mechanical Characterization

The compression test was performed to evaluate the effect of NaOH treatment on the mechanical properties of 4PCLMA-based PolyHIPE scaffolds. The tests were conducted following the modified version of the American Society for Testing and Materials standard (ASTM). For compression tests, 10 mm x 6 mm cylindrical moulds were fabricated. Polydimethylsiloxane (PDMS) was used to obtain the cylindrical moulds. An elastomer and crosslinking agent were mixed by using a ratio of 10:1 (w/w) to prepare PDMS and placed in a petri dish with a height of 6 mm. Then, a vacuum pump was used to remove air bubbles in the resulting mixture. Finally, the mixture was cured

at 65°C for 4 h. Molds were obtained from the cured PDMS with the help of a biopsy punch with a diameter of 10 mm. Then, prepared HIPEs were transferred into the cylindrical moulds. After that, HIPEs were photo-polymerised for 2 min for each side (4 min total). A mechanical test device (SHIMADZU Scientific Instruments EZ-LX) with a 100 N load cell was used to perform the compression test. The compression test was set at a rate of 1 mm/min, with a maximum load of 95 N and a strain limit of 60%. The diameter and height of all samples were measured before the experiment.

Force displacement data was obtained as raw data as a result of the experiment. Stress-strain data is obtained from force-displacement data using Equation 5, where F is the applied force to the sample, A is the cross-sectional area where the force is applied, and Equation 6, where ΔL is the displacement of the sample and L_0 is the initial length of the sample.

$$Stress = \frac{F}{A} \tag{5}$$

$$Strain = \frac{\Delta L}{L_0} \tag{6}$$

Young's Modulus was calculated using the linear area of this stress-strain chart. The slope of the line of the linear area of the stress-strain graphic gives the compression modulus of the samples (Corti et al. 2019). 5 samples were used for each group. Compression modulus was calculated according to Equation (Biron 2016). where E is compression modulus, σ is the applied compressive stress, and ε is the strain.

$$E = \frac{\sigma}{\varepsilon} \tag{7}$$

2.2.11. Brunauer-Emmett-Teller (BET) Analysis

BET analysis was performed to determine the effect of NaOH treatment on the surface area and porosity of 4PCLMA-based PolyHIPE scaffolds. BET analyses were performed for the N0, N1M24H and N5M3H groups. All samples were placed in glass sample holders and degassed at 250 °C for 12 h. Following this, the samples were rapidly cooled to −196 °C. The surface area of the scaffolds was evaluated through nitrogen adsorption at 77 K using a Micromeritics Gemini V analyzer. The specific surface areas of the materials are determined by fitting the adsorption isotherms using the BET model (Hong, Wang, and Liu 2024).

2.2.12. Protein Adsorption

The Pierce BCA protein assay was utilized to examine the impact of NaOH treatment on the ability of PolyHIPE scaffolds to bind proteins. First, 0.1% (*w*/*v*) bovine serum albumin (BSA) solution was prepared using a 2 mg/mL concentration of BSA stock solution. Then, three experiment groups (N0, N1M24h and N5M3h) and four scaffolds from each group were used for the protein adsorption test. Additionally, three scaffolds from each group that had not been incubated in BSA solution were used as blanks in the experiment. The scaffolds were transferred to 48-well plates using forceps in a biological cabinet. After that, 0.1% BSA solution was added to the well, and the incubation was allowed for 24 h at 37 °C. Following the incubation period, the scaffolds were taken out of the well plates. 25 µL of the solution in each well was taken and transferred to 96 well plates. The working agent was prepared using Reagent A and Reagent B (50:1). The working agent (200 µL) was transferred to 96 well plates. After that, well plates were put in the incubator and left for 30 min at 37 °C. A spectrophotometer was used to measure the absorbance at 562 nm (Tamburaci and Tihminlioglu 2018).

2.2.13. Biological Characterization

2.2.13.1. General *In Vitro* Cell Culture

A mouse fibroblast (L929) cell line was utilized to perform cytotoxicity testing of scaffolds following the ISO standards (ISO 10993-5:2009, Biological evaluation of medical devices) (Nedeljkovic et al. 2022; Koymen et al. 2022). The L929 cell line originates from the subcutaneous areolar and adipose tissue of a 100-day-old male C3H/ mouse (Lackner et al. 2013). For monolayers, the average doubling time of this cell line was calculated as 21 h (Torabi et al. 2023). This cell line is a standard for cytotoxicity tests.

Assays for cell proliferation and seeding efficiency were conducted using the Saos-2 cell line. Saos-2 is a human osteosarcoma cell line. This cell line was isolated from the primary osteosarcoma of an 11-year-old white girl in 1975 (Fogh, Wright, and Loveless 1977). An adult osteoblast phenotype is seen in these cells. Saos-2 synthesizes collagen with a structure similar to that of primary human osteoblast cells (Fernandes et al. 2007). The Saos-2 cell line can differentiate like osteoblasts and has an average doubling time of approximately 45.7 ± 3.3 h. These properties make it a useful model for bone biology and bone tissue engineering studies. For this reason, the Saos-2 cell line is frequently utilized in tissue engineering, mainly due to its osteoblastic (bone-forming) properties (Xu and Liu 2023).

The cryopreserved Saos-2 cell line between P22 and P23 and the L929 cell line between P21 and P22 were taken out from the liquid nitrogen tank. Then, cryovials were soaked in a 37 °C water bath until two-thirds of the ice melted. The cells were thawed gently in a fresh medium and taken from the cryovials. After that, it was put into centrifuge tubes and centrifuged at 1550 rpm for 5 min. Subsequently, supernatants were discarded, and the cell pellets were re-suspended in high glucose DMEM (4.5 g/L) supplemented with 10% FBS and 1% PS and transferred to T-75 cell culture flasks. Following that, the flasks were placed in an incubator with a humidified environment, 5% CO_2, at 37 °C. The culture was continued until the cell confluency reached 90%, and the medium was changed with a new fresh medium every 2-3 days.

2.2.13.2. Scaffold Preparation for Cell Culture

PolyHIPE discs were prepared, as explained in Section 2.2.2. Then, they were incubated in 70% ethanol in a biological safety cabinet for 2 h for disinfection. Afterwards, PBS was gradually added to the scaffolds to ensure the exchange of ethanol with PBS. Finally, when completely switched to PBS, washing was repeated three more times with PBS. Scaffolds were not conditioned either in media or in FBS. The tests for cytotoxicity and cell proliferation were conducted using scaffolds with a diameter of around 2.5 mm, and 6 mm were used for the cytotoxicity test and cell proliferation test, respectively.

2.2.13.3. Direct Cytotoxicity Test

2.2.13.3.1. Alamar blue Assay

The cytotoxicity tests were performed following the procedures outlined in ISO 10993-5:2009, which is the standard for the biological evaluation of medical devices, especially focused on *in vitro* cytotoxicity tests. For the cytotoxicity tests, a L929 cell line was used following the guidelines. L929 cells are widely used in cytotoxicity testing because of their reproducible growth rates and high biological responses (such as biocompatibility, cell attachment, cell proliferation and cell differentiation) (Meneses et al. 2020; Ozdemir, Yilmaz, and Yilmaz 2009; Wadajkar et al. 2014).

A direct contact test was performed to determine the cytotoxicity of NaOH-treated scaffolds on the cells. Cytotoxicity testing was performed in 48 well plates and tested with five samples from each group. A concentration of 30.000 cells/mL was seeded in each well in 48 well plates and incubated for 1 day. They were subjected to PBS for washing after the first day, and new media was used. The scaffolds were taken from PBS using forceps and placed in the wells containing the cells, and they were incubated for 1 more day. Following the period of incubation, the scaffolds were taken out of the well

plates, and the cell viability was investigated using the resazurin reduction assay (RR, Alamar blue assay). The resazurin assay is an easy, quick, and accurate test to check the viability of bacteria and mammalian cells. Living cells have a metabolic activity and, using mitochondrial reductase enzymes, reduce resazurin (non-fluorescent dye, blue) to resorufin (strong fluorescent dye, pink) (Figure 16) (O'Brien et al. 2000).

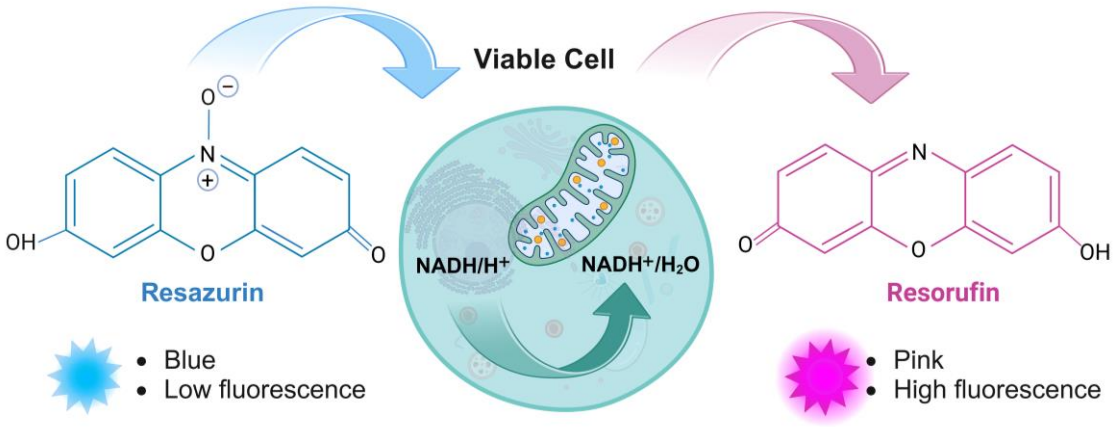

Figure 16. Resazurin is enzymatically converted to resorufin in living cells.

For this experiment, firstly, 1 mM resazurin (M_w: 251.17 g) stock solution was prepared in dH_2O and filtered. A growing medium was used to dilute the 1 mM resazurin stock solution to 100 µM under aseptic conditions to obtain the working solution. Then, media was aspirated from the well plates, and PBS was used to wash the wells. After adding the Alamar blue working solution, the solution was incubated for 4 h. After the incubation period, the reduction solution in each well was transferred to 96-well plates in triplicate. Finally, fluorometric measurements (540 nm and 635 nm) were performed using a spectrophotometer (Thermo Scientific™ Varioskan Lux Multimodal Microplate Reader) for the solutions in a 96-well plate.

2.2.13.3.2. Live & Dead Assay

NaOH-treated scaffolds were tested for cytotoxicity using a live/dead assay on the cells. The 48 well plates were seeded with L929 fibroblasts at a density of 3 x 10^4 cells/mL and incubated for one day at 37 °C, 5% CO_2, and a humidified environment. Subsequently, 1 mL of new media was added after the old media was removed. Afterwards, the scaffolds prepared to correspond to one-tenth of the surface area of the wells were taken into the well with the help of forceps and then incubated for 24 h in an incubator at 37 °C, 5% CO_2, and a humidified environment. At that, the media was discarded, and the scaffolds were taken from the well plate. The dye solution was prepared using 1 mM Calcein-AM, and 1 μg / ml PI was put into the well and left the incubation for 30 min (X. Wang et al. 2023). After the incubation period, a fluorescence microscope (Zeiss ApoTome.2) was used to examine the results. All procedures were carried out in a dark environment. The experiment was performed with triplicates.

2.2.13.4. Cell Seeding Efficiency and Cell Proliferation

2.2.13.4.1. Cell Seeding to Scaffolds

Cells that reached at least 90% confluence were detached from the surface by trypsinization and suspended in a fresh medium. Neubauer cell counting slide was used to count the cells. The cells were placed in centrifuge tubes and centrifuged at 1550 rpm for 5 min. After centrifugation, the supernatant was discarded. Then, the cells were prepared by re-suspending them in fresh media at a concentration of 3 x 10^4 cells/8 μL. The scaffolds were transferred to 48-well culture plates under aseptic conditions as one scaffold per well, and 8 μL of cell suspension was homogeneously transferred to each scaffold. After cell seeding, the well plates were left in the incubator for 15 min or 60 min to examine the cell seeding efficiency of the cells on the scaffolds. After that, non-adhered cells were removed from the scaffolds with PBS washing. Afterwards, the cells

were cultured for 5 days after 1 mL of new media was added to each well. Meanwhile, the medium was changed to a fresh medium every 2-3 days.

2.2.13.4.2. Initial Cell Attachment Behaviour

The initial cell attachment behaviour was investigated using SEM to examine the impact of the NaOH treatment. For this purpose, Saos-2 cells were seeded onto N0, N1M24h, and N5M3h PolyHIPE scaffolds at the concentration of 3 x 10^4 cells/8 μL. Then, the scaffolds were left to incubate in the incubator for 1h. Then, fresh medium was added, and the scaffolds were incubated in the incubator for 3h more. Following a 4 h incubation period, non-adhered cells were removed from the scaffolds with PBS washing. Then, the scaffolds were fixed in 2.5% glutaraldehyde, as described in Section 2.2.13.5, to preserve cell morphology and examine cell attachment behaviour using SEM.

2.2.13.4.3. Cell Seeding Efficiency and Cell Proliferation

The metabolic activities of the cells cultured on PolyHIPE scaffolds were evaluated using the Alamar Blue test. In 48-well culture plates, after adding 1 mL of RR solution to each well, the scaffolds were transferred to the wells with the help of forceps. Cell culture well plates were placed in an incubator, protected from the light, and incubated for 4 h at 37 °C. 200 μL of the reduced solution in triplicate from each well was transferred to 96-well culture plates at the end of the incubation time. The scaffolds were subjected to PBS washing, a fresh medium was added, and incubation was continued for subsequent analysis. RR analysis was performed on days 1, 3, and 5 using four fresh scaffolds for each time point, and four scaffolds without cells were used as blanks. Using a spectrofluorometer, the resulting reduced solutions were measured three times at 540 nm and 635 nm for excitation and emission, respectively.

2.2.13.5. Biological SEM

The adherence and spreading morphologies of cells on PolyHIPE scaffolds were investigated using SEM. Before examining with SEM, a water removal protocol was applied to biological samples. The scaffolds were subjected to PBS washing three times after the discarding of the culture medium. After that, the scaffolds were fixed for 1 h at room temperature in 2.5% glutaraldehyde to keep the cell morphology. Afterwards, the scaffolds were subjected to PBS three times and 15 min each. Following the PBS wash, a dH_2O wash (5 min) was performed. Following the water wash, serial ethanol washes (35, 60, 80, 90 and 100%) were performed for 15 min each to dehydrate the samples. Following ethanol washes, the scaffolds were exposed to HMDS, a drying agent. The samples were treated for 1 h with HMDS/ethanol (1:1) and then for 5 min with 100% HMDS. The scaffolds were finally allowed to air-dry for the overnight. An SEM (FEI QUANTA 250 FEG) device was utilized to examine the morphologies of the dried PolyHIPE scaffolds. To increase conductivity, the samples were first coated with gold for 45 sec at 15 kV. (Aldemir Dikici, Reilly, and Claeyssens 2020). Then, micro images of the samples were recorded at different magnifications.

2.2.14. Statistical Analysis

GraphPad Prism Software (GraphPad Prism Version 9.3.0 for Windows, California USA) was used to analyze the data. Mean values are reported as ± standard deviation. Statistically significant differences between experimental groups were determined using the ANOVA test for multiple comparisons. Comparisons with a p-value less than 0.05 were considered significant statistical differences and indicated on the graphs.

CHAPTER 3

RESULTS & DISCUSSIONS

3.1. Synthesis and Characterization of 4PCLMA

Following synthesis, the structure and DM of the resultant pre-polymer were verified using ^{1}H NMR spectroscopy. The methylene groups neighbour to the hydroxyl end groups in the structure of 4PCL correspond to the peak that is seen at 3.6 ppm. The number of groups corresponding to this peak decreases in 4PCL as it is converted into methacrylate groups by the methacrylation process. This decreasing peak transforms into groups corresponding to the peaks at 1.9, 5.5, and 6.1 ppm. In the 4PCL structure, these peaks do not appear, but they appear only in the 4PCLMA structure. The peaks here, corresponding to values of 1.9, 5.5, and 6.1, confirm that the methacrylation reaction successfully occurred (Figure 17). The ^{1}H NMR analysis results of the previously synthesized and reported PCL methacrylate-related studies also confirm the result of the 4PCLMA structure obtained in this study (Field et al. 2021). DM of 4PCLMA pre-polymer was calculated using the integrals of these peaks and found to be 96.5%. Methacrylation time and the amount of MAAn and TEA have a direct effect on DM. In our study, a DM of pre-polymer was obtained ~100% by using a 68 h reaction time. Field *et al.* synthesised PCL tri-methacrylate polymers with different DMs by varying the reaction parameters (methacrylation time, MAAn and TEA amount). They showed that DM is directly affecting the mechanical properties of the polymer (Field et al. 2021). In this study, we aimed to obtain maximum DM, as polymers with higher DM show higher mechanical strength, and the scaffold was designed to be used in bone tissue engineering.

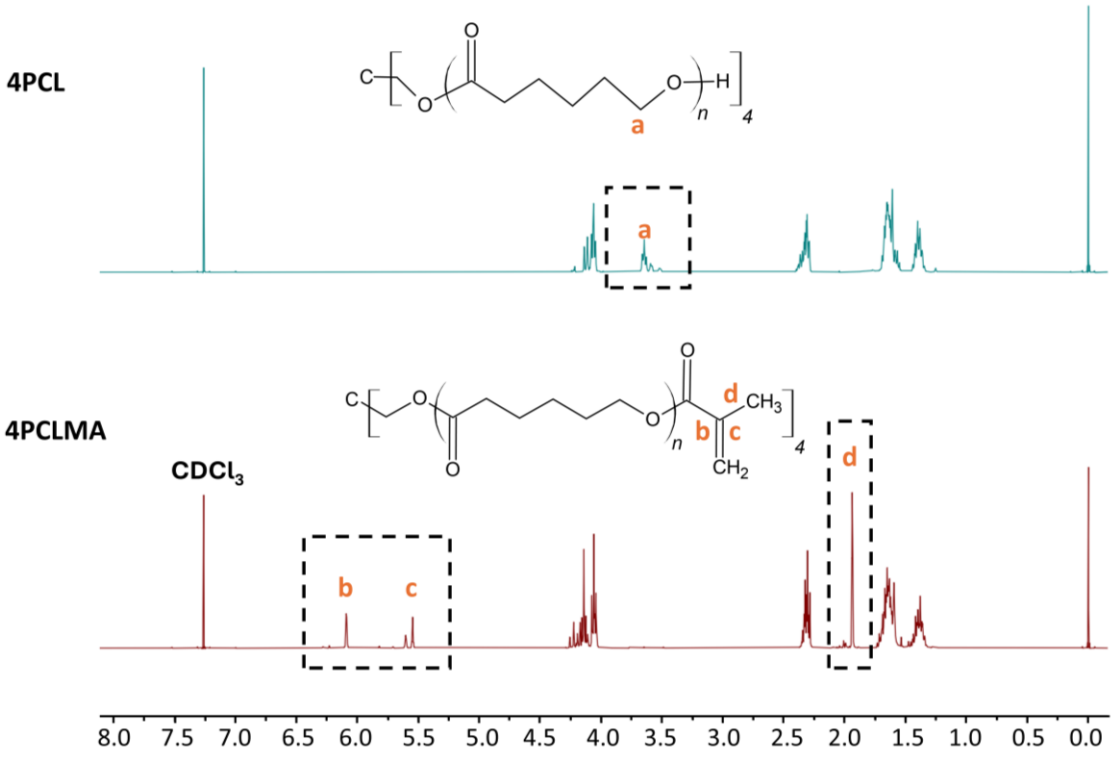

Figure 17. The ^{1}H NMR spectra and chemical structure of 4PCL and 4PCLMA.

When chemicals used in the synthesis were considered, the theoretical M_w of 4PCLMA was calculated as 2266 g/mol. GPC results showed that the M_w value of this polymer was 2069, and the M_n value was 1771 g/mol. The polydispersity index (PDI) was 1.17 (M_w/M_n). The molecular mass distribution in each polymer sample was measured by PDI. It is calculated as the ratio of the average molecular to the average molecular weight (M_n). The PDI value provides a sense of the uniformity of polymer chains. When the PDI value is 1, the polymer sample is monodispersed, meaning all polymer chains have the same molecular weight. In cases where the PDI value is more than 1, it causes a wider distribution of molecular weights in the polymer sample. A higher PDI indicates that the polymer has a wider molecular weight range, which affects the mechanical and physical properties of the polymer (Whitfield et al. 2019).

3.2. Preparation of HIPEs and PolyHIPEs

While preparing the HIPEs, during the emulsification process, no observable phase separation was detected at any stage until the polymerization. Once water incorporation was initiated, the transparent polymer gradually turned into an opaque white colour. The final emulsion has a mayonnaise-like consistency and viscosity. 74% water was incorporated into the emulsion composition as an internal phase. After the polymerization of HIPE and drying of PolyHIPE, the porosity was measured as 68.0 ± 0.4%. As the incorporated water amount was responsible for porosity, the porosity value was expected to be close to the internal phase volume. However, porosity was found to be around 8% lower than the internal phase volume. This is likely due to the shrinkage of the PolyHIPE after cross-linking the polymer and drying the sample (J. H. Chen, Le, and Hsu 2018; Ovadia and Silverstein 2016). After cross-linking and drying, shrinkage was observed in each dimension of the samples. Figure 18 shows the cross-section of 4PCLMA-based PolyHIPE at different magnifications. PolyHIPEs have interconnected and homogeneous porosity and open cellular architecture. Cells can establish pathways for nutrients and waste owing to their porosity and interconnected structure of PolyHIPE. The interconnectivity of the scaffolds is essential for cell infiltration, tissue integration, and vascularization (Lyu, Yu, and Chen 2016; Somo et al. 2015). No microstructural collapse was noticed in the scaffolds' SEM images. Qualitative information can be obtained from the SEM images. The pore and window diameter can be obtained using software such as ImageJ, which measures them manually. However, the measurements taken manually have a very high margin of human error, making multiple measurements challenging. To avoid these disadvantages, Karaca and her colleagues developed a deep learning model (Pore D^2) that enables the automated measurement of the morphological features of emulsion-templated scaffolds. With the help of this deep learning model, errors resulting from manual measurements can be minimized, and rapid measurement is achieved (Karaca and Aldemir Dikici 2024).

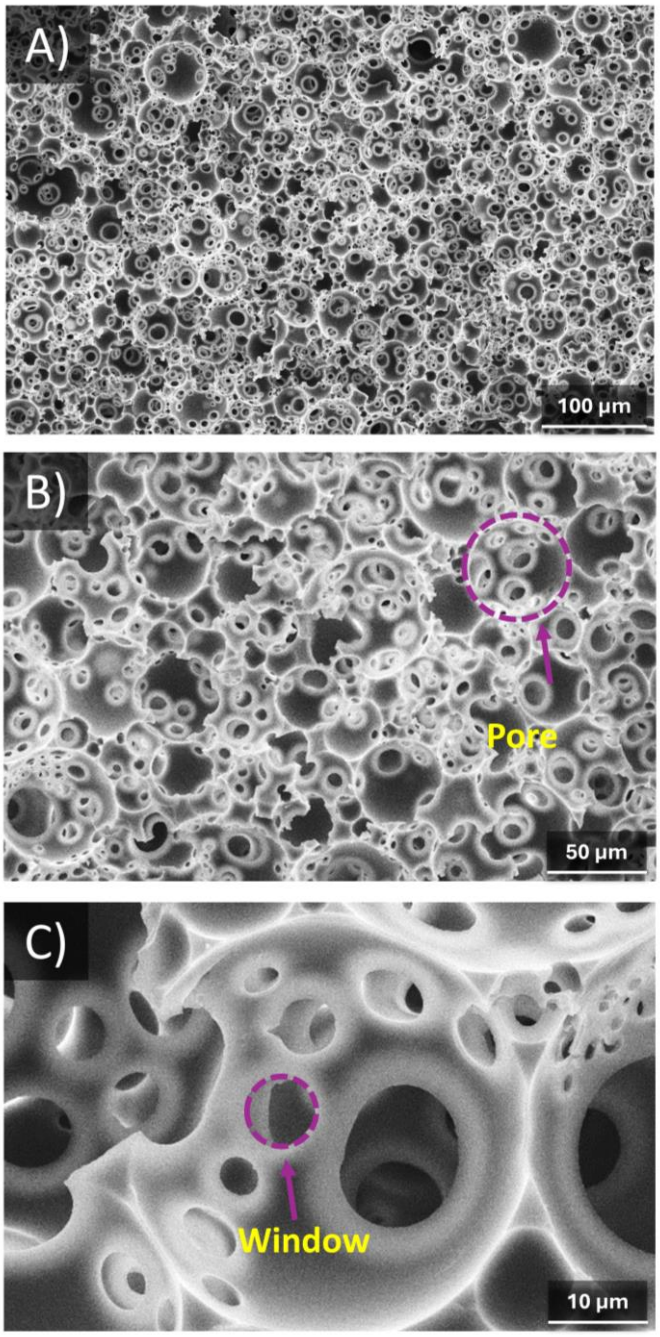

Figure 18. SEM images of non-treated PolyHIPEs emphasizing A) the overall morphology, B) pore, and C) window architectures, respectively.

In this study, ImageJ software was used to estimate the pore and window diameters of the scaffolds using the SEM images. The PCL PolyHIPE disk has varied pore diameters ranging from 7 to 66 µm. The average pore diameter (D) has been determined to be 22 ± 12 µm (Figure 19A). The window sizes of PolyHIPE are obtained

between 1-17 µm, and 3.7 ± 2.7 µm was found to be the average window size (d) (Figure 19B), giving the d/D of 0.16.

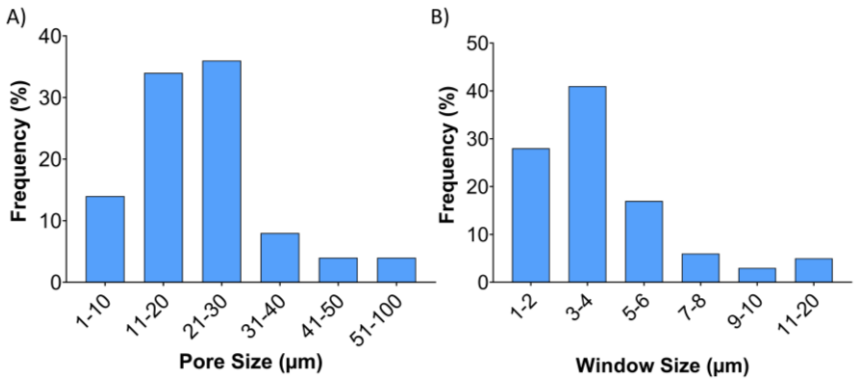

Figure 19. Histograms of A) pore size and B) window size of the PolyHIPE scaffolds.

In an earlier study, the same solvent combination (80:20 chloroform: toluene (w/w)) was used, and the average window size and pore size were determined to be 4 ± 2 and 20 ± 7 µm, respectively (Aldemir Dikici et al. 2019). The DOI value was found to be 0.17, and the DOO value was found to be 0.05. This value should be considered during the scaffold fabrication. This value affects the open area within the walls, and increasing this value causes a decrease in the mechanical strength (Kravchenko et al. 2018). The properties of non-treated 4PCLMA-based polyHIPEs are shown in Table 5.

In tissue engineering scaffolds, pore and window diameter are critical (J. Li et al. 2022). Porosity and interconnectivity affect the settlement of cells into scaffolds, the transport of nutrients and waste products, and biocompatibility (Loh and Choong 2013). A study on porous implants noted the pore sizes required for significant bone growth. According to this study, it was revealed that the minimum pore size is 75-100 µm, and the optimum range is 100-135 µm (Klawitter et al. 1976). Subsequently, studies have suggested that the pore size should exceed 300 µm for bone formation and vascularization. However, pores larger than 300 µm cause osteogenesis, while pore size smaller than 300 µm promotes osteochondral ossification. Furthermore, by increasing the void volume, large porous could affect the mechanical properties of scaffolds, so an increase in pore size may not always be advantageous (Klawitter et al. 1976). We found that the average pore size in our study was around 22 µm. It has been observed during *in*

vitro studies that the current pore size value does not restrict early cell adhesion and growth. Conversely, it might limit cell penetration in long-term culture. The composition that our group had previously produced was used to obtain the PolyHIPEs utilized in this study. However, during our other studies, different compositions that increase porosity and have a positive effect on morphology have been developed. The impact of the NaOH treatment on the resulting PolyHIPEs was assessed as part of this study. In subsequent studies, this approach, which was developed as a proof-of-concept by performing optimization studies, will be applied to scaffolds with higher pore sizes.

In emulsions, different parameters affect pore and window diameters. The concentration of the polymer used affects the size and pore distribution of the pores. The volume of the proportion of the internal phase affects the pore size. In addition, the type and number of surfactants used when creating emulsions also affect the pore structure. Considering all this, the desired porosity and connectivity can be achieved by changing these parameters (Aldemir Dikici and Claeyssens 2020).

When the emulsion is formed during the production of PolyHIPE, the internal phase droplets are dispersed in the continuous phase, and this structure initially has a very high porosity. Because the solvent is still present in the system before polymerization, the porosity of the emulsion is initially at least 74%, as calculated by the ratio of the internal phase volume to the total volume. Afterwards, when the continuous phase is solidified by the polymerization process, the solvent is washed away from the system after polymerization. At this stage, shrinkage occurs with the removal of the solvent. After solvent elimination, the final porosity of the porous structure is identified as PolyHIPE porosity (68%). Due to shrinkage, the final porosity becomes lower than the initial porosity, as shown in Table 5.

Table 5. Morphological properties of non-treated 4PCLMA-based PolyHIPEs.

$D_{average}$ (µm)	**$d_{average}$ (µm)**	**DOI (d/D)**	**DOO**	**$\rho_{Polymer}$ (g/cm^3)**	**Internal phase (%) (w/solvent)**	**Internal phase (%) (w/o solvent)**	**Porosity (%)**
22±12	3.7±2.7	0.17	0.05	1.05	63	74	68

3.3. Development of Alkali Treated 4PCLMA-based PolyHIPEs

Alkali treatment of the scaffolds with NaOH is a process performed to change the surface properties of the polymeric materials (Schneider et al. 2020; Jaidev and Chatterjee 2019; Abdul Hamid, Tham, and Ahmad 2018). These modifications can significantly improve the integration of biomaterials with biological tissues and increase cell-material interaction (Smith et al. 2007). Accordingly, in this study, NaOH treatment was performed on 4PCLMA-based PolyHIPE scaffolds with three different NaOH concentrations (0.1 M, 1 M and 5 M) and three different incubation times (3 h, 6 h and 24 h). When NaOH interacts with the polymer, it breaks the ester bonds in the polymer backbone and reveals hydroxyl and carboxylic acid groups on the surface (Tham et al. 2014). The chemical drawing of NaOH hydrolysis is shown in Figure 20.

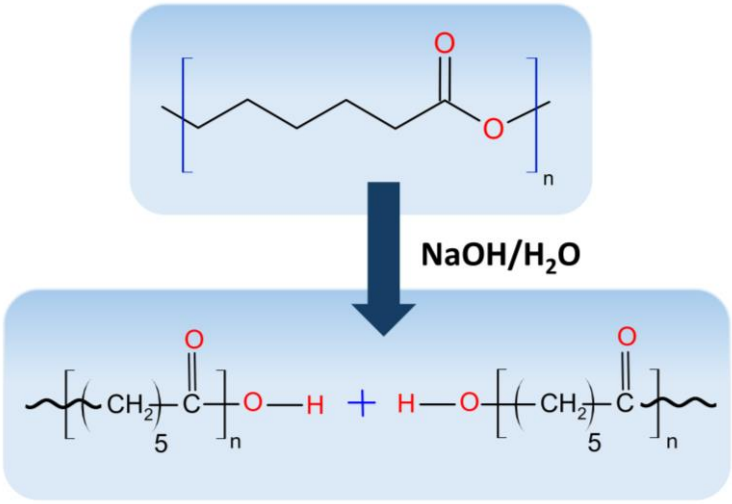

Figure 20. NaOH hydrolysis of PCL.

3.4. Chemical Characterization of Scaffolds Using FTIR Analysis

The functional groups of 4PCLMA-based scaffolds after surface modification in different NaOH concentrations and incubation times were analyzed using FTIR. The IR

spectrum of 4PCLMA-based PolyHIPE scaffolds after NaOH treatment is shown in Figure 21. The FTIR spectrum shows how NaOH treatment changes the chemical structural properties of 4PCLMA-based PolyHIPE scaffolds. The peaks between 3400-3200 cm^{-1} represent broad bands of -OH groups, resulting from stretch vibrations of hydroxyl groups. The increase in these bands indicates that the scaffolds tend to hydrolyze and deteriorate. The most intense peak belongs to the N5M24h group. The presence of -OH groups indicates that these polymers have free hydroxyl groups that interact with water (Zamani et al. 2019). The peaks between 3000-2800 cm^{-1} represent CH_2 groups. C-H stretch vibrations in this area indicate that PCL has aliphatic carbon-hydrogen bonds. No significant change in these peaks indicates that the chemical structure of the polymer is preserved and its structural integrity is not compromised (Suárez et al. 2022).

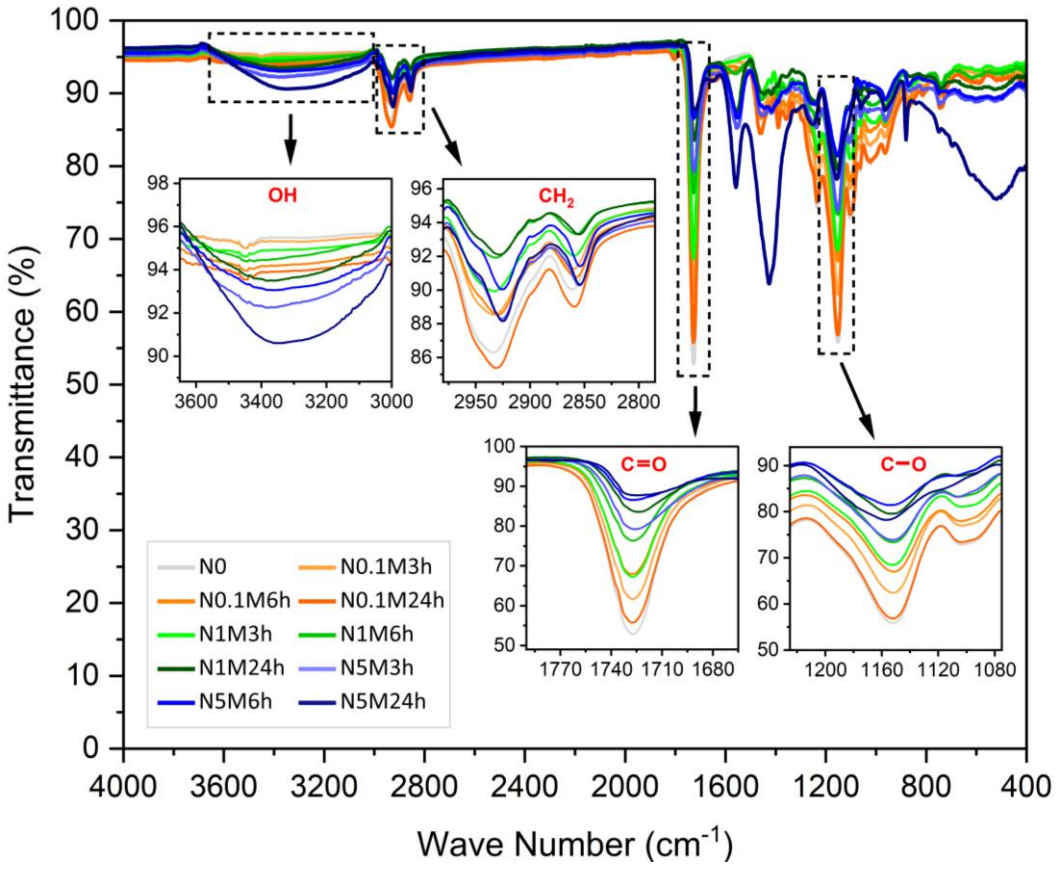

Figure 21. FTIR analysis of PolyHIPE scaffolds.

The peaks between 1750-1700 cm^{-1} represent the C=O group. These peaks provide information about ester bonds. The decrease in these peaks indicates the destruction of the ester bonds in the polymer chain, and as a matter of fact, the lowest peak intensity is seen in the N5M24h group (Benkaddour et al. 2013). The peaks between 1200-1000 cm^{-1} are seen in this region as C-O stretch vibrations of ester bonds and give information about the ester functional groups of PCL. Overall, these peaks provide information about the chemical changes of the polymer via NaOH hydrolysis (Oyane et al. 2005).

3.5. SEM Analysis

The effect of NaOH treatment on the morphological properties of the scaffolds was examined using SEM. Micrographs of 4PCLMA-based PolyHIPEs treated with NaOH are shown in Figure 22.

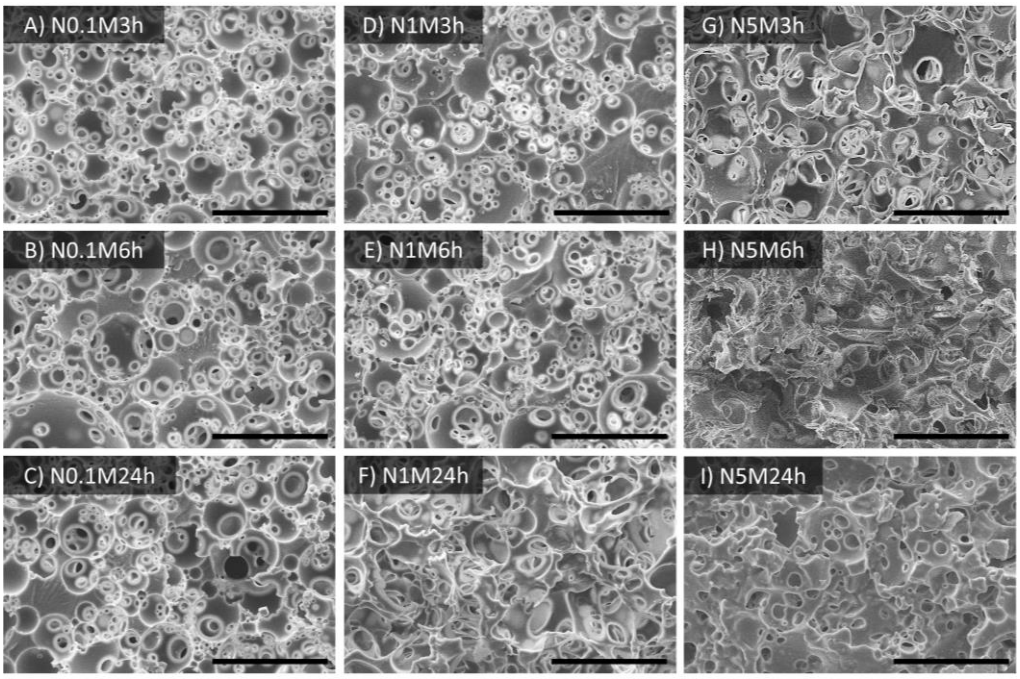

Figure 22. SEM images of NaOH-treated 4PCLMA PolyHIPE scaffolds (Scale bar: 50 μm).

There was no change in surface morphology in the groups treated with 0.1M NaOH. In the groups treated with 1M NaOH, pore structures were affected with an increase in incubation time, and especially in the group that remained in the 24 h incubation period, deteriorations in the pore structures were observed. In groups treated with 5M NaOH, there were dramatic changes in the morphology of PolyHIPE depending on the incubation time. These results showed that NaOH concentration and treatment time play an important role in changing the pore structures and surface morphology of the material.

The average pore sizes of non-treated and NaOH-treated scaffolds were measured. As seen in the results, NaOH treatments did not cause a dramatic change in the average pore size of scaffolds. The resulting average pore diameters of different scaffolds were close to each other (Figure 23).

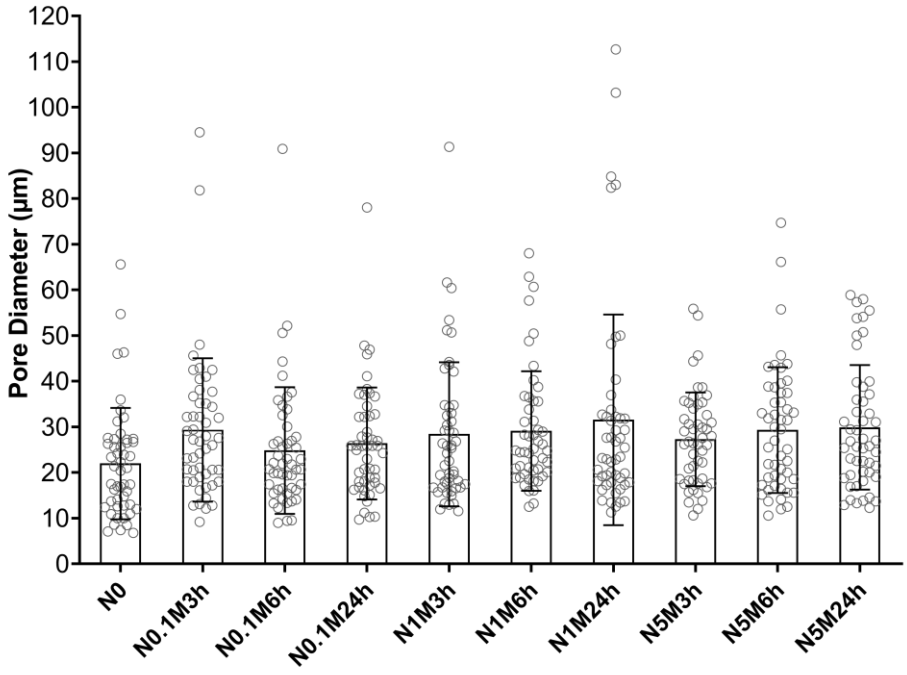

Figure 23. Pore size distributions of PolyHIPE scaffolds.

The impact of NaOH treatment on the window diameter was examined and shown in Figure 24. Although there was a slight increase in average window diameters due to

the increase in incubation time in the groups treated with 0.1 M NaOH, there was no significant change. In the groups treated with 1M NaOH, this increase was more apparent, especially in PolyHIPEs treated with NaOH for 24 h. Although there was no significant difference between the window diameters of the samples treated for 3 h and 6 h incubation periods, there was a significant increase in the window diameter in the group exposed to NaOH for 24 h. In groups treated with 5M NaOH, the pore diameter significantly increased compared to the control group. The highest window diameter was observed in the groups exposed to NaOH for 6 h and 24 h incubation periods. This increase in window diameter may be due to the degradation of windows with smaller diameters due to NaOH and the merging of smaller windows to form windows with larger diameters. These results in pore diameter and window diameter show that although the NaOH concentration and treatment time did not affect the pore diameter critically, they caused an increase in the window diameter, especially in the groups treated with high concentrations of NaOH for long incubation time.

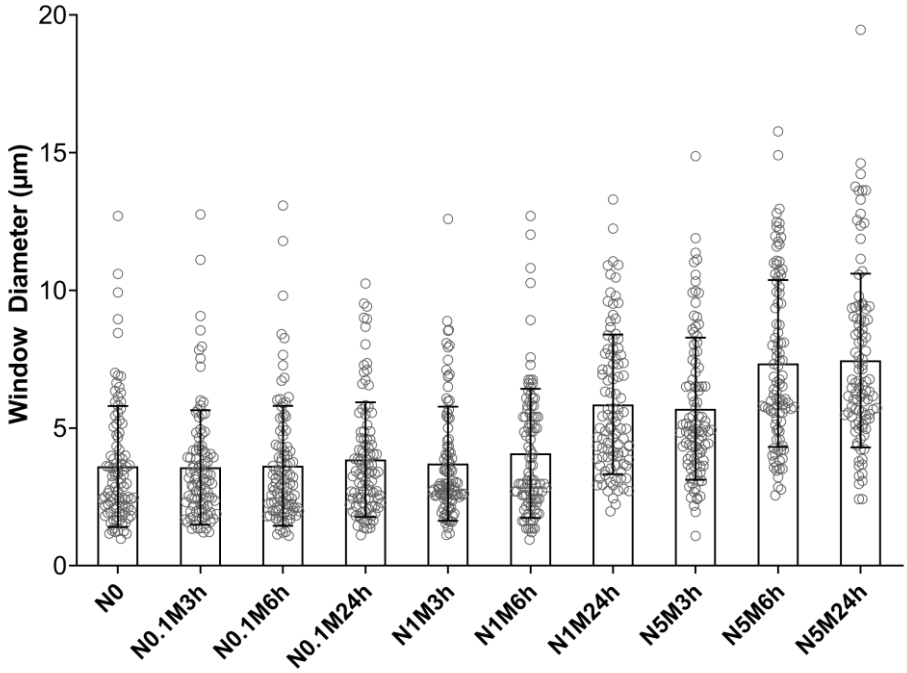

Figure 24. Window size distributions of PolyHIPE scaffolds.

3.6. Determination of Mass Change

The mass loss graphic is shown in Figure 25. NaOH hydrolysis causes mass loss by breaking the ester bonds in the polymer backbone and exposes hydroxyl and carboxylic acid groups (W. Wang et al. 2016). Therefore, increasing the NaOH concentration or incubation time broke a higher number of bonds in the polymer chain and resulted in enhanced mass loss.

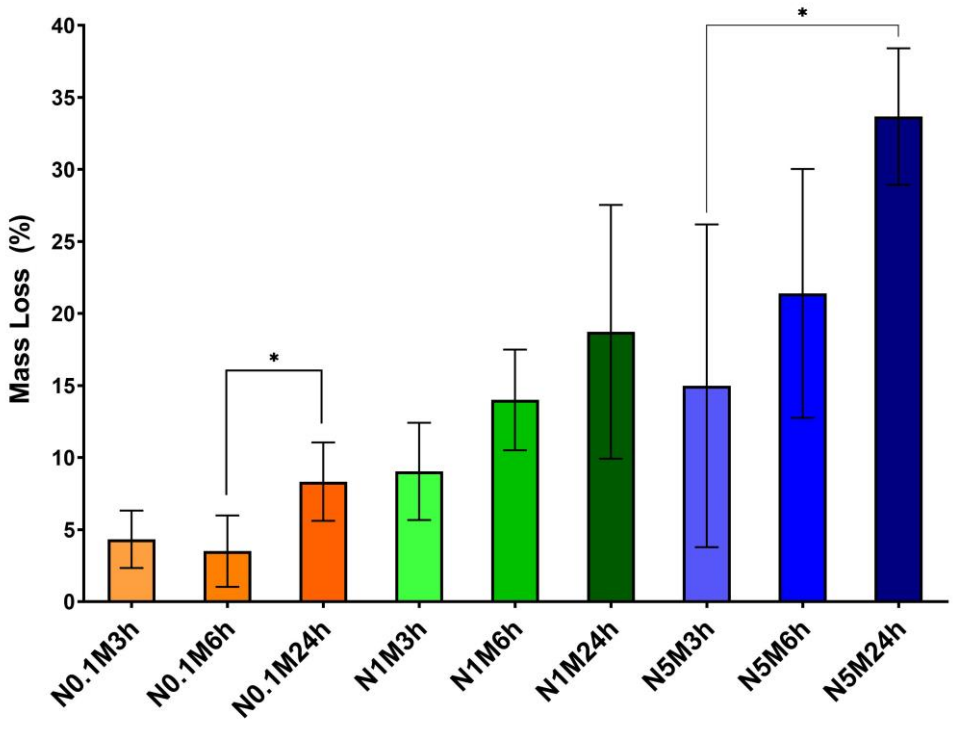

Figure 25. The mass loss of scaffolds after NaOH treatment (n=3). * : $p \leq 0.05$, and no significant difference was observed in unlabelled groups ($p > 0.05$).

Measurements of weight loss in 0.1M NaOH treated groups exhibit a minor increase in comparison to the control group (N0), meaning a slight degradation of the material occurs. Although a greater increase was observed in measurements in 1M NaOH than in measurements in 0.1M NaOH, the most aggressive changes were observed in PolyHIPEs treated with 5M NaOH. Especially in the last group (N5M24), the weight loss

reached up to 32%, which shows that degradation accelerates at higher concentrations and incubation times. This study shows that the structural integrity of the scaffolds is significantly stressed under high alkalinity and long-term incubation.

Jirofti *et al.* developed PCL/Polyurethane (PU) based scaffolds and modified the surface with NaOH (Jirofti, Mohebbi-Kalhori, and Masoumi 2022). They used three different concentrations (1M, 2M and 3M) of NaOH with three different incubation times (1 h, 2 h and 3 h). Mass loss data presented after hydrolysis of PCL with varying concentrations of NaOH over different periods revealed that the degradation behaviours of the polymer were dependent on NaOH concentration and incubation time. After they hydrolysed PCL scaffolds with different NaOH concentrations and incubation time, they observed 0.45% to 11.80% mass loss on the PCL scaffolds. In the results, scaffolds treated with 1M NaOH for 3h showed 9.20% mass loss. In our study, we observed 6.73% mass loss in the same group. Although they used thermoplastic PCL with a longer chain and a molecular weight of 80,000 g/mol as a mixture with PU in their studies, we obtained less mass loss in our study with 4PCLMA pre-polymer, which has an approximately 2,100 g/mol M_w before the crosslinking of pre-polymer. Scaffold fabrication methods used may also have an impact on this difference. Electrospinning and emulsion templating methods provide different porous structures for the scaffolds. This may affect the interaction between the NaOH solution and the scaffolds.

Overall, it can be concluded that there is a clear correlation between NaOH concentration/incubation time and the degradation rate of PCL. Their increase leads to greater and faster degradation.

3.7. Water Absorption Capacity

Water absorption is a crucial property that affects scaffold hydrolytic degradation (Sultana and Wang 2008). Since water uptake capacity affects nutrient transport (H. Zhu et al. 2010), cell attachment and proliferation, materials with enhanced hydrophilicity are preferred in tissue engineering applications (Kouhi et al. 2018). The water absorption capacity of scaffolds after being treated with NaOH at different times (3h, 6h, 24 h) and various concentrations (0.1 M, 1 M and 5 M) is shown in Figure 26A and Figure 26B.

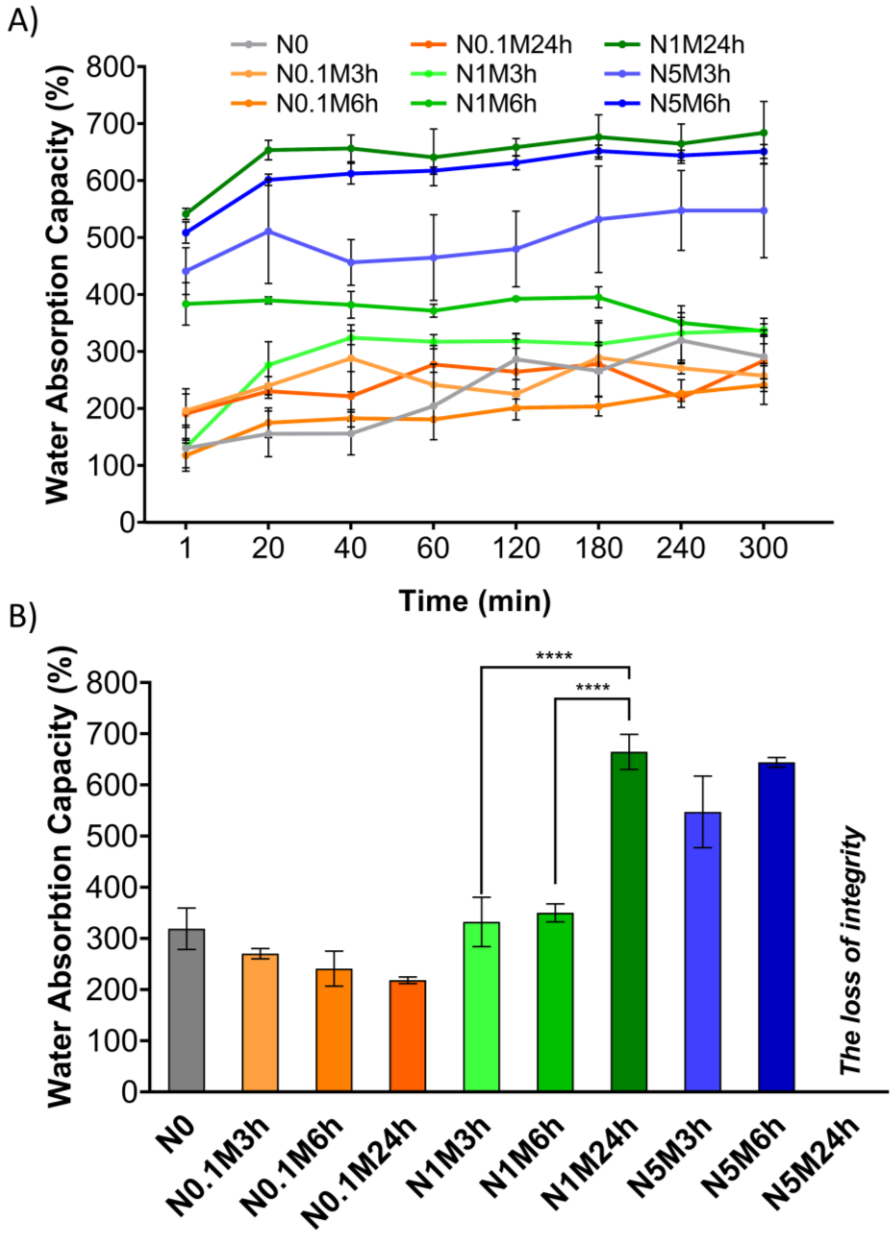

Figure 26. A) Time-dependent and B) ultimate (after 300 min) water absorption capacity of PolyHIPEs (n=3). ****$p < 0.0001$, and no significant difference was observed in unlabelled groups ($p > 0.05$).

The water adsorption capacity test was performed for 5 h. There was no significant difference in the initial absorption capacity of the scaffolds treated with 0.1 M NaOH compared to the control group. However, scaffolds treated with 1M NaOH exhibit a steady increase in water absorption capacity, reaching the highest level after 24 h. For groups treated with 5M NaOH, there was a sharp increase in water absorption capacity

even at 3 h when compared with the control group (N0). N5M6h groups showed higher water absorption capacity compared to the N5M3h group. The water absorption capacity of N5M24h group samples could not be determined due to losing integrity. The highest water absorption capacity, with 665%, was observed in the N1M24h group.

Thadavirul *et al*. used solvent casting and salt particle leaching methods to produce PCL/HA-based scaffolds. To increase the hydrophilicity of the PCL/HA dual-leached scaffolds, they treated the PCL/HA scaffolds with an alkaline solution. For this purpose, they treated the scaffolds in 1M NaOH at 37 ºC for 1h. They performed water uptake tests for 3 days to investigate the HA addition and NaOH treatment on the water absorption capacity of the scaffolds. There was a decrease in the water absorption capacity of the scaffolds with the addition of HA. The scaffolds with HA added showed decreased water absorption capabilities compared to the samples in the control group. On the other hand, PCL/HA scaffolds treated with NaOH had higher water absorption capacity than untreated PCL/HA scaffolds. Considering this result, 1M 1h NaOH treatment shows significant increases in the water absorption capacity of the scaffolds even in alkaline treatment (Thadavirul, Pavasant, and Supaphol 2014).

In our study, NaOH treatment applied at different concentrations and incubation times showed higher water retention capacity at higher concentrations and immersion times. On the other hand, it was noted that during incubation and at concentrations over a certain level, the integrity of scaffolds was compromised. Although alkaline hydrolysis increases the hydrophilic properties of materials, it affects the material integrity. This fact was taken into consideration when determining the ideal concentration and incubation time for 4PCLMA-based PolyHIPE scaffolds.

3.8. Water Contact Angle

Measurements of the water contact angle were conducted on the NaOH-treated and non-treated scaffold surfaces to quantify their hydrophilic properties. The results are shown in Figure 27.

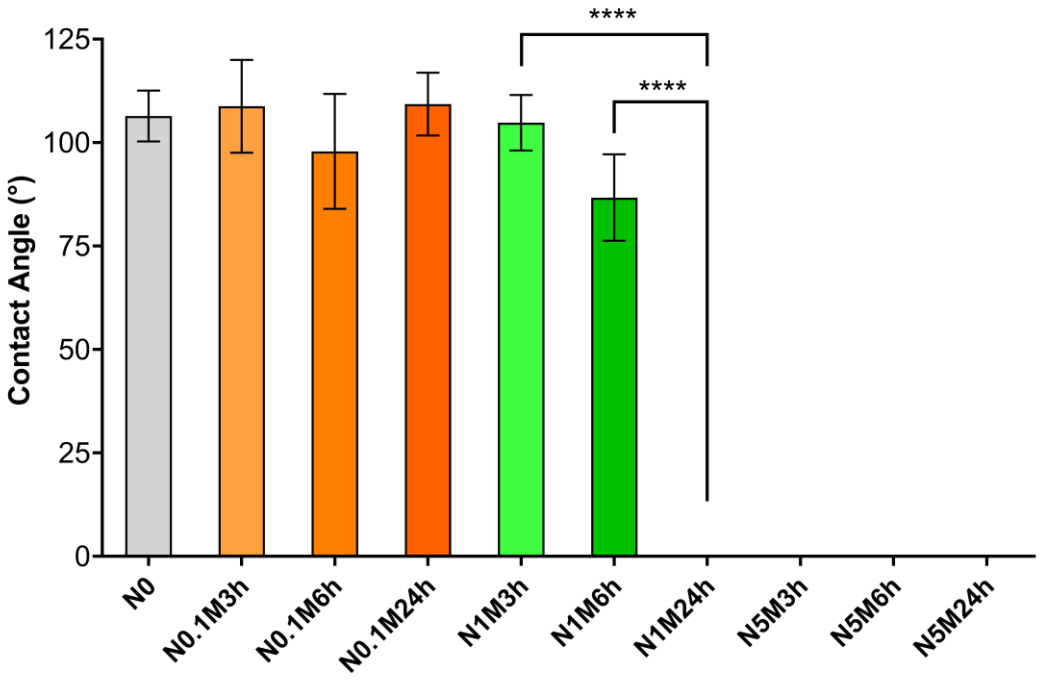

Figure 27. Water contact angles on the PolyHIPE scaffolds after 60 s (n=3). ****$p < 0.0001$, and no significant difference was observed in unlabelled groups ($p > 0.05$).

According to the results of static contact angle measurements, a decrease in contact angles was observed after NaOH treatment of the material. A significant difference was not seen in the scaffolds between the N0 and N1M6h groups. While the contact angles of the scaffolds 60 s after water was dropped were above 90° until the N1M6h group, they decreased below 90° starting from the 1NM6h group. Starting from the N1M24h group, the scaffolds started to show hydrophilic properties and a significant difference was seen in the results. Especially after the N1M24h group, the contact angle of the scaffolds decreased to 0°. The contact angles were measured as 0° in all 5M NaOH-treated groups. These results showed that 3 h of treatment in 5 M NaOH was sufficient to improve the hydrophilicity of PCL without the need for long-term hydrolysis.

Zhou *et al*. wanted to examine the effect of NaOH treatment on PCL films. For this purpose, they performed a contact angle experiment to evaluate the hydrophilic properties of NaOH-treated samples. They treated the scaffolds in NaOH with a concentration of 5 M at three different time points (5 min, 15 min, and 30 min). They

investigated the contact angles of the NaOH-treated scaffolds. They observed that as time increased, the contact angle of PCL films decreased. These results also showed that a soaking time of 30 min in 5 M NaOH was sufficient to improve the hydrophilicity of thermoplastic PCL (M_n = 80,000) without long-term soaking times (Z.-X. Zhou et al. 2020). The results indicated that NaOH treatment decreased the contact angle of the scaffolds and improved their hydrophilic properties. The breaking of ester bonds on the polymer structure can yield hydrophilic carboxyl and hydroxyl groups on the PCL surface as a result of the polymer hydrolysis in NaOH solutions (W. Wang et al. 2016).

Contact angle images of the scaffolds were captured at four different time points (1 s, 10 s, 30 s and 60 s) (Figure 28). Mostly, the contact angle of hydrophobic groups did not change from 1 s to 60 s. However, the contact angle of the N1M6h group was changed to the hydrophilic range from the hydrophobic range, and the contact angle of scaffolds between N1M24h and N5M3h groups decreased to 0 ° at the beginning stage.

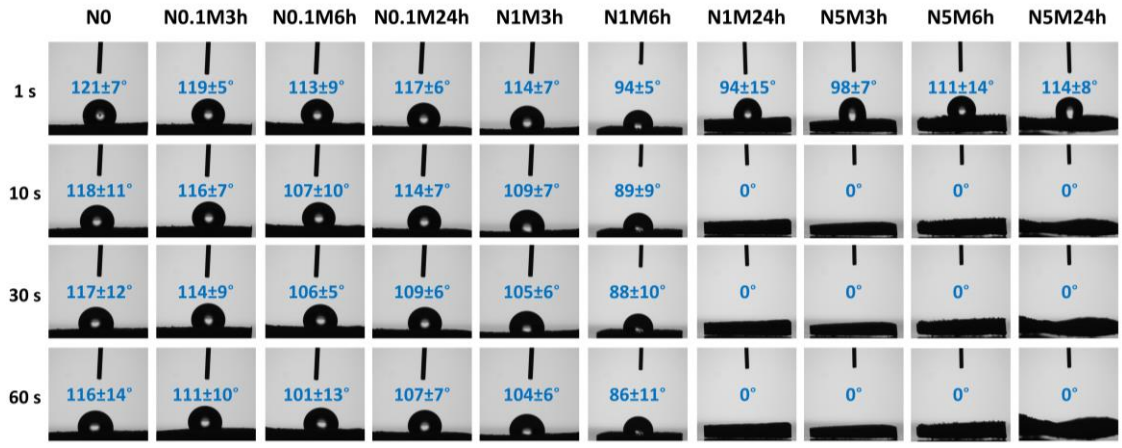

Figure 28. Contact angle images of PolyHIPE scaffolds at four different time points.

3.9. Mechanical Characterization

Scaffolds need to have sufficient mechanical properties to resist the forces involved in tissue regeneration for utilization in bone tissue engineering. Maintaining the structural integrity of scaffolds supports cell growth and tissue formation under

physiological conditions. Designing scaffolds by considering mechanical properties such as stiffness, compressive strength and load-bearing capacity to support successful tissue repair and regeneration is crucial (Yazdanpanah et al. 2022). Compression tests were applied to the scaffold to characterize the mechanical properties. The compressive modulus of the samples calculated from the linear region of the stress-strain curve is shown in Figure 29A. The stress-strain chart is shown in Figure 29B. The maximum stress value was limited to a strain of 60%, where the sample is almost fully compressed. While this value does not correlate with a material fracture, it does indicate the point where stress reaches its maximum level without exceeding the maximum force limit of the device and with the minimum change in strain. A very high local modulus value is observed here.

Treatment of the scaffolds with NaOH at different concentrations and incubation times resulted in a decrease in the compressive modulus of the scaffolds, as shown in Figure 29B. The compressive modulus of the control group (N0) was 3.4 ± 0.4 MPa. Among the groups treated with 0.1M NaOH and the control group, there was no noticeable difference. Although there was no significant difference between N0 and N1M6h groups, there was a significant difference between N0 and N1M3h groups. The reason for this may be air bubbles in the emulsion formed during sample preparation or the samples having different properties due to being obtained in different batches. It was observed that the compression modulus decreased significantly in the group treated 1M for 24 h. In 5M NaOH-treated groups, although there was a decrease in the compressive modulus in the group treated for 3 h, there was no statistical difference compared to the control group. There were serious decreases in the compressive modulus in the groups treated for 6 h and 24 h. Due to the high degree of degradation in the scaffolds in this group, their mechanical strength may have decreased significantly.

Gupta *et al.* have a study investigating the effect of NaOH treatment on PCL-based 3D printed scaffold. In this study, researchers applied NaOH treatment at different concentrations (5 M, 10 M and 20 M), different temperatures (room temperature and 37 °C) and different incubation times (24 h and 48 h). The results showed that the Young's modulus of each group decreased, and mechanical properties were affected more with increasing incubation time and concentration.

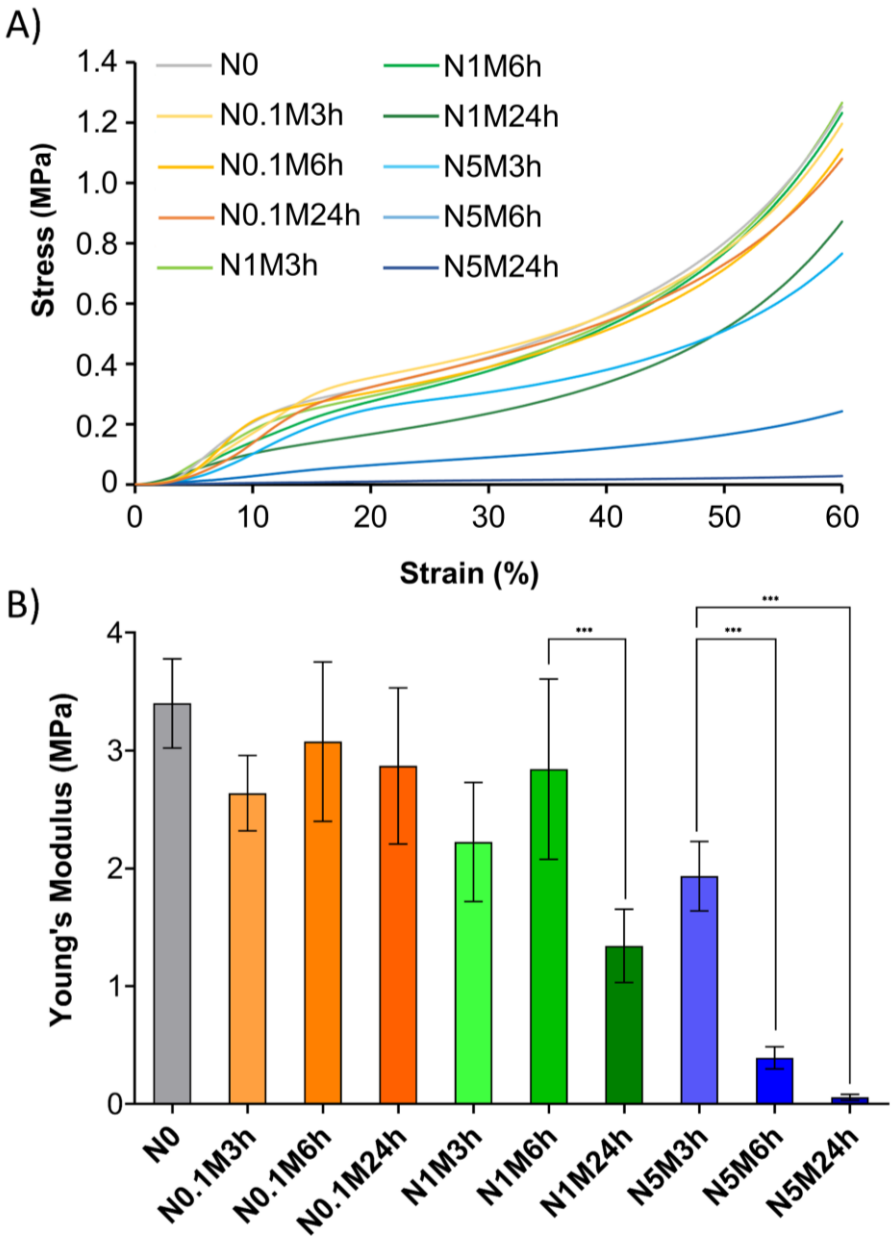

Figure 29. A) Stress-strain curve of compression-tested PolyHIPE scaffolds, B) Young's modulus of compression-tested PolyHIPE scaffolds (n=5). ***$p < 0.001$, and no significant difference was observed in unlabelled groups ($p > 0.05$).

Although there was a decrease in Young's modulus in the group treated at 5M room temperature and 24 h compared to the control group, there was no significant difference. In contrast, in our study, it is seen that at such a high concentration and incubation time, the Young's modulus of the scaffold significantly decreased. One of the

potential reasons for that is likely to be the polymers used are different; one is linear PCL with high M_w, while the other is 4PCLMA pre-polymer, which is a polymer with lower M_w. Another reason may be that the scaffolds are produced using different production methods. Scaffolds produced by emulsion templating have a porous morphology and different porosity, and the scaffolds fabricated by electrospinning have different porous structures (Gupta et al. 2019). Emulsion-templated scaffolds have more surface area due to their highly porous structure. It causes higher liquid absorption, and due to this absorption capacity, NaOH can be exposed more on the scaffolds even with the same concentration and immersion time applied to scaffolds.

3.10. Determination of the Ideal Immersion Time and NaOH Concentration

4PCLMA PolyHIPE scaffolds were exposed to nine different test conditions for NaOH treatment. The hydrophilicity after NaOH treatment was evaluated by measuring the contact angle of dH_2O droplets on the scaffold surface prepared with different test conditions. Ester bonds were broken after NaOH treatment of the scaffolds, and hydroxyl and carboxylic acid groups were obtained on the surfaces of the samples. The hydrophilic characteristics of the scaffolds increased as a result of increases in hydroxyl and carboxylic acid groups on their surface. Although the contact angle determines the hydrophilicity of the scaffolds, it is necessary to examine the effects of NaOH treatment on other properties of the material. By breaking down the ester bonds within the polymer chains, the mechanical strength of materials is significantly affected by NaOH treatment. In this sense, the compressive mechanical test results of NaOH-treated scaffolds were evaluated. In addition to evaluating the hydrophilicity and mechanical properties of these nine test conditions, the change in bulk mass of the scaffold before and after NaOH treatment was also examined. As a result, two groups, N1M24h and N5M3h, which showed hydrophilic properties after NaOH treatment, preserved the integrity of the scaffold, which had more mechanical strength and less mass loss, were selected as test groups for ongoing characterizations.

3.11. BET analysis

The surface areas and porosity of the samples were examined using BET. The results of the BET analysis of PolyHIPE scaffolds are shown in Table 6. The BET surface area and Langmuir surface area of the 1M 24h NaOH treated group (N1M24h) are higher than the N0 group but lower than the N5M3h group. This sample has more surface area and larger pores than N0. In the 5M3h NaOH-treated group (N5M3h), the pore size is significantly larger than the other groups. BET and Langmuir's surface areas are also higher than those of the other groups. In bone tissue engineering, the surface area and pore size of the biomaterials used are important for cell growth and tissue integration (Amini, Laurencin, and Nukavarapu 2012). A larger surface area is generally ideal for cell growth and integration of bone tissue (Jiao et al. 2023). The pore size of the control group sample (N0) is smaller than the other samples.

Table 6. BET analysis of PolyHIPE scaffolds.

Sample	**N0**	**N1M24h**	**N5M3h**
BET Surface Area (m^2/g)	1.0579	1.6885	2.5052
Langmuir Surface Area (m^2/g)	1.7731	2.8672	4.0663
t-Plot External Surface Area (m^2/g)	1.1995	2.2990	3.0072
Pore Size (Å)	39.2838	41.3382	77.9087

3.12. Protein Adsorption

One significant component that affects cell adherence to the scaffold is cell-substrate interaction. Cell migration, spreading, and proliferation are all regulated through protein adsorption on the scaffold surface, resulting in an impact on the interaction between cells and materials. Protein adsorption takes place on the surface of a biomaterial when it comes into interaction with a liquid (blood, body fluid, or cell cultivation medium) that contains soluble protein. Thus, when the cells are seeded, they contact

directly the adsorbed protein layer instead of the molecular structure of the biomaterial (Latour 2008).

In our study, protein adsorption of the scaffolds was determined using the BCA colourimetric kit, a protein assay kit. Protein adsorption of the scaffolds was performed in 0.1% BSA solution for 24 h. The colour change obtained for the working solution is shown in Figure 30. Four replicates were used from each sample group, and three replicates were used from each sample group as blank. The colour of the working agent is close to turquoise, and when it interacts with BSA, it turns darker and purple. The colour of the blanks of each sample group did not change after 30 min and remained the same colour. However, in the wells where only BSA is placed, we see the colour change as the working agent and BSA interact. This colour change was close to purple. Compared to the scaffold groups adsorbing BSA, more colour change was seen in the group with less BSA-adsorbed group (N0) because the solution contained more BSA than the other groups. Since the N1M24h and N5M3h groups adsorbed more BSA, less BSA remained in the well after the scaffolds were removed from the well, and accordingly, the colour change was less than the N0 group (Figure 28).

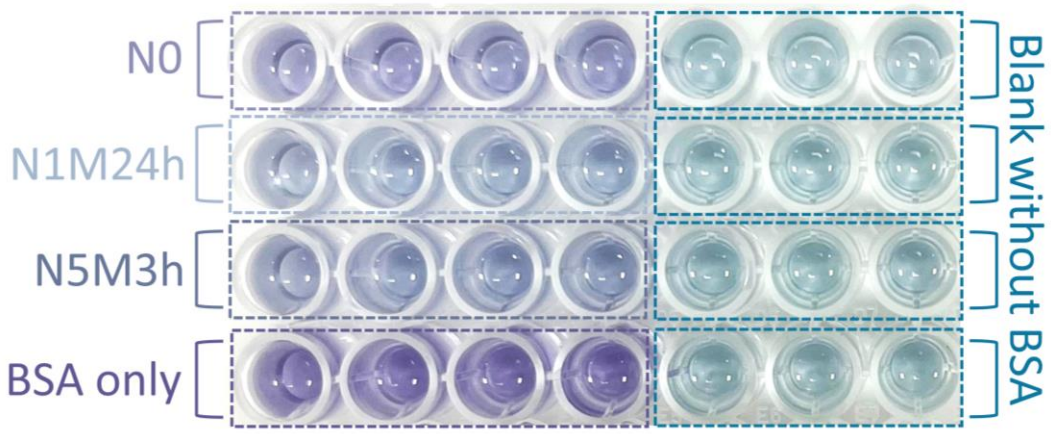

Figure 30. Experimental set-up of BSA adsorption test. Images were taken after 30 min of scaffold removal and the addition of working agents to the wells.

The adsorption graph of the resulting protein is given in Figure 31. As a result, the group showing the highest protein adsorption was N1M24h. The protein adsorption

value of this group was observed as 67.1 µg/mL. The N5M3h group showed 57.5 µg/mL protein adsorption. In general, scaffolds with more surface area are expected to show greater protein adsorption. In this case, higher protein adsorption is expected in the 5M3h sample group, which has more surface area because of BET analysis. However, the N1M24h group showed higher protein adsorption. The potential reason for this may be that different treatment times and intensities between N1M24h and 5M3h samples may have caused the formation of different chemical groups on the surface or different surface morphologies. Different chemical groups formed on the surface may also have decreased or increased protein binding ability. The lowest protein adsorption value was shown in the N0 group with 34.6 µg/mL. When the N5M3h and N1M24h groups were compared with the control (N0) group, these two groups showed statistically significantly more protein adsorption than the control group. As a result, treating the scaffolds with NaOH significantly increased the protein adsorption of the scaffolds.

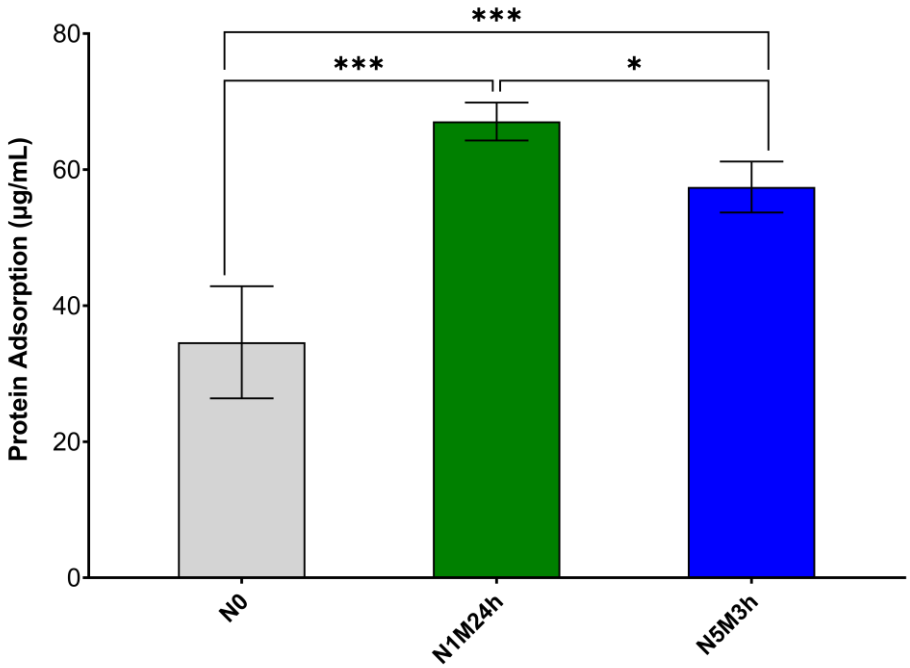

Figure 31. Protein adsorption studies of the PolyHIPE scaffolds (n=3). *$p < 0.05$, ***$p < 0.001$.

3.13. Biological Characterization

3.13.1. Cytotoxicity of The Scaffolds

The cytotoxicity of the scaffolds was tested by culturing L929 cell lines for 48 h (Figure 32A). In the first-day results, relative fluorescence values were similar in all groups, and no significant differences were observed. This result shows that the N0, N1M24h, and N5M3h did not show any cytotoxic effect on the cells compared to the tissue culture plate (TCP). Similar fluorescence values in all groups indicate that the cytotoxicity of the scaffolds was not affected by NaOH treatment. Results on 48 h showed an increase in relative fluorescence compared to 24 h in all groups. This result indicates that cell viability increased over time. The fact that this increase occurred in all groups shows that the material and NaOH treatment did not create a cytotoxic effect, and the cells continued to proliferate. As a result, it can be said that none of the tested samples (N1M24h, N5M3h, N0 and TCP) exhibited cytotoxic effects within these 48 h. It shows consistency in relative fluorescence between groups on both days and does not appear to negatively affect cell viability.

Thadavirul and his colleagues produced PCL and PCL/HA dual-leached scaffolds using solvent casting, polymer leaching, and salt particulate leaching methods. Afterwards, the scaffold surfaces were modified by applying NaOH treatment to the produced scaffolds. In their study, they performed an indirect cytotoxicity test to examine the cytotoxic effects of NaOH treatment. For this test, mouse calvaria-derived preosteoblastic cells and L929 cell lines were used. According to MTT results, the cell viability was always above 80% compared to TCP on days 1, 3, and 7. They showed that NaOH treatment of scaffolds did not cause cytotoxicity (Thadavirul, Pavasant, and Supaphol 2014).

Also, a live/dead assay was performed using calcein and propidium iodide (PI) stains to confirm the Alamar blue test for cell cytotoxicity. Fluorescence microscope images are presented in Figure 32B. Since live/dead stain is used, the cells shown in green in the images are live cells, and the cells shown in red are dead cells. Yellow arrows indicate the dead cells on the images. Cellular viability of cells in wells containing

untreated and NaOH-treated scaffolds was very high and close to each other after 48 h of culture.

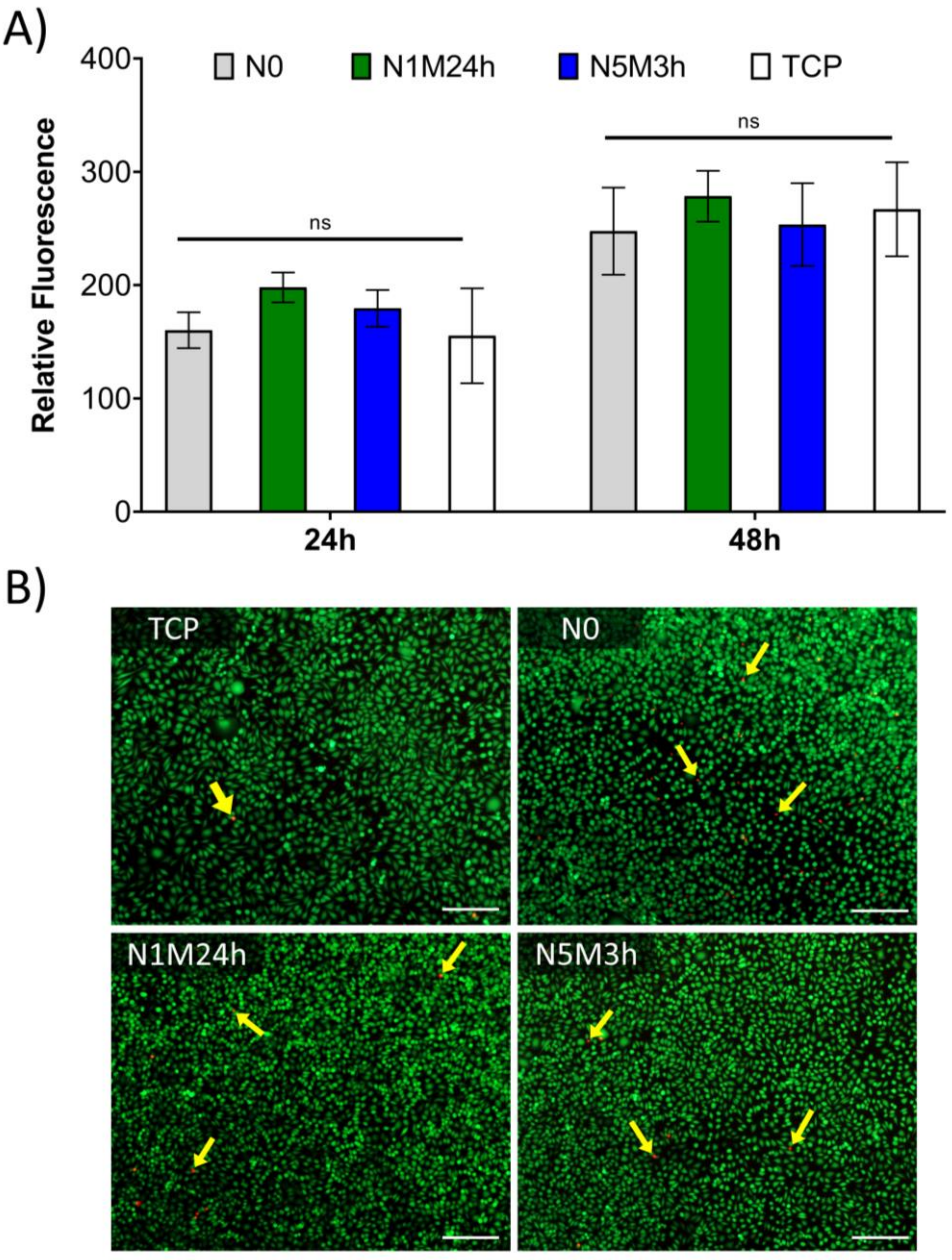

Figure 32. A) Cytotoxicity of PolyHIPE scaffolds (n=5). No significant difference was observed as labelled ($p>0.05$). B) Fluorescence microscope images of PolyHIPE scaffolds and TCP after live/dead staining (Scale bar: 100 µm).

3.13.2. Initial Cell Attachment Behaviour

Initial cell adhesion is a crucial phase for the healthy proliferation, differentiation and tissue regeneration of cells. Ensuring initial cell attachment is an important goal for the development of biomaterials and tissue scaffolds (Lotfi, Nejib, and Naceur 2013). SEM analysis was performed to examine the cell attachment behaviour of cells on the surfaces of NaOH-treated and untreated scaffolds. This study was conducted to observe initial cell interaction with NaOH-treated and non-treated scaffolds after 4 h of cell seeding. SEM images of cell-seeded PolyHIPE scaffolds are shown in Figure 33.

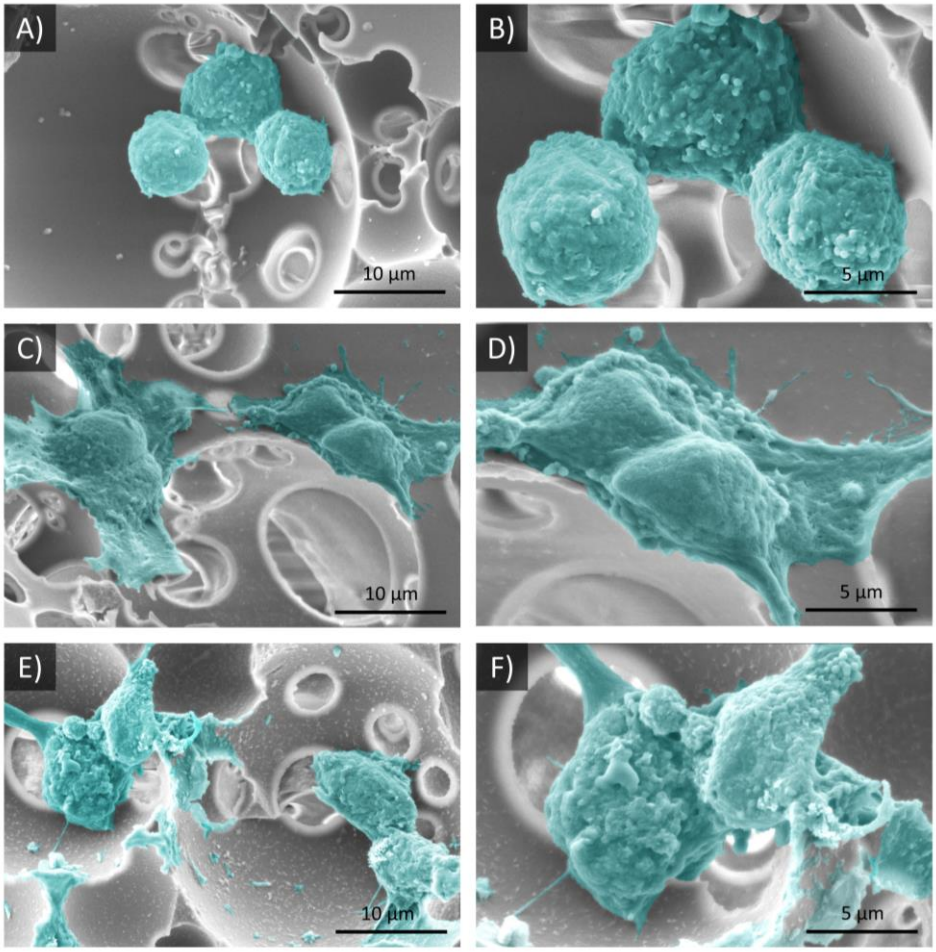

Figure 33. False-coloured biological SEM images of PolyHIPE scaffolds. Morphological images of Saos-2 cells cultured on A-B) N0, C-D) N1M24h and E-F) 5M24h PolyHIPE scaffolds after 4h incubation.

The morphology formed by the cell after its interaction with the material after 4 h of cell seeding is given in these figures. Cells adhere to the surface and do not spread on the control group (N0). On the surfaces of NaOH-treated scaffolds (N1M24h and N5M3h), the cells adhered to the hills and valleys on the rough surface and spread slightly more on the surfaces. Also, cells produced filamentous extensions on the scaffold surface to attach to these valleys. NaOH treatment enabled the cells to spread and produced filamentous extension to attach onto the scaffold surface.

Gupta *et al*. also investigated the cell attachment behaviours of the scaffolds obtained from PCL scaffolds with 3D printing technology. They investigated initial cell attachment behaviours on non-treated and NaOH-treated scaffolds. They also used the Saos-2 cell line in their study and showed that the cells on the scaffolds treated with NaOH showed better cell attachment than the non-treated groups after 4 and 8 hours (Gupta et al. 2019).

3.13.3. Cell Seeding Efficiency and Cell Proliferation

Following the cytotoxicity tests of the scaffolds, cell seeding efficiency and proliferation experiments were carried out using Saos-2 cell lines to examine the effect of NaOH treatment on the initial adhesion of the scaffolds and subsequent proliferation. 15 min and 60 min time points were selected for cell seeding efficiency. These time points were chosen to understand the critical stages of cell attachment and initial interaction with the scaffold surface. The 15 min time point was chosen to evaluate the initial attachment efficiency of cells to the scaffold surface.

Since NaOH-treated scaffolds showed hydrophilic properties compared to the control group, it was predicted that the cells would attach to the scaffold surface within 15 min, and there would be an enhancement in cell attachment compared with the control group. The attachment of cells onto the scaffold surface in such a short time shows that the scaffold supports surface compatibility and cell adhesion.

The 60 min time point will allow the initially connected cells to spread further and form more stable connections. So, while the early process (15 min) will provide insight into how well the cells recognize the scaffold and adhere to the surface, the later process

(60 min) will provide insight into whether the cells maintain their attachment and begin to spread and proliferate on the surface. Cell seeding efficiency and cell proliferation graphs of scaffolds are shown in Figure 34.

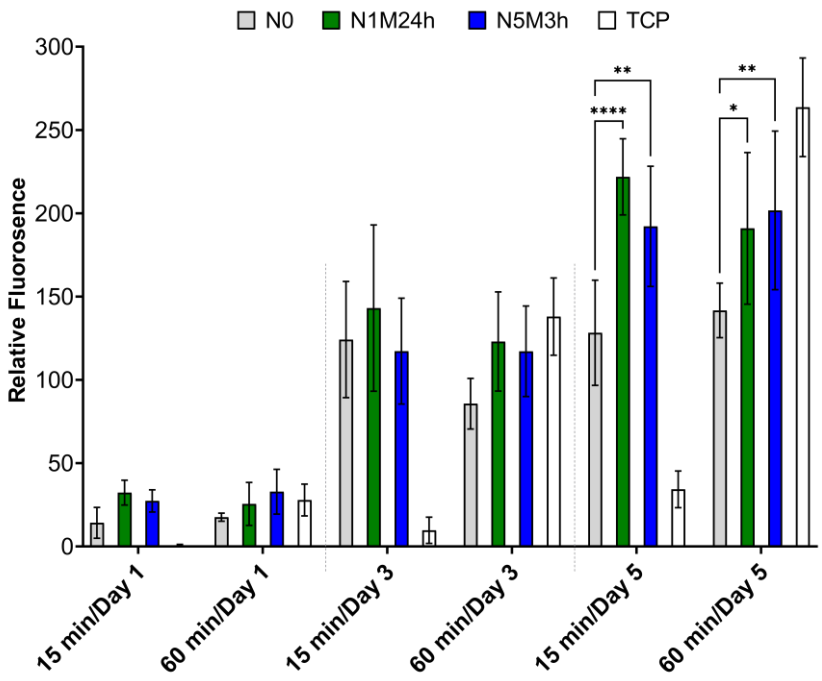

Figure 34. Cell seeding efficiency and cell proliferation of Saos-2 cells on PolyHIPE scaffolds (n=5). *$p < 0.05$, **$p < 0.01$, ****$p < 0.0001$, and no significant difference was observed in unlabelled groups ($p > 0.05$).

In the results, although there was a difference in relative fluorescent values, it was not significant for both the 15 min and 60 min groups after 1 day of cell culture. That is, cell proliferation or metabolic activity was found to be similar in each group after the first day. Only a difference was seen between 15 min and 60 min only in the TCP groups. While the cells adhered less to TCP at 15 min, it was observed that the cells adhered more at 60 min. On day 3, no significant difference was seen between both the 15 min and 60 min groups, so it can be assumed that there was no significant change in cell proliferation between the sample groups at this time point. Day 5 results showed significantly higher fluorescence in N1M24h and N5M3h scaffolds in the 15 min groups compared to N0 scaffolds. In other words, cell proliferation was observed to increase in these groups. It

was observed that at 60 min, N5M3h scaffolds in the groups showed significantly higher fluorescence than N0 scaffolds, so they provided significantly higher cell proliferation.

In conclusion, although initial cell proliferation was similar in all groups, day 5 results show that the NaOH-treated groups (N1M24h and N5M3h) showed enhanced cell activity, especially at the 15 min interval. The observed increase in cell proliferation is consistent with previously reported findings that surface modifications can enhance cellular responses.

Thadavirul and colleagues investigated the capacity to facilitate bone cell adhesion and proliferation on PCL/HA-doped scaffolds with MC3T3-E1 cells. In their study, cells were seeded and cultured onto the scaffold surface and TCP for 4, 8, or 16 h or 1, 2, or 3 days. They measured the viability of cells in the scaffolds using the Alamar blue test. The number of cells seeded in TCP at an early seeding density of $4x10^4$ cells/well increased to 100% in 4h cell culture and then to 133% in 16h cell culture. It was determined that the vitality of cells on PCL and PCL/HA double-leached scaffolds treated with NaOH was greater compared to that of cells seeded on TCP. The rough and hydrophobic surface of the PCL/HA double-leached scaffolds likely contributed to the higher number of cells on the NaOH-treated scaffold than the nontreated scaffold. In the results on days 1, 2 and 3, higher cell proliferation was observed in the groups that applied NaOH treatment. As a result, it can be said that NaOH treatment accelerated cell proliferation at different time points (Thadavirul, Pavasant, and Supaphol 2014).

Wang and his colleagues produced a PCL-based scaffold, and they modified the scaffolds with NaOH treatment and pristine graphene, adding at different ratios. They used human adipose-derived stem cells (ADSCs) for cell culture studies. They performed the Alamar blue test to compare cell viability. In the results, the scaffolds treated with 5M NaOH for 3 h and then added pristine graphene at different rates showed higher cell proliferation than the non-treated scaffolds from day 3 to day 14 (W. Wang et al. 2016).

Zamani and his colleagues also used different concentrations of NaOH treatment in the PCL-based scaffolds they fabricated using 3D printing. They also applied arginylglycylaspartic acid (RGD) immobilization on the scaffolds. They investigated the cell behaviours of the scaffold that NaOH treated and RGD immobilized. For this, they performed cell culture studies with pre-osteoblast cells. In the results, although they did not see a significant difference in cell proliferation after 3 days of cell culture, from day 7 onwards, NaOH-treated and RGD-immobilized scaffolds began to show higher cell proliferation than unmodified scaffolds (Zamani et al. 2019). Consequently, it was found

that treating the scaffolds with NaOH enhanced cell proliferation, both in our study and in the studies reported in the literature.

Cell attachment and cell proliferation on the scaffolds with 15 min (Figure 35) and 60 min (Figure 36) cell seeding were investigated using SEM after 5 day cell culture.

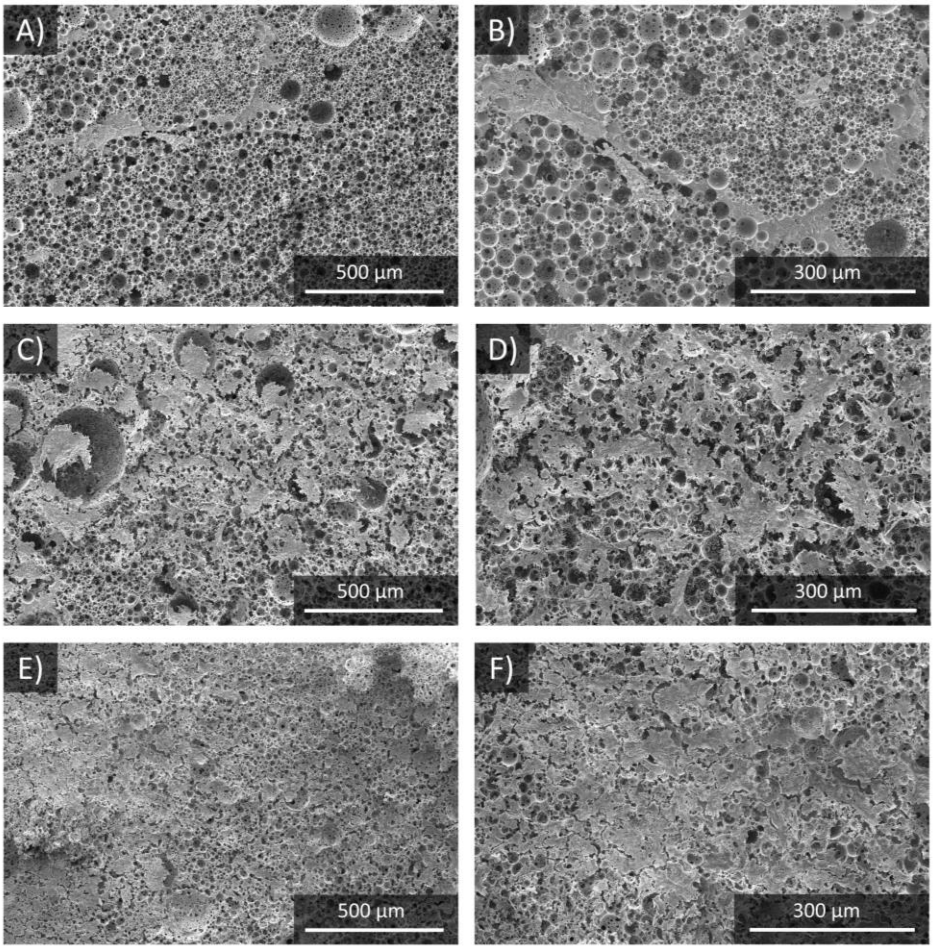

Figure 35. Cell morphological images of Saos-2 cells on A-B) N0, C-D) N1M24h and E-F) N5M24h PolyHIPE scaffolds after 5-day culture with 15 min incubation after cell seeding.

In the untreated group (N0), where cell seeding was performed for both 15 min and 60 min, cells adhered and spread on the scaffold surface, but cells were concentrated in certain areas on the scaffold surface. In addition, in 15 min and 60 min cell seeded NaOH-treated scaffold groups (N1M24h and N5M3h), cells adhered to the surface of the

scaffolds. Cells were spread on the surface, covering almost the entire scaffold surface. After NaOH treatment, cell adhesion behaviour and proliferation were positively affected. The obtained SEM results also confirm the Alamar blue tests. In Alamar blue results, more metabolic activity was also seen in NaOH-treated scaffold groups (N1M24h and N5M3h). In general, there are many studies in the literature showing that cell adhesion and proliferation are enhanced with hydrophilic surfaces (Gupta et al. 2019; Z.-X. Zhou et al. 2020).

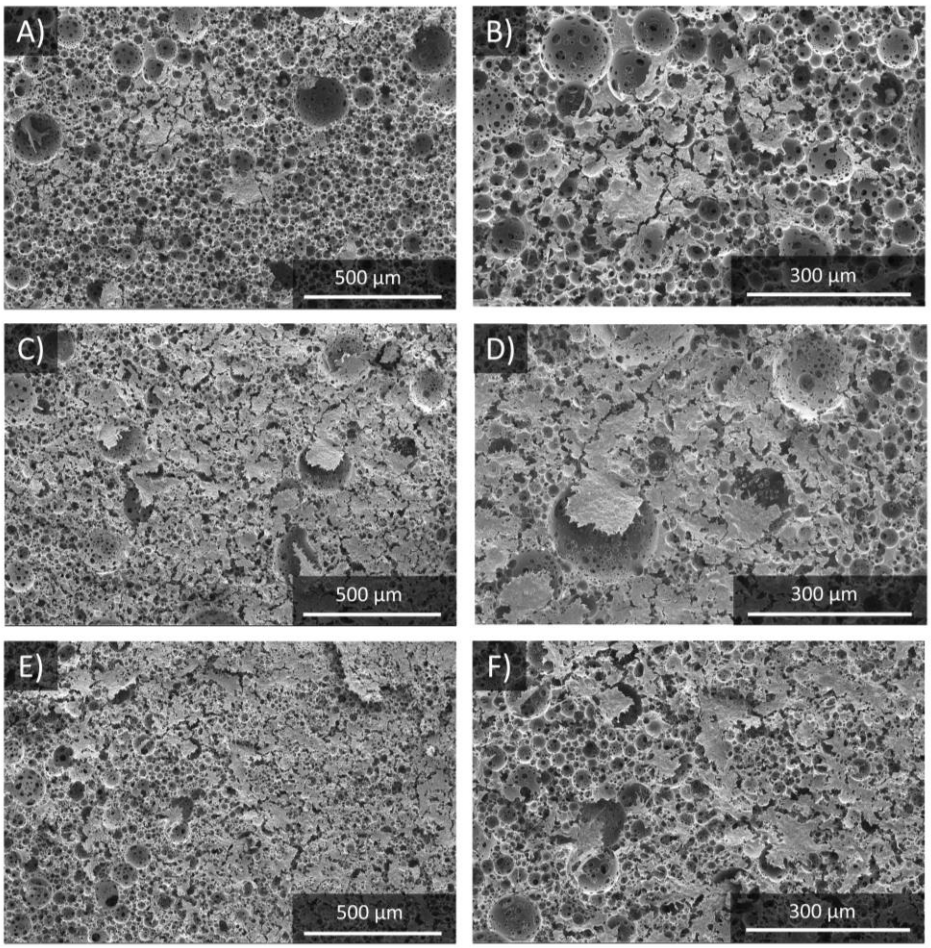

Figure 36. Cell morphological images of Saos-2 cells on A-B) N0, C-D) N1M24h and E-F) N5M24h PolyHIPE scaffolds after 5-day culture with 60 min incubation after cell seeding.

CHAPTER 4

CONCLUSION

The main aim of this thesis was to develop surface-modified 4PCLMA-based PolyHIPE scaffolds with enhanced hydrophilicity and cell-material interactions to be used in bone tissue engineering applications.

In the scope of this thesis, 4PCLMA pre-polymer was successfully synthesized in two steps: ring-opening polymerization and methacrylate functionalization. The polymer structure and the polymer molecular weight distributions were confirmed successfully with NMR and GPC analysis. 4PCMA-based PolyHIPEs were developed, and alkaline treatment of PolyHIPE scaffolds was implemented with NaOH to increase their hydrophilicities. The effect of NaOH treatment on the morphological, mechanical, chemical, physical and biological characteristics of scaffolds was examined and characterized using SEM, mechanical test device, FTIR, contact angle analysis, BET analysis, swelling study, and protein adsorption assay. *In vitro* cytotoxicity of NaOH-treated PolyHIPE scaffolds was determined by Alamar blue and live/dead assays. Cytotoxicity of scaffolds was performed with L929, and cell attachment and cell proliferation tests were performed with Saos-2 cells.

As a result, the polymer was successfully synthesized with ~97% DM and 2420 g/mol molecular weight. Then, emulsion templating was used in the fabrication of 4PCLMA-based polyHIPE scaffolds. The resulting PolyHIPE was found to have an average pore size of 20 ± 7 μm and a window size of 4 ± 2, respectively. Following NaOH treatment, although the NaOH concentration and treatment time did not affect the pore diameter critically, they caused an increase in the window diameters. Although the pore and window diameter of the scaffolds developed in the scope of this thesis has less diameter than required for bone tissue engineering scaffolds, the proof-of-concept approach that is presented in this study showed that the NaOH treatment of emulsion templated scaffolds is applicable without causing a deteriorating effect on their morphologies. This technique can be applied to scaffolds that will be developed with

larger pore and window pore sizes by changing the process parameters of emulsion templating.

NaOH-treated scaffolds were analyzed using FTIR, which indicated that NaOH treatment successfully changed the surface chemistry of 4PCLMA PolyHIPEs. Accordingly, in contact angle results, an increase in NaOH concentration and incubation time significantly decreased the contact angles of scaffolds. In the same direction, water absorption capacity increased depending on the increase in NaOH concentration and incubation time.

The mass loss showed that degradation accelerates at higher concentrations and incubation times. An increase in NaOH concentration and incubation time caused lower mechanical strength on scaffolds.

Two groups, N1M24h and N5M3h, which showed hydrophilic character after NaOH treatment, preserving the integrity of the scaffold, which had more mechanical strength and less mass loss, were selected as test groups for ongoing characterizations. They are further investigated using BET analysis, protein adsorption, and biological characterization.

As a result of BET analysis, NaOH treatment on the PolyHIPE scaffolds caused more porosity and greater surface area. Accordingly, in the protein adsorption assay, both N1M24h and N5M3h groups adsorbed significantly higher degrees of protein compared to the control.

The cytotoxicity of both non-treated and treated scaffolds was tested using the L929 cell line, and no cytotoxicity was observed for 48 h period. Also, according to the live/dead assay, NaOH treatment did not show any cytotoxic effect. In cell proliferation experiments, a higher degree of cell proliferation was observed in NaOH-treated groups at the end of the 5-day culture period.

In the biological SEM investigation, whilst cells adhere to the surface and do not spread on the untreated group, the cells adhere on the surface and spread on the NaOH-treated scaffold surface following 4 h incubation. In 5-day cell proliferation images, cells adhered and spread on all of the NaOH-treated scaffolds (N1M24h and 5M3h) and covered almost the surface homogeneously. Conversely, cells adhered and spread on the non-treated (N0) scaffolds but did not cover the scaffold surface homogeneously and cells were concentrated on certain areas of the scaffold surface.

NaOH treatment is an advantageous technique because of its simplicity, scalability, and cost-effectiveness. NaOH treatment on the 4PCLMA-based scaffolds

increased the hydrophilic properties of the scaffolds. Also, it provides better protein adsorption, cell attachment, and cell proliferation on the scaffolds.

In addition to all these advantages of NaOH treatment, significant disadvantages have also emerged. NaOH treatment had a very destructive effect on the scaffolds, negatively affecting their mechanical properties. Even in the groups that showed the highest mechanical strength in the hydrophilic range, compression modulus losses were observed at around 50%.

In future work, intermediate concentrations and incubation times can be applied to reduce the destructive effect caused by NaOH treatment while staying in the hydrophilic region. In addition, mechanical properties can be increased by combining NaOH treatment with other surface modifications. Modifications such as HA coating and CaP dipping can increase both the bioactivity and mechanical properties of the scaffolds. Additionally, by synthesizing lower molecular weight polymers with lower degrees of polymerization, the intrinsic mechanical properties of the polymer can be increased, which will eventually result in modified scaffolds with higher compression modulus.

Also, future work has been planned to develop scaffolds with larger pore sizes for cell culture studies and longer periods for better cell infiltration. *In vitro* culture of mesenchymal stem cells, their differentiation, long-term culture, and further characterization can give a better understanding of the performance of NaOH-treated 4PCLMA scaffolds as bone tissue engineering scaffolds.

Overall, this thesis provides a proof-of-concept approach that successfully enhances the hydrophilicity and biological performance of 4PCLMA PolyHIPE scaffolds. The material properties can be enhanced for more clinically relevant materials, and further *in vitro* and *in vivo* characterization is needed to evaluate the biological performance of the material better.

REFERENCES

Abdul Hamid A. Zuratul, Cho Y. Tham, and Zulkilfi Ahmad. 2018. “Preparation and Optimization of Surface-Engineered Poly(Lactic Acid) Microspheres as a Drug Delivery Device.” *Journal of Materials Science* 53 (7): 4745–58. https://doi.org/10.1007/s10853-017-1840-9.

Agarwal, Seema, Joachim H. Wendorff, and Andreas Greiner. 2008. “Use of Electrospinning Technique for Biomedical Applications.” *Polymer* 49 (26): 5603–21. https://doi.org/10.1016/j.polymer.2008.09.014.

Ahmad A. Fahad, Akhtar R. Razali, and Intan Suhana M. Razelan. 2017. “Utilization of Polyethylene Terephthalate (PET) in Asphalt Pavement: A Review.” *IOP Conference Series: Materials Science and Engineering* 203 (5): 012004. https://doi.org/10.1088/1757-899X/203/1/012004.

Aldemir Dikici, Betül, and Frederik Claeyssens. 2020. “Basic Principles of Emulsion Templating and Its Use as an Emerging Manufacturing Method of Tissue Engineering Scaffolds.” *Frontiers in Bioengineering and Biotechnology* 8 (875): 1-32. https://doi.org/10.3389/fbioe.2020.00875.

Aldemir Dikici, Betül, Gwendolen C. Reilly, and Frederik Claeyssens. 2020. “Boosting the Osteogenic and Angiogenic Performance of Multiscale Porous Polycaprolactone Scaffolds by in Vitro Generated Extracellular Matrix Decoration.” *ACS Applied Materials and Interfaces* 12 (11): 12510–24. https://doi.org/10.1021/acsami.9b23100.

Aldemir Dikici, Betül, Colin Sherborne, Gwendolen C. Reilly, and Frederik Claeyssens. 2019. “Emulsion Templated Scaffolds Manufactured from Photocurable Polycaprolactone.” *Polymer* 175 (5): 243–54. https://doi.org/10.1016/j.polymer.2019.05.023.

Amin, Shreyasee, Sara J Achenbach, Elizabeth J Atkinson, Sundeep Khosla, and Joseph L Melton. 2014. “Trends in Fracture Incidence: A Population-Based Study Over 20 Years.” *Journal of Bone and Mineral Research* 29 (3): 581–89. https://doi.org/10.1002/jbmr.2072.

Amini R. Ami, Cato T. Laurencin, and Syam P. Nukavarapu. 2012. “Bone Tissue Engineering: Recent Advances and Challenges.” *Critical Reviews in Biomedical Engineering* 40 (5): 363–408.

https://doi.org/10.1615/CritRevBiomedEng.v40.i5.10.

Andrews D. Kristie, John A. Hunt, and Richard A. Black. 2007. “Effects of Sterilisation Method on Surface Topography and In-Vitro Cell Behaviour of Electrostatically Spun Scaffolds.” *Biomaterials* 28 (6): 1014–26. https://doi.org/10.1016/j.biomaterials.2006.10.014.

Annabi, Nasim, Jason W. Nichol, Xia Zhong, Chengdong Ji, Sandeep Koshy, Ali Khademhosseini, and Fariba Dehghani. 2010. “Controlling the Porosity and Microarchitecture of Hydrogels for Tissue Engineering.” *Tissue Engineering Part B: Reviews* 16 (4): 371–83. https://doi.org/10.1089/ten.teb.2009.0639.

Arabpour, Zohreh, Farshad Abedi, Majid Salehi, Seyed Mahbod Baharnoori, Mohammad Soleimani, and Ali R. Djalilian. 2024. “Hydrogel-Based Skin Regeneration.” *International Journal of Molecular Sciences* 25 (4): 1–25. https://doi.org/10.3390/ijms25041982.

Archunan W Maheswaran, and Sandris Petronis. 2021. “Bone Grafts in Trauma and Orthopaedics.” *Cureus* 13 (9): 1-6. https://doi.org/10.7759/cureus.17705.

Asadian, Mahtab, Ke Vin Chan, Mohammad Norouzi, Silvia Grande, Pieter Cools, Rino Morent, and Nathalie De Geyter. 2020. “Fabrication and Plasma Modification of Nanofibrous Tissue Engineering Scaffolds.” *Nanomaterials* 10 (1): 119. https://doi.org/10.3390/nano10010119.

Aslam Khan, Muhammad Umar, Saiful Izwan Abd Razak, Wafa Shamsan Al Arjan, Samina Nazir, Joseph Sahaya Anand, Hassan Mehboob, and Rashid Amin. 2021. “Recent Advances in Biopolymeric Composite Materials for Tissue Engineering and Regenerative Medicines: A Review.” *Molecules* 26 (3): 619. https://doi.org/10.3390/molecules26030619.

Avossa, Joshua, Gordon Herwig, Claudio Toncelli, Fabian Itel, and René Michel Rossi. 2022. “Electrospinning Based on Benign Solvents: Current Definitions, Implications and Strategies.” *Green Chemistry* 24 (6): 2347–75. https://doi.org/10.1039/D1GC04252A.

Awwad, Nancy, Anh Thy Bui, Evgeny O. Danilov, and Felix N. Castellano. 2020. “Visible-Light-Initiated Free-Radical Polymerization by Homomolecular Triplet-Triplet Annihilation.” *Chem* 6 (11): 3071–85. https://doi.org/10.1016/j.chempr.2020.08.019.

Bajaj, Piyush, Ryan M. Schweller, Ali Khademhosseini, Jennifer L. West, and Rashid Bashir. 2014. "3D Biofabrication Strategies for Tissue Engineering and Regenerative Medicine." *Annual Review of Biomedical Engineering* 16 (1): 247–76. https://doi.org/10.1146/annurev-bioeng-071813-105155.

Bancroft, D Wilder. 1912. "The Theory of Emulsification. II." *Journal of Physical Chemistry* 16 (5): 345–72. https://doi.org/10.1021/j150131a001.

Baran, Eda Hazal, and Husnu Yildirim Erbil. 2019. "Surface Modification of 3D Printed PLA Objects by Fused Deposition Modeling: A Review." *Colloids and Interfaces* 3 (2): 43. https://doi.org/10.3390/colloids3020043.

Basko, Andrey, Tatyana Lebedeva, Mikhail Yurov, Anna Ilyasova, Galina Elyashevich, Viktor Lavrentyev, Denis Kalmykov, Alexey Volkov, and Konstantin Pochivalov. 2023. "Mechanism of PVDF Membrane Formation by NIPS Revisited: Effect of Precipitation Bath Nature and Polymer–Solvent Affinity." *Polymers* 15 (21): 4307. https://doi.org/10.3390/polym15214307.

Bauso, Luana Vittoria, Valeria La Fauci, Clelia Longo, and Giovanna Calabrese. 2024. "Bone Tissue Engineering and Nanotechnology: A Promising Combination for Bone Regeneration." *Biology* 13 (4): 237. https://doi.org/10.3390/biology13040237.

Benaddi, Aurelie Ohana, Orit Cohen, Krzysztof Matyjaszewski, and Michael S. Silverstein. 2021. "RAFT Polymerization within High Internal Phase Emulsions: Porous Structures, Mechanical Behaviors, and Uptakes." *Polymer* 213 (8): 123327. https://doi.org/10.1016/j.polymer.2020.123327.

Benkaddour, Abdelhaq, Khalil Jradi, Sylvain Robert, and Claude Daneault. 2013. "Study of the Effect of Grafting Method on Surface Polarity of Tempo-Oxidized Nanocellulose Using Polycaprolactone as the Modifying Compound: Esterification versus Click-Chemistry." *Nanomaterials* 3 (4): 638–54. https://doi.org/10.3390/nano3040638.

Bernardo P. Marcela, Bruna C. R. da Silva, Ahmed E. I. Hamouda, Marcelo A. S. de Toledo, Carmen Schalla, Stephan Rütten, Roman Goetzke, Luiz H. C. Mattoso, Martin Zenke, and Antonio Sechi. 2022. "PLA/Hydroxyapatite Scaffolds Exhibit in Vitro Immunological Inertness and Promote Robust Osteogenic Differentiation of Human Mesenchymal Stem Cells without Osteogenic Stimuli." *Scientific Reports* 12 (1): 2333. https://doi.org/10.1038/s41598-022-05207-w.

Bhardwaj, Nandana, and Subhas C. Kundu. 2010. "Electrospinning: A Fascinating Fiber

Fabrication Technique." *Biotechnology Advances* 28 (3): 325–47. https://doi.org/10.1016/j.biotechadv.2010.01.004.

Bhushan, Sakchi, Sandhya Singh, Tushar Kanti Maiti, Chhavi Sharma, Dharm Dutt, Shubham Sharma, Changhe Li, and Elsayed Mohamed Tag Eldin. 2022. "Scaffold Fabrication Techniques of Biomaterials for Bone Tissue Engineering: A Critical Review." *Bioengineering* 9 (12): 728. https://doi.org/10.3390/bioengineering9120728.

Bîrcă, Alexandra, Oana Gherasim, Valentina Grumezescu, and Alexandru Mihai Grumezescu. 2019. "Introduction in Thermoplastic and Thermosetting Polymers." In *Materials for Biomedical Engineering*, 1–28. https://doi.org/10.1016/B978-0-12-816874-5.00001-3.

Biron, Michel. 2016. "Mechanical Properties." *In Material Selection for Thermoplastic Parts*, 261–337. https://doi.org/10.1016/B978-0-7020-6284-1.00007-6.

Blumer J.F. Michael. 2021. "Bone Tissue and Histological and Molecular Events during Development of the Long Bones." *Annals of Anatomy* 235 (1): 151704. https://doi.org/10.1016/j.aanat.2021.151704.

Bokhari, A. Maria, Galip Akay, Shuguang Zhang, and Mark A. Birch. 2005. "The Enhancement of Osteoblast Growth and Differentiation in Vitro on a Peptide Hydrogel - PolyHIPE Polymer Hybrid Material." *Biomaterials* 26 (25): 5198–5208. https://doi.org/10.1016/j.biomaterials.2005.01.040.

Bolívar-Monsalve, Edna Johana, Mario Moisés Alvarez, Samira Hosseini, Michelle Alejandra Espinosa-Hernandez, Carlos Fernando Ceballos-González, Margarita Sanchez-Dominguez, Su Ryon Shin, et al. 2021. "Engineering Bioactive Synthetic Polymers for Biomedical Applications: A Review with Emphasis on Tissue Engineering and Controlled Release." *Materials Advances* 2 (14): 4447–78. https://doi.org/10.1039/d1ma00092f.

Busby Wendy, Neil R. Cameron, and Colin A.B. Jahoda. 2001. "Emulsion-Derived Foams (PolyHIPEs) Containing Poly(Sε-Caprolactone) as Matrixes for Tissue Engineering." *Biomacromolecules* 2 (1): 154–64. https://doi.org/10.1021/bm0000889.

Busby, Wendy, Neil R. Cameron, and Colin A.B. Jahoda. 2002. "Tissue Engineering Matrixes by Emulsion Templating." *Polymer International* 51 (10): 871–81. https://doi.org/10.1002/pi.934.

Cabezas-Sáinz Pablo, Alba Pensado-López, Sáinz Bruno, and Sánchez Laura. 2020. "Modeling Cancer Using Zebrafish Xenografts : Drawbacks for Mimicking The." *Cells Review* 9 (1978): 1–29. https://doi.org/10.3390/cells9091978.

Caldwell, Sally, David W. Johnson, Matthew P. Didsbury, Bridgid A. Murray, Jun Jie Wu, Stefan A. Przyborski, and Neil R. Cameron. 2012. "Degradable Emulsion-Templated Scaffolds for Tissue Engineering from Thiol-Ene Photopolymerisation." *Soft Matter* 8 (40): 10344–51. https://doi.org/10.1039/c2sm26250a.

Capuana, Elisa, Francesco Lopresti, Francesco Carfì Pavia, Valerio Brucato, and Vincenzo La Carrubba. 2021. "Solution-Based Processing for Scaffold Fabrication in Tissue Engineering Applications: A Brief Review." *Polymers* 13 (13): 2041. https://doi.org/10.3390/polym13132041.

Carnachan J. Ross, Maria Bokhari, Stefan A. Przyborski, and Neil R. Cameron. 2006. "Tailoring the Morphology of Emulsion-Templated Porous Polymers." *Soft Matter* 2 (7): 608. https://doi.org/10.1039/b603211g.

Castillo-Henríquez, Luis, Rolando Vargas-Zúñiga, Jorge Pacheco-Molina, and Jose Vega-Baudrit. 2020. "Electrospun Nanofibers: A Nanotechnological Approach for Drug Delivery and Dissolution Optimization in Poorly Water-Soluble Drugs." *ADMET and DMPK* 8 (4): 325–53. https://doi.org/10.5599/admet.844.

Chan, B. P., and Sarah K. W. Leong. 2008. "Scaffolding in Tissue Engineering: General Approaches and Tissue-Specific Considerations." *European Spine Journal* 17 (4): 1-13. https://doi.org/10.1007/s00586-008-0745-3.

Cheerarot, Onanong, and Sunan Saikrasun. 2023. "Effects of Different Preparation Methods (Solvent Casting and Melt Blending) on Properties of Chitosan-Filled Polylactic Acid Biocomposite Films." *Journal of Elastomers & Plastics* 55 (8): 1173–98. https://doi.org/10.1177/00952443231198468.

Chen, Fulin, Chuen N. Lee, and Swee H. Teoh. 2007. "Nanofibrous Modification on Ultra-Thin Poly(e-Caprolactone) Membrane via Electrospinning." *Materials Science and Engineering C* 27 (2): 325–32. https://doi.org/10.1016/j.msec.2006.05.004.

Chen, Jyh Herng, Thi Tuyet Mai Le, and Kai Chung Hsu. 2018. "Application of PolyHIPE Membrane with Tricaprylmethylammonium Chloride for Cr(VI) Ion Separation: Parameters and Mechanism of Transport Relating to the Pore Structure." *Membranes* 8 (1): 11. https://doi.org/10.3390/membranes8010011.

Chen, Shixuan, Ruiquan Li, Xiaoran Li, and Jingwei Xie. 2018. “Electrospinning: An Enabling Nanotechnology Platform for Drug Delivery and Regenerative Medicine.” *Advanced Drug Delivery Reviews* 132 (7): 188–213. https://doi.org/10.1016/j.addr.2018.05.001.

Chiu, Yu-Chieh, Ming-Huei Cheng, Holger Engel, Shu-Wei Kao, Jeffery C. Larson, Shreya Gupta, and Eric M. Brey. 2011. “The Role of Pore Size on Vascularization and Tissue Remodeling in PEG Hydrogels.” *Biomaterials* 32 (26): 6045–51. https://doi.org/10.1016/j.biomaterials.2011.04.066.

Conoscenti, Gioacchino, Tobias Schneider, Katharina Stoelzel, Francesco Carfì Pavia, Valerio Brucato, Clemens Goegele, Vincenzo La Carrubba, and Gundula Schulze-Tanzil. 2017. “PLLA Scaffolds Produced by Thermally Induced Phase Separation (TIPS) Allow Human Chondrocyte Growth and Extracellular Matrix Formation Dependent on Pore Size.” *Materials Science and Engineering: C* 80 (1): 449–59. https://doi.org/10.1016/j.msec.2017.06.011.

Corti, Marco, Enrica Calleri, Sara Perteghella, Anna Ferrara, Roberto Tamma, Chiara Milanese, Delia Mandracchia, et al. 2019. “Polyacrylate/Polyacrylate-PEG Biomaterials Obtained by High Internal Phase Emulsions (HIPEs) with Tailorable Drug Release and Effective Mechanical and Biological Properties.” *Materials Science and Engineering C* 105 (7): 110060. https://doi.org/10.1016/j.msec.2019.110060.

Dahlin L. Rebecca, Kurtis F. Kasper, and Antonios G. Mikos. 2011. “Polymeric Nanofibers in Tissue Engineering.” *Tissue Engineering Part B: Reviews* 17 (5): 349–64. https://doi.org/10.1089/ten.teb.2011.0238.

Deliormanlı, Aylin M., and Harika Atmaca. 2020. “Effect of Pore Architecture on the Mesenchymal Stem Cell Responses to Graphene/Polycaprolactone Scaffolds Prepared by Solvent Casting and Robocasting.” *Journal of Porous Materials* 27 (1): 49–61. https://doi.org/10.1007/s10934-019-00791-1.

Devi, Yashaswini, Ashwini Prabhu, Sukumaran Anil, and Jayachandran Venkatesan. 2021. “Preparation and Characterization of Dexamethasone Loaded Sodium Alginate-Graphene Oxide Microspheres for Bone Tissue Engineering.” *Journal of Drug Delivery Science and Technology* 64 (8): 102624. https://doi.org/10.1016/j.jddst.2021.102624.

Dikici, Betül Aldemir, Serkan Dikici, Gwendolen C. Reilly, Sheila MacNeil, and Frederik Claeyssens. 2019. “A Novel Bilayer Polycaprolactone Membrane for Guided Bone Regeneration: Combining Electrospinning and Emulsion Templating.” *Materials* 12 (16): 2643. https://doi.org/10.3390/ma12162643.

Drobota, Mioara, Stefan Ursache, and Magdalena Aflori. 2022. “Surface Functionalities of Polymers for Biomaterial Applications.” *Polymers* 14 (12): 2307. https://doi.org/10.3390/polym14122307.

Duchstein, Patrick, and Dirk Zahn. 2011. “Atomistic Modeling of Apatite-Collagen Composites from Molecular Dynamics Simulations Extended to Hyperspace.” *Journal of Molecular Modeling* 17 (1): 73–79. https://doi.org/10.1007/s00894-010-0707-7.

Dumur, Frédéric. 2023. “Recent Advances on Water-Soluble Photoinitiators of Polymerization.” *European Polymer Journal* 189 (5): 111942. https://doi.org/10.1016/j.eurpolymj.2023.111942.

Eltom, Abdalla, Gaoyan Zhong, and Ameen Muhammad. 2019. “Scaffold Techniques and Designs in Tissue Engineering Functions and Purposes: A Review.” *Advances in Materials Science and Engineering* 2019 (3): 1–13. https://doi.org/10.1155/2019/3429527.

Feng, Xu. 2009. “Chemical and Biochemical Basis of Cell-Bone Matrix Interaction in Health and Disease.” *Current Chemical Biology* 3 (2): 189–96. https://doi.org/10.2174/187231309788166398.

Fernandes J. Russell, Michael A. Harkey, Maryann Weis, Jennifer W. Askew, and David R. Eyre. 2007. “The Post-Translational Phenotype of Collagen Synthesized by SAOS-2 Osteosarcoma Cells.” *Bone* 40 (5): 1343–51. https://doi.org/10.1016/j.bone.2007.01.011.

Field Jonathan, John W. Haycock, Fiona M. Boissonade, and Frederik Claeyssens. 2021. “A Tuneable, Photocurable, Poly(Caprolactone)-Based Resin for Tissue Engineering—Synthesis, Characterisation and Use in Stereolithography.” *Molecules* 26 (5): 1199. https://doi.org/10.3390/molecules26051199.

Fleith Sandrine, Arnaud Ponche, Reine Bareille, Joëlle Amédée, and Michael Nardin. 2005. “Effect of Several Sterilisation Techniques on Homogeneous Self Assembled Monolayers.” *Colloids and Surfaces B: Biointerfaces* 44 (1): 15–24. https://doi.org/10.1016/j.colsurfb.2005.05.009.

Fogh, Jørgen, William C. Wright, and James D. Loveless. 1977. “Absence of HeLa Cell Contamination in 169 Cell Lines Derived from Human Tumors.” *Journal of the National Cancer Institute* 58 (2): 209–14. https://doi.org/10.1093/jnci/58.2.209.

Fratzl Peter, Hari S. Gupta, Eleftherios P. Paschalis, and Andreas Roschger. 2004. "Structure and Mechanical Quality of the Collagen–Mineral Nano-Composite in Bone." *J. Mater. Chem.* 14 (14): 2115–23. https://doi.org/10.1039/B402005G.

Fuchs K. Robyn, William R. Thompson, and Stuart J. Warden. 2018. *Bone Biology*. *Bone Repair Biomaterials: Regeneration and Clinical Applications, Second Edition*. 15-52. https://doi.org/10.1016/B978-0-08-102451-5.00002-0.

Garcia, Jan Ulric, Tatsuhiro Iwama, Eva Y. Chan, Douglas R. Tree, Kris T. Delaney, and Glenn H. Fredrickson. 2020. "Mechanisms of Asymmetric Membrane Formation in Nonsolvent-Induced Phase Separation." *ACS Macro Letters* 9 (11): 1617–24. https://doi.org/10.1021/acsmacrolett.0c00609.

Ghalia, Mustafa Abu, and Yaser Dahman. 2016. "Advanced Nanobiomaterials in Tissue Engineering." In *Nanobiomaterials in Soft Tissue Engineering*, 141–72. https://doi.org/10.1016/B978-0-323-42865-1.00006-4.

Gunatillake, Pathiraja Arachchillage and Raju Adhikari. 2003. "Biodegradable Synthetic Polymers for Tissue Engineering." *European Cells and Materials* 5: 1–16. https://doi.org/10.22203/eCM.v005a01.

Gupta, Deepak, Atul Kumar Singh, Neelakshi Kar, Ashwin Dravid, and Jayesh Bellare. 2019. "Modelling and Optimization of NaOH-Etched 3-D Printed PCL for Enhanced Cellular Attachment and Growth with Minimal Loss of Mechanical Strength." *Materials Science and Engineering C* 98 (7): 602–11. https://doi.org/10.1016/j.msec.2018.12.084.

Hales, Thomas. 2005. "A Proof of the Kepler Conjecture." *Annals of Mathematics* 162 (3): 1065–1185. https://doi.org/10.4007/annals.2005.162.1065.

Hesari, Sahar M, Farimah Ghorbani, Farnaz Ghorbani, Ali Zamanian, and Alireza Khavandi. 2021. "Plasma Surface Modification Technique–Induced Gelatin Grafting on Bio-Originated Polyurethane Porous Matrix: Physicochemical and in Vitro Study." *Polymers and Polymer Composites* 29 (6): 640–51. https://doi.org/10.1177/0967391120929076.

Ho, Ming-Hua, Pei-Yun Kuo, Hsyue-Jen Hsieh, Tzu-Yang Hsien, Lein-Tuan Hou, Juin-Yih Lai, and Da-Ming Wang. 2004. "Preparation of Porous Scaffolds by Using Freeze-Extraction and Freeze-Gelation Methods." *Biomaterials* 25 (1): 129–38. https://doi.org/10.1016/S0142-9612(03)00483-6.

Hong, Ziyi, Shaohui Wang, and Fengyu Liu. 2024. “Synthesis of Tubular Hydroxyapatite and Its Application in Polycaprolactone Scaffold Materials.” *Journal of Functional Biomaterials* 15 (1): 22. https://doi.org/10.3390/jfb15010022.

Hutmacher, Dietmar Werner, Jan Thorsten Schantz, Christopher Xu Fu Lam, Kim Cheng Tan, and Thiam Chye Lim. 2007. “State of the Art and Future Directions of Scaffold-Based Bone Engineering from a Biomaterials Perspective.” *Journal of Tissue Engineering and Regenerative Medicine* 1 (4): 245–60. https://doi.org/10.1002/term.24.

Ielo, Ileana, Giovanna Calabrese, Giovanna De Luca, and Sabrina Conoci. 2022. “Recent Advances in Hydroxyapatite-Based Biocomposites for Bone Tissue Regeneration in Orthopedics.” *International Journal of Molecular Sciences* 23 (17): 9721. https://doi.org/10.3390/ijms23179721.

Jacobs, Tinneke, Rino Morent, Nathalie De Geyter, Peter Dubruel, and Christophe Leys. 2012. “Plasma Surface Modification of Biomedical Polymers: Influence on Cell-Material Interaction.” *Plasma Chemistry and Plasma Processing* 32 (5): 1039–73. https://doi.org/10.1007/s11090-012-9394-8.

Jaidev, L. R. Chakka, and Kaushik Chatterjee. 2019. “Surface Functionalization of 3D Printed Polymer Scaffolds to Augment Stem Cell Response.” *Materials and Design* 161: 44–54. https://doi.org/10.1016/j.matdes.2018.11.018.

Jain, Krishan G., Sujata Mohanty, Alok R. Ray, Rajesh Malhotra, and Balram Airan. 2015. “Culture & Differentiation of Mesenchymal Stem Cell into Osteoblast on Degradable Biomedical Composite Scaffold: In Vitro Study.” *Indian Journal of Medical Research* 142 (6): 747. https://doi.org/10.4103/0971-5916.174568.

Janmohammadi, Mahsa, Mohammad Sadegh Nourbakhsh, Marjan Bahraminasab, and Lobat Tayebi. 2023. “Effect of Pore Characteristics and Alkali Treatment on the Physicochemical and Biological Properties of a 3D-Printed Polycaprolactone Bone Scaffold.” *ACS Omega* 8 (8): 7378–94. https://doi.org/10.1021/acsomega.2c05571.

Javid-Naderi, Mohammad Javad, Javad Behravan, Negar Karimi-Hajishohreh, and Shirin Toosi. 2023. “Synthetic Polymers as Bone Engineering Scaffold.” *Polymers for Advanced Technologies* 34 (7): 2083–96. https://doi.org/10.1002/pat.6046.

Jiang, Jiang, Mark A. Carlson, Matthew J. Teusink, Hongjun Wang, Matthew R. MacEwan, and Jingwei Xie. 2015. “Expanding Two-Dimensional Electrospun Nanofiber Membranes in the Third Dimension By a Modified Gas-Foaming

Technique." *ACS Biomaterials Science & Engineering* 1 (10): 991–1001. https://doi.org/10.1021/acsbiomaterials.5b00238.

Jiao, Juyang, Qimin Hong, Dachen Zhang, Minqi Wang, Haozheng Tang, Jingzhou Yang, Xinhua Qu, and Bing Yue. 2023. "Influence of Porosity on Osteogenesis, Bone Growth and Osteointegration in Trabecular Tantalum Scaffolds Fabricated by Additive Manufacturing." *Frontiers in Bioengineering and Biotechnology* 11: 1117954. https://doi.org/10.3389/fbioe.2023.1117954.

Jirofti, Nafiseh, Davod Mohebbi-Kalhori, and Ramin Masoumi. 2022. "Enhancing Biocompatibility of PCL/PU Nano-Structures to Control the Water Wettability by NaOH Hydrolysis Treatment for Tissue Engineering Applications." *Journal of Industrial Textiles* 51 (2): 3278–96. https://doi.org/10.1177/1528083720963268.

Johnson W. Drew, Caitlin R. Langford, M. P. Didsbury, Benjamin Lipp, Stefan A. Przyborski, and Neil R. Cameron. 2015. "Fully Biodegradable and Biocompatible Emulsion Templated Polymer Scaffolds by Thiol-Acrylate Polymerization of Polycaprolactone Macromonomers." *Polymer Chemistry* 6 (41): 7256–63. https://doi.org/10.1039/c5py00721f.

Jongprateep, Oratai, Nonthaporn Jitanukul, Khotamy Saphongxay, Benjamon Petchareanmongkol, Ampika Bansiddhi, Apirat Laobuthee, Amornrat Lertworasirikul, and Ratchatee Techapiesancharoenkij. 2022. "Hydroxyapatite Coating on an Aluminum/Bioplastic Scaffold for Bone Tissue Engineering." *RSC Advances* 12 (41): 26789–99. https://doi.org/10.1039/D2RA03285F.

Jung, Jun Tae, Jeong F. Kim, Ho Hyun Wang, Emanuele di Nicolo, Enrico Drioli, and Young Moo Lee. 2016. "Understanding the Non-Solvent Induced Phase Separation (NIPS) Effect during the Fabrication of Microporous PVDF Membranes via Thermally Induced Phase Separation (TIPS)." *Journal of Membrane Science* 514 (9): 250–63. https://doi.org/10.1016/j.memsci.2016.04.069.

Karaca, Ilayda, and Betül Aldemir Dikici. 2024. "Quantitative Evaluation of the Pore and Window Sizes of Tissue Engineering Scaffolds on Scanning Electron Microscope Images Using Deep Learning." *ACS Omega* 9 (23): 24695–706. https://doi.org/10.1021/acsomega.4c01234.

Khan, Barkat Ali, Naveed Akhtar, Haji Muhammad Shoaib Khan, Khalid Waseem, Tariq Mahmood, Akhtar Rasul, Muhammad Iqbal, and Haroon Khan. 2011. "Basics of Pharmaceutical Emulsions: A Review." *African Journal of Pharmacy and Pharmacology* 5 (25): 2715–25. https://doi.org/10.5897/AJPP11.698.

Kim, Ha Sung, Jong Keun Seon, and Ah Reum Jo. 2013. “Current Trends in Anterior Cruciate Ligament Reconstruction.” *Knee Surgery and Related Research* 25 (4): 165–73. https://doi.org/10.5792/ksrr.2013.25.4.165.

Klawitter, Jonathan J., Jennifer. J. Bagwell, Miriam Weinstein, Braun. W. Sauer, and Benjamin J. R. Pruitt. 1976. “An Evaluation of Bone Growth into Porous High Density Polyethylene.” *Journal of Biomedical Materials Research* 10 (2): 311–23. https://doi.org/10.1002/jbm.820100212.

Koga, Yoshikatsu, and Atsushi Ochiai. 2019. “Systematic Review of Patient-Derived Xenograft Models for Preclinical Studies of Anti-Cancer Drugs in Solid Tumors.” *Cells* 8 (5): 418. https://doi.org/10.3390/cells8050418.

Kohnken, Rebecca, Pierluigi Porcu, and Anjali Mishra. 2017. “Overview of the Use of Murine Models in Leukemia and Lymphoma Research.” *Frontiers in Oncology* 7 (22): 1-11. https://doi.org/10.3389/fonc.2017.00022.

Kouhi, Monireh, Mohammadhossein Fathi, Molamma P. Prabhakaran, Morteza Shamanian, and Seeram Ramakrishna. 2018. “Enhanced Proliferation and Mineralization of Human Fetal Osteoblast Cells on PHBV-Bredigite Nanofibrous Scaffolds.” *Materials Today: Proceedings* 5 (7): 15702–9. https://doi.org/10.1016/j.matpr.2018.04.181.

Koymen, Safiye Selin, Nazmiye Donmez, Vildan Betul Yenigun, Fatemeh Bahadori, and Abdurrahim Kocyigit. 2022. “Investigating the Cytotoxicity of Dual-Cure Bulk-Fill Resin Materials on L929 Cells.” *Prosthesis* 4 (3): 447–57. https://doi.org/10.3390/prosthesis4030036.

Krajnc, Peter, Dejan Štefanec, and Irena Pulko. 2005. “Acrylic Acid ‘Reversed’ PolyHIPEs.” *Macromolecular Rapid Communications* 26 (16): 1289–93. https://doi.org/10.1002/marc.200500353.

Kravchenko, Oleksandr G., Gabriel Gedler, Sergii G. Kravchenko, Donald L. Feke, and Ica Manas-Zloczower. 2018. “Modeling Compressive Behavior of Open-Cell Polymerized High Internal Phase Emulsions: Effects of Density and Morphology.” *Soft Matter* 14 (9): 1637–46. https://doi.org/10.1039/C7SM02043K.

Kumar, Abinash, and Anu Jacob. 2022. “Techniques in Scaffold Fabrication Process for Tissue Engineering Applications: A Review.” *Journal of Applied Biology & Biotechnology* 10 (3): 163–76. https://doi.org/10.7324/JABB.2022.100321.

Lackner, Juergen M., Claudia Meindl, Christian Wolf, Alexander Fian, Clemens Kittinger, Marcin Kot, Lukasz Major, et al. 2013. “Gas Permeation, Mechanical Behavior and Cytocompatibility of Ultrathin Pure and Doped Diamond-like Carbon and Silicon Oxide Films.” *Coatings* 3 (4): 268–300. https://doi.org/10.3390/coatings3040268.

Latour, Robert. 2008. “Biomaterials: Protein–Surface Interactions.” In *Encyclopedia of Biomaterials and Biomedical Engineering, Second Edition - Four Volume Set*, 270–84. https://doi.org/10.1201/b18990-27.

Lee, Hwa Sun, Soo Hwan Byun, Seoung Won Cho, and Byoung Eun Yang. 2019. “Past, Present, and Future of Regeneration Therapy in Oral and Periodontal Tissue: A Review.” *Applied Sciences (Switzerland)* 9 (6): 1-19. https://doi.org/10.3390/app9061046.

Lee, Seunghun S., Xiaoyu Du, Inseon Kim, and Stephen J. Ferguson. 2022. “Scaffolds for Bone-Tissue Engineering.” *Matter* 5 (9): 2722–59. https://doi.org/10.1016/j.matt.2022.06.003.

Lee, Sungsoo S., Brian J. Huang, Stuart R. Kaltz, Shantanu Sur, Christina J. Newcomb, Stuart R. Stock, Ramille N. Shah, and Samuel I. Stupp. 2013. “Bone Regeneration with Low Dose BMP-2 Amplified by Biomimetic Supramolecular Nanofibers within Collagen Scaffolds.” *Biomaterials* 34 (2): 452–59. https://doi.org/10.1016/j.biomaterials.2012.10.005.

Li, Jinyu, Hao Huang, Taotao Xu, Jinsheng Li, Tailin Guo, Xiong Lu, Jing Ren, Xiaohua Ren, Yandong Mu, and Jie Weng. 2022. “Effect of the Interconnecting Window Diameter of Hydroxyapatite Scaffolds on Vascularization and Osteoinduction.” *Ceramics International* 48 (17): 25070–78. https://doi.org/10.1016/j.ceramint.2022.05.162.

Li, Lei, and You-Lo Hsieh. 2005. “Ultra-Fine Polyelectrolyte Hydrogel Fibres from Poly(Acrylic Acid)/Poly(Vinyl Alcohol).” *Nanotechnology* 16 (12): 2852–60. https://doi.org/10.1088/0957-4484/16/12/020.

Li, Wei, Bo Jiao, Sisheng Li, Shah Faisal, Aimin Shi, Weiming Fu, Yiying Chen, and Qiang Wang. 2022. “Recent Advances on Pickering Emulsions Stabilized by Diverse Edible Particles: Stability Mechanism and Applications.” *Frontiers in Nutrition* 9 (5): 1–17. https://doi.org/10.3389/fnut.2022.864943.

Li, Ya, Jiadeng Zhu, Hui Cheng, Guoqing Li, Hyunjin Cho, Mengjin Jiang, Qiang Gao, and Xiangwu Zhang. 2021. “Developments of Advanced Electrospinning

Techniques: A Critical Review." *Advanced Materials Technologies* 6 (11): 1-29. https://doi.org/10.1002/admt.202100410.

Liang, Xiangyu, Yongli Qi, Zhen Pan, Yao He, Xiangnan Liu, Shuquan Cui, and Jiandong Ding. 2018. "Design and Preparation of Quasi-Spherical Salt Particles as Water-Soluble Porogens to Fabricate Hydrophobic Porous Scaffolds for Tissue Engineering and Tissue Regeneration." *Materials Chemistry Frontiers* 2 (8): 1539–53. https://doi.org/10.1039/C8QM00152A.

Liu, Jingyu, and Cheng Yan. 2018. "3D Printing of Scaffolds for Tissue Engineering." *In 3D Printing*. 1-18. https://doi.org/10.5772/intechopen.78145.

Loh, Qiu Li, and Cleo Choong. 2013. "Three-Dimensional Scaffolds for Tissue Engineering Applications: Role of Porosity and Pore Size." *Tissue Engineering Part B: Reviews* 19 (6): 485–502. https://doi.org/10.1089/ten.teb.2012.0437.

Lotfi, Mahmoud, Mohamed Nejib, and Mohamed Naceur. 2013. "Cell Adhesion to Biomaterials: Concept of Biocompatibility." In *Advances in Biomaterials Science and Biomedical Applications*. InTech. 1-34. https://doi.org/10.5772/53542.

Louis D. V. Johnson, Mina Aleemardani, Simon Atkins, Fiona M. Boissonade, and Frederik Claeyssens. 2024. "Emulsion Templated Composites: Porous Nerve Guidance Conduits for Peripheral Nerve Regeneration." *Materials & Design* 239 (3): 112779. https://doi.org/10.1016/j.matdes.2024.112779.

Lyu, Zhonglin, Qian Yu, and Hong Chen. 2016. "Interactions of Biomaterial Surfaces with Proteins and Cells. " *Polymeric Biomaterials for Tissue Regeneration: From Surface/Interface Design to 3D Constructs*. 103-121. https://doi.org/10.1007/978-981-10-2293-7_5.

Ma, Yuyao, Yuxia Ma, Min Liu, Yang Chen, Xun Hu, Zhengmao Ye, and Dehua Dong. 2019. "Study on Nanofibrous Catalysts Prepared by Electrospinning for Methane Partial Oxidation." *Catalysts* 9 (5): 479. https://doi.org/10.3390/catal9050479.

Ma, Zuwei, Changyou Gao, and Jiacong Shen. 2003. "Surface Modification of Poly-L-Lactic Acid (PLLA) Membrane by Grafting Acrylamide: An Effective Way to Improve Cytocompatibility for Chondrocytes." *Journal of Biomaterials Science, Polymer Edition* 14 (1): 13–25. https://doi.org/10.1163/15685620360511119.

Maghsoudi, Saeid, Bahareh Taghavi Shahraki, Navid Rabiee, Yousef Fatahi, Rassoul Dinarvand, Maryam Tavakolizadeh, Sepideh Ahmadi, et al. 2020. "Burgeoning

Polymer Nano Blends for Improved Controlled Drug Release: A Review." *International Journal of Nanomedicine* 15: 4363–92. https://doi.org/10.2147/IJN.S252237.

Malikmammadov, Elbay, Tugba Endogan Tanir, Aysel Kiziltay, Vasif Hasirci, and Nesrin Hasirci. 2018. "PCL and PCL-Based Materials in Biomedical Applications." *Journal of Biomaterials Science, Polymer Edition*. 29(7-9): 863-893. https://doi.org/10.1080/09205063.2017.1394711.

Mankin, Henry J., Francis J. Hornicek, and Kevin A. Raskin. 2005. "Infection in Massive Bone Allografts." *Clinical Orthopaedics and Related Research* 432 (432): 210–16. https://doi.org/10.1097/01.blo.0000150371.77314.52.

Márquez, Andrés L., Alejandra Medrano, Luis A. Panizzolo, and Jorge R. Wagner. 2010. "Effect of Calcium Salts and Surfactant Concentration on the Stability of Water-in-Oil (w/o) Emulsions Prepared with Polyglycerol Polyricinoleate." *Journal of Colloid and Interface Science* 341 (1): 101–8. https://doi.org/10.1016/j.jcis.2009.09.020.

Marrale, Jonathan, Matthew C. Morrissey, and Fares S. Haddad. 2007. "A Literature Review of Autograft and Allograft Anterior Cruciate Ligament Reconstruction." *Knee Surgery, Sports Traumatology, Arthroscopy* 15 (6): 690–704. https://doi.org/10.1007/s00167-006-0236-1.

Massy, Jim. 2017. "Thermoplastic and Thermosetting Polymers." *In: A Little Book about BIG Chemistry,* 19–26. https://doi.org/10.1007/978-3-319-54831-9_5.

Mavis, Bora, Tolga T. Demirtaş, Menemşe Gümüşderelioğlu, Güngör Gündüz, and Üner Çolak. 2009. "Synthesis, Characterization and Osteoblastic Activity of Polycaprolactone Nanofibers Coated with Biomimetic Calcium Phosphate." *Acta Biomaterialia* 5 (8): 3098–3111. https://doi.org/10.1016/j.actbio.2009.04.037.

McDonald, Samantha M., Quansan Yang, Yen Hao Hsu, Shantanu P. Nikam, Ziying Hu, Zilu Wang, Darya Asheghali, et al. 2023. "Resorbable Barrier Polymers for Flexible Bioelectronics." *Nature Communications* 14 (1): 7299. https://doi.org/10.1038/s41467-023-42775-5.

Meeremans, Marguerite, Gerlinde R. Van de Walle, Sandra Van Vlierberghe, and Catharina De Schauwer. 2021. "The Lack of a Representative Tendinopathy Model Hampers Fundamental Mesenchymal Stem Cell Research." *Frontiers in Cell and Developmental Biology* 9: 1-28. https://doi.org/10.3389/fcell.2021.651164.

Meneses, João, João C. Silva, Sofia R. Fernandes, Abhishek Datta, Frederico Castelo Ferreira, Carla Moura, Sandra Amado, Nuno Alves, and Paula Pascoal-Faria. 2020. "A Multimodal Stimulation Cell Culture Bioreactor for Tissue Engineering: A Numerical Modelling Approach." *Polymers* 12 (4): 940. https://doi.org/10.3390/POLYM12040940.

Menut, Paul, Su S. Yushen, Watchanida. Chinpa, C. Pochat-Bohatier, André Deratani, Ming, D. Wang, Patrice Huguet, Chunyin Kuo, Juin-Yih Lai, and Claude Dupuy. 2008. "A Top Surface Liquid Layer during Membrane Formation Using Vapor-Induced Phase Separation (VIPS)—Evidence and Mechanism of Formation." *Journal of Membrane Science* 310 (1–2): 278–88. https://doi.org/10.1016/j.memsci.2007.11.016.

Metwally, Sara, and Urszula Stachewicz. 2019. "Surface Potential and Charges Impact on Cell Responses on Biomaterials Interfaces for Medical Applications." *Materials Science and Engineering: C* 104: 109883. https://doi.org/10.1016/j.msec.2019.109883.

Moghadam M. Zahedi, Shadi Hassanajili, Feridun Esmaeilzadeh, Maryam Ayatollahi, and Misagh Ahmadi. 2017. "Formation of Porous HPCL/LPCL/HA Scaffolds with Supercritical CO2 Gas Foaming Method." *Journal of the Mechanical Behavior of Biomedical Materials* 69 (1): 115–27. https://doi.org/10.1016/j.jmbbm.2016.12.014.

Moglia, Robert, Michael Whitely, Megan Brooks, Jennifer Robinson, Michael Pishko, and Elizabeth Cosgriff-Hernandez. 2014. "Solvent-Free Fabrication of PolyHIPE Microspheres for Controlled Release of Growth Factors." *Macromolecular Rapid Communications* 35 (14): 1301–5. https://doi.org/10.1002/marc.201400145.

Mohapatra, Subrajeet. 2017. "Sterilization and Disinfection." *Essentials of Neuroanesthesia*, 929–44. https://doi.org/10.1016/B978-0-12-805299-0.00059-2.

Mudassir, Muhammad Ahmad, Hafiz Zohaib Aslam, Tariq Mahmood Ansari, Haifei Zhang, and Irshad Hussain. 2021. "Fundamentals and Design-Led Synthesis of Emulsion-Templated Porous Materials for Environmental Applications." *Advanced Science* 8 (22): 1-60. https://doi.org/10.1002/advs.202102540.

Murphy, Ciara M., Matthew G. Haugh, and Fergal J. O'Brien. 2010. "The Effect of Mean Pore Size on Cell Attachment, Proliferation and Migration in Collagen–Glycosaminoglycan Scaffolds for Bone Tissue Engineering." *Biomaterials* 31 (3): 461–66. https://doi.org/10.1016/j.biomaterials.2009.09.063.

Murray, Eoin, Brianna C. Thompson, Sepidar Sayyar, and Gordon G. Wallace. 2015. "Enzymatic Degradation of Graphene/Polycaprolactone Materials for Tissue Engineering." *Polymer Degradation and Stability* 111: 71–77. https://doi.org/10.1016/j.polymdegradstab.2014.10.010.

Nedeljkovic, Ivana, Behrouz Zandieh Doulabi, Marwa Abdelaziz, Albert J. Feilzer, Rob A.M. Exterkate, Slawomir Szafert, Nurbey Gulia, Ivo Krejci, and Cornelis J. Kleverlaan. 2022. "Cytotoxicity and Anti-Biofilm Properties of Novel Hybrid-Glass-Based Caries Infiltrant." *Dental Materials* 38 (12): 2052–61. https://doi.org/10.1016/j.dental.2022.11.018.

Nemani, Srinivasa Kartik, Rama Kishore Annavarapu, Behrouz Mohammadian, Asif Raiyan, Jamie Heil, Md Ashraful Haque, Ahmed Abdelaal, and Hossein Sojoudi. 2018. "Surface Modification of Polymers: Methods and Applications." *Advanced Materials Interfaces* 5 (24): 1–26. https://doi.org/10.1002/admi.201801247.

Nikolov, Svetoslav, and Dierk Raabe. 2008. "Hierarchical Modeling of the Elastic Properties of Bone at Submicron Scales: The Role of Extrafibrillar Mineralization." *Biophysical Journal* 94 (11): 4220–32. https://doi.org/10.1529/biophysj.107.125567.

Niu, Yifan, Lei Chen, and Tianfu Wu. 2023. "Recent Advances in Bioengineering Bone Revascularization Based on Composite Materials Comprising Hydroxyapatite." *International Journal of Molecular Sciences* 24 (15): 12492. https://doi.org/10.3390/ijms241512492.

Nogueira, João C. F., Ketevan Paliashvili, Alexandra Bradford, Francesco Di Maggio, Daniel A. Richards, Richard M. Day, and Vijay Chudasama. 2020. "Functionalised Thermally Induced Phase Separation (TIPS) Microparticles Enabled for 'Click' Chemistry." *Organic & Biomolecular Chemistry* 18 (12): 2215–18. https://doi.org/10.1039/D0OB00106F.

O'Brien, John, Ian Wilson, Terry Orton, and François Pognan. 2000. "Investigation of the Alamar Blue (Resazurin) Fluorescent Dye for the Assessment of Mammalian Cell Cytotoxicity." *European Journal of Biochemistry* 267 (17): 5421–26. https://doi.org/10.1046/j.1432-1327.2000.01606.x.

Oladele, Isiaka Oluwole, Christian Junior Okoro, Anuoluwapo Samuel Taiwo, Linus N. Onuh, Newton Itua Agbeboh, Oluwayomi Peter Balogun, Peter Apata Olubambi, and Senzeni Sipho Lephuthing. 2023. "Modern Trends in Recycling Waste Thermoplastics and Their Prospective Applications: A Review." *Journal of Composites Science* 7 (5): 198. https://doi.org/10.3390/jcs7050198.

Ovadia, Maya, and Michael S. Silverstein. 2016. “High Porosity, Responsive Hydrogel Copolymers from Emulsion Templating.” *Polymer International* 65 (3): 280–89. https://doi.org/10.1002/pi.5052.

Owen, Robert, Colin Sherborne, Richard Evans, Gwendolen C. Reilly, and Frederik Claeyssens. 2020. “Combined Porogen Leaching and Emulsion Templating to Produce Bone Tissue Engineering Scaffolds.” *International Journal of Bioprinting* 6 (2): 99–113. https://doi.org/10.18063/ijb.v6i2.265.

Oyane, Ayako, Masaki Uchida, Cleo Choong, James Triffitt, John Jones, and Atsuo Ito. 2005. “Simple Surface Modification of Poly(ε-Caprolactone) for Apatite Deposition from Simulated Body Fluid.” *Biomaterials* 26 (15): 2407–13. https://doi.org/10.1016/j.biomaterials.2004.07.048.

Ozdemir, Kutlu Gokhan, Handan Yilmaz, and Sukran Yilmaz. 2009. “In Vitro Evaluation of Cytotoxicity of Soft Lining Materials on L929 Cells by MTT Assay.” *Journal of Biomedical Materials Research - Part B Applied Biomaterials* 90 B (1): 82–86. https://doi.org/10.1002/jbm.b.31256.

Ozkendir, Ozgu, Ilayda Karaca, Selin Cullu, Oğul Can Erdoğan, Hüsniye Nur Yaşar, Serkan Dikici, Robert Owen, and Betül Aldemir Dikici. 2024. “Engineering Periodontal Tissue Interfaces Using Multiphasic Scaffolds and Membranes for Guided Bone and Tissue Regeneration.” *Biomaterials Advances* 157: 213732. https://doi.org/10.1016/j.bioadv.2023.213732.

Pakeyangkoon, Pornsri, Rathanawan Magaraphan, Pomthong Malakul, and Manit Nithitanakul. 2012. “Surface Modification of High Internal Phase Emulsion Foam as a Scaffold for Tissue Engineering Application via Atmospheric Pressure Plasma Treatment.” *Adaptive, Active and Multifunctional Smart Materials Systems* 77: 172–77. https://doi.org/10.4028/www.scientific.net/ast.77.172.

Park Jeng Soo, Kim Jung-Man, Lee Sung Jun, Lee Se Geun, Jeong Joung-Keun, Kim Sung Eun, and Lee Cheon. 2007. “Surface Hydrolysis Of Fibrous Poly(ε-Caprolactone) Scaffolds for Enhanced Osteoblast Adhesion and Proliferation.” *Macromolecular Research* 15 (5): 424–29. https://doi.org/10.1007/BF03218809

Park, Sangbae, Jae Eun Kim, Jinsub Han, Seung Jeong, Jae Woon Lim, Myung Chul Lee, Hyunmok Son, et al. 2021. “3D-Printed Poly(ε-Caprolactone)/Hydroxyapatite Scaffolds Modified with Alkaline Hydrolysis Enhance Osteogenesis In Vitro.” *Polymers* 13 (2): 257. https://doi.org/10.3390/polym13020257.

Parks, John Rabon. 1982. “The Theory” 883: 109–57. https://doi.org/10.1007/978-3-642-

68330-5_7.

Pavan Kalyan, BG, and Lalit Kumar. 2022. “3D Printing: Applications in Tissue Engineering, Medical Devices, and Drug Delivery.” *AAPS PharmSciTech* 23 (4): 92. https://doi.org/10.1208/s12249-022-02242-8.

Pereira, Helena Filipa, Ibrahim Fatih Cengiz, Filipe Samuel Silva, Rui Luís Reis, and Joaquim Miguel Oliveira. 2020. “Scaffolds and Coatings for Bone Regeneration.” *Journal of Materials Science: Materials in Medicine* 31 (3): 27. https://doi.org/10.1007/s10856-020-06364-y.

Phutane, Prasanna, Darshan Telange, Surendra Agrawal, Mahendra Gunde, Kunal Kotkar, and Anil Pethe. 2023. “Biofunctionalization and Applications of Polymeric Nanofibers in Tissue Engineering and Regenerative Medicine.” *Polymers* 15 (5): 1–38. https://doi.org/10.3390/polym15051202.

Place, Elsie S., Julian H. George, Charlotte K. Williams, and Molly M. Stevens. 2009. “Synthetic Polymer Scaffolds for Tissue Engineering.” *Chemical Society Reviews* 38 (4): 1139–51. https://doi.org/10.1039/b811392k.

Princen, M. Hencirus. 1979. “Highly Concentrated Emulsions. I. Cylindrical Systems.” *Journal of Colloid And Interface Science* 71 (1): 55–66. https://doi.org/10.1016/0021-9797(79)90221-2.

Pulko, Irena, Jennifer Wall, Peter Krajnc, and Neil R. Cameron. 2010. “Ultra-High Surface Area Functional Porous Polymers by Emulsion Templating and Hypercrosslinking: Efficient Nucleophilic Catalyst Supports.” *Chemistry – A European Journal* 16 (8): 2350–54. https://doi.org/10.1002/chem.200903043.

Qu, Huawei, Hongya Fu, Zhenyu Han, and Yang Sun. 2019. “Biomaterials for Bone Tissue Engineering Scaffolds: A Review.” *RSC Advances* 9 (45): 26252–62. https://doi.org/10.1039/c9ra05214c.

Radlmaier, Veronika, Catharina Heckel, Malte Winnacker, Andreas Erber, and Hannes Koerber. 2017. “Effects of Thermal Cycling on Polyamides during Processing.” *Thermochimica Acta* 648: 44–51. https://doi.org/10.1016/j.tca.2016.12.011.

Rahmati, Maryam, David K. Mills, Aleksandra M. Urbanska, Mohammad Reza Saeb, Jayarama Reddy Venugopal, Seeram Ramakrishna, and Masoud Mozafari. 2021. “Electrospinning for Tissue Engineering Applications.” *Progress in Materials Science* 117: 100721. https://doi.org/10.1016/j.pmatsci.2020.100721.

Rahmati, Maryam, Eduardo A. Silva, Janne E. Reseland, Catherine A. Heyward, and Håvard J. Haugen. 2020. "Biological Responses to Physicochemical Properties of Biomaterial Surface." *Chemical Society Reviews* 49 (15): 5178–5224. https://doi.org/10.1039/D0CS00103A.

Recek, Nina. 2019. "Biocompatibility of Plasma-Treated Polymeric Implants." *Materials* 12 (2): 240. https://doi.org/10.3390/ma12020240.

Rezwan, Kurosch., Chen Z. Qizhi, Blaker J. Jonny, and Aldo Roberto Boccaccini. 2006. "Biodegradable and Bioactive Porous Polymer/Inorganic Composite Scaffolds for Bone Tissue Engineering." *Biomaterials* 27 (18): 3413–31. https://doi.org/10.1016/j.biomaterials.2006.01.039.

Rinaldo Florencio-Silva, Gisela Rodrigues da Silva Sasso, Estela Sasso-Cerri, Manuel Jesus Simões, Paulo Sérgio Cerri. 2015. "Physiology of Bone Tissue." *Immuno-Analyse & Biologie Spécialisée* 7 (6): 17–24. https://doi.org/10.1155/2015/421746.

Roberts T. Timothy, and Andrew J. Rosenbaum. 2012. "Bone Grafts, Bone Substitutes and Orthobiologics." *Organogenesis* 8 (4): 114–24. https://doi.org/10.4161/org.23306.

Robinson L. Jennifer, Brudnicki A.P. Philip, and Lu H. Helen. 2017. "1.21 Polymer-Bioactive Ceramic Composites." In *Comprehensive Biomaterials II*, 1: 460–77. https://doi.org/10.1016/B978-0-12-803581-8.09345-0.

Robinson L. Jennifer, Madison A.P. McEnery, Hannah Pearce, Michael E. Whitely, Dany J. Munoz-Pinto, Mariah S. Hahn, Huinan Li, Nicholas A. Sears, and Elizabeth Cosgriff-Hernandez. 2016. "Osteoinductive PolyHIPE Foams as Injectable Bone Grafts." *Tissue Engineering - Part A* 22 (5–6): 403–14. https://doi.org/10.1089/ten.tea.2015.0370.

Rohani Shirvan, Anahita, Nahid Hemmatinejad, S. Hajir Bahrami, and Azadeh Bashari. 2022. "A Comparison between Solvent Casting and Electrospinning Methods for the Fabrication of Neem Extract-Containing Buccal Films." *Journal of Industrial Textiles* 51 (1): 311–35. https://doi.org/10.1177/15280837211027785.

Rutala, William A., and David J. Weber. 2016. "Disinfection, Sterilization, and Antisepsis: An Overview." *American Journal of Infection Control* 44 (5): 1–6. https://doi.org/10.1016/j.ajic.2015.10.038.

Satchanska, Galina, Slavena Davidova, and Petar D. Petrov. 2024. “Natural and Synthetic Polymers for Biomedical and Environmental Applications.” *Polymers* 16 (8): 1159. https://doi.org/10.3390/polym16081159.

Schneider, Matthias, Nora Fritzsche, Agnieszka Puciul-Malinowska, Andrzej Baliś, Amr Mostafa, Ilko Bald, Szczepan Zapotoczny, and Andreas Taubert. 2020. “Surface Etching of 3D Printed Poly(Lactic Acid) with NaOH: A Systematic Approach.” *Polymers* 12 (8): 1711. https://doi.org/10.3390/POLYM12081711.

Shafiei, Masoud, Yousef Kazemzadeh, Ghazal Mohammadzadeh Shirazy, and Masoud Riazi. 2022. “Evaluating the Role of Salts on Emulsion Properties during Water-Based Enhanced Oil Recovery: Ion Type, Concentration, and Water Content.” *Journal of Molecular Liquids* 364: 120028. https://doi.org/10.1016/j.molliq.2022.120028.

Sheikh, Zeeshan, Corneliu Sima, and Michael Glogauer. 2015. “Bone Replacement Materials and Techniques Used for Achieving Vertical Alveolar Bone Augmentation.” *Materials* 8 (6): 2953–93. https://doi.org/10.3390/ma8062953.

Sherborne, Colin, Robert Owen, Gwendolen C. Reilly, and Frederik Claeyssens. 2018. “Light-Based Additive Manufacturing of PolyHIPEs: Controlling the Surface Porosity for 3D Cell Culture Applications.” *Materials and Design* 156: 494–503. https://doi.org/10.1016/j.matdes.2018.06.061.

Silverstein, Michael S. 2014. “PolyHIPEs: Recent Advances in Emulsion-Templated Porous Polymers.” *Progress in Polymer Science* 39 (1): 199–234. https://doi.org/10.1016/j.progpolymsci.2013.07.003.

Silverstein, Michael S., Huiwen Tai, Anatoly Sergienko, Yulia Lumelsky, and Svet Pavlovsky. 2005. “PolyHIPE: IPNs, Hybrids, Nanoscale Porosity, Silica Monoliths and ICP-Based Sensors.” *Polymer* 46 (17): 6682–94. https://doi.org/10.1016/j.polymer.2005.05.022.

Simons, W. Brian, and Brayton F. Cory. 2017. “Challenges and Limitations of Mouse Xenograft Models of Cancer.”*Patient Derived Tumor Xenograft Models* 25-36. https://doi.org/10.1016/B978-0-12-804010-2.00003-5.

Sin, DongChoon, Xigeng Miao, Gang Liu, Fan Wei, Gary Chadwick, Cheng Yan, and Thor Friis. 2010. “Polyurethane (PU) Scaffolds Prepared by Solvent Casting/Particulate Leaching (SCPL) Combined with Centrifugation.” *Materials Science and Engineering: C* 30 (1): 78–85. https://doi.org/10.1016/j.msec.2009.09.002.

Smith, Lester L., Paul J. Niziolek, Karen M. Haberstroh, Eric A. Nauman, and Thomas J. Webster. 2007. “Decreased Fibroblast and Increased Osteoblast Adhesion on Nanostructured NaOH-Etched PLGA Scaffolds.” *International Journal of Nanomedicine* 2 (3): 383–88. PMID: 18019837

Somo, Sami I., Banu Akar, Elif S. Bayrak, Jeffery C. Larson, Alyssa A. Appel, Hamidreza Mehdizadeh, Ali Cinar, and Eric M. Brey. 2015. “Pore Interconnectivity Influences Growth Factor-Mediated Vascularization in Sphere-Templated Hydrogels.” *Tissue Engineering - Part C: Methods* 21 (8): 773–85. https://doi.org/10.1089/ten.tec.2014.0454.

Song, Jialing, Xuanhao Lin, Liang Ying Ee, Sam Fong Yau Li, and Manhong Huang. 2023. “A Review on Electrospinning as Versatile Supports for Diverse Nanofibers and Their Applications in Environmental Sensing.” *Advanced Fiber Materials* 5 (2): 429–60. https://doi.org/10.1007/s42765-022-00237-5.

Song, Ping, Changchun Zhou, Hongyuan Fan, Boqing Zhang, Xuan Pei, Yujiang Fan, Qing Jiang, et al. 2018. “Novel 3D Porous Biocomposite Scaffolds Fabricated by Fused Deposition Modeling and Gas Foaming Combined Technology.” *Composites Part B: Engineering* 152: 151–59. https://doi.org/10.1016/j.compositesb.2018.06.029.

Su, Nan, Jing Yang, Yangli Xie, Xiaolan Du, Hangang Chen, Hong Zhou, and Lin Chen. 2019. “Bone Function, Dysfunction and Its Role in Diseases Including Critical Illness.” *International Journal of Biological Sciences* 15 (4): 776–87. https://doi.org/10.7150/ijbs.27063.

Suárez, Diego Fernando, Ana Delia Pinzón-García, Rubén Darío Sinisterra, Anderson Dussan, Fredy Mesa, and Sandra Ramírez-Clavijo. 2022. “Uniaxial and Coaxial Nanofibers PCL/Alginate or PCL/Gelatine Transport and Release Tamoxifen and Curcumin Affecting the Viability of MCF7 Cell Line.” *Nanomaterials* 12 (19): 3348. https://doi.org/10.3390/nano12193348.

Sultana, Naznin, and Min Wang. 2008. “Fabrication of HA/PHBV Composite Scaffolds through the Emulsion Freezing/Freeze-Drying Process and Characterisation of the Scaffolds.” *Journal of Materials Science: Materials in Medicine* 19 (7): 2555–61. https://doi.org/10.1007/s10856-007-3214-3.

Sundaramurthi, Dhakshinamoorthy, Uma Maheswari Krishnan, and Swaminathan Sethuraman. 2014. “Electrospun Nanofibers as Scaffolds for Skin Tissue Engineering.” *Polymer Reviews* 54 (2): 348–76. https://doi.org/10.1080/15583724.2014.881374.

Sušec, Maja, Robert Liska, Günter Russmüller, Jiři Kotek, and Peter Krajnc. 2015. "Microcellular Open Porous Monoliths for Cell Growth by Thiol-Ene Polymerization of Low-Toxicity Monomers in High Internal Phase Emulsions." *Macromolecular Bioscience* 15 (2): 253–61. https://doi.org/10.1002/mabi.201400219.

Szczęsny, Grzegorz, Mateusz Kopec, Denis J. Politis, Zbigniew L. Kowalewski, Adam Łazarski, and Tomasz Szolc. 2022. "A Review on Biomaterials for Orthopaedic Surgery and Traumatology: From Past to Present." *Materials* 15 (10): 3622. https://doi.org/10.3390/ma15103622.

Tamburaci, Sedef, and Funda Tihminlioglu. 2018. "Biosilica Incorporated 3D Porous Scaffolds for Bone Tissue Engineering Applications." *Materials Science and Engineering C* 91: 274–91. https://doi.org/10.1016/j.msec.2018.05.040.

Tanaka, Takaaki, Takashi Tsuchiya, Hidema Takahashi, Masayuki Taniguchi, and Douglas R. Lloyd. 2006. "Microfiltration Membrane of Polymer Blend of Poly(l-Lactic Acid) and Poly(ε-Caprolactone)." *Desalination* 193 (1–3): 367–74. https://doi.org/10.1016/j.desal.2005.06.068.

Tanaka, Takaaki, Takashi Tsuchiya, Hidema Takahashi, Masayuki Taniguchi, Hitomi Ohara, and Douglas R. Lloyd. 2006. "Formation of Biodegradable Polyesters Membranes via Thermally Induced Phase Separation." *Journal Of Chemical Engineering Of Japan* 39 (2): 144–53. https://doi.org/10.1252/jcej.39.144.

Teimouri, Reihaneh, Khalil Abnous, Seyed Mohammad Taghdisi, Mohammad Ramezani, and Mona Alibolandi. 2023. "Surface Modifications of Scaffolds for Bone Regeneration." *Journal of Materials Research and Technology* 24: 7938–73. https://doi.org/10.1016/j.jmrt.2023.05.076.

Temtem, Márcio, Teresa Casimiro, João F. Mano, and Ana Aguiar-Ricardo. 2008. "Preparation of Membranes with Polysulfone/Polycaprolactone Blends Using a High Pressure Cell Specially Designed for a CO2-Assisted Phase Inversion." *Journal of Supercritical Fluids* 43 (3): 542–48. https://doi.org/10.1016/j.supflu.2007.07.012.

Teo, Wee, and Seeram Ramakrishna. 2006. "A Review on Electrospinning Design and Nanofibre Assemblies." *Nanotechnology* 17 (14): 89–106. https://doi.org/10.1088/0957-4484/17/14/R01.

Tessmar, Jörg, Antonios Mikos, and Achim Göpferich. 2003. "The Use of Poly(Ethylene Glycol)-Block-Poly(Lactic Acid) Derived Copolymers for the Rapid Creation of

Biomimetic Surfaces." *Biomaterials* 24 (24): 4475–86. https://doi.org/10.1016/S0142-9612(03)00345-4.

Thadavirul, Napaphat, Prasit Pavasant, and Pitt Supaphol. 2014. "Improvement of Dual-Leached Polycaprolactone Porous Scaffolds by Incorporating with Hydroxyapatite for Bone Tissue Regeneration." *Journal of Biomaterials Science, Polymer Edition* 25 (17): 1986–2008. https://doi.org/10.1080/09205063.2014.966800.

Tham, C. Yin, Zuratul, A. Abdul Hamid, Zulkifli. Ahmad, and Hanafi Ismail. 2014. "Surface Modification of Poly (Lactic Acid) (PLA) via Alkaline Hydrolysis Degradation." *Advanced Materials Research* 970: 324–27. https://doi.org/10.4028/www.scientific.net/AMR.970.324.

Thang, Nguyen Hoc, Truong Bach Chien, and Dang Xuan Cuong. 2023. "Polymer-Based Hydrogels Applied in Drug Delivery: An Overview." *Gels* 9 (7): 1–38. https://doi.org/10.3390/gels9070523.

Torabi, S. Ali, Shima Oleimani, Homayoon Mahravani, Mehdi M. Ebrahimi, and Shahla Shahsavandi. 2023. "Mouse Fibroblast L929 Cell Line as a Useful Tool for Replication and Adaptation of Infectious Bursal Disease Virus." *Archives of Razi Institute* 78 (3): 863–71. https://doi.org/10.22092/ARI.2023.361584.2663.

Turnbull, Gareth, Jon Clarke, Frédéric Picard, Philip Riches, Luanluan Jia, Fengxuan Han, Bin Li, and Wenmiao Shu. 2018. "3D Bioactive Composite Scaffolds for Bone Tissue Engineering." *Bioactive Materials* 3 (3): 278–314. https://doi.org/10.1016/j.bioactmat.2017.10.001.

Vacanti, Charles. 2006. "The History of Tissue Engineering." *Journal of Cellular and Molecular Medicine* 1 (3): 569–76. https://doi.org/10.2755/jcmm010.003.20.

Venault, Antoine, Yung Chang, Da-Ming Wang, and Denis Bouyer. 2013. "A Review on Polymeric Membranes and Hydrogels Prepared by Vapor-Induced Phase Separation Process." *Polymer Reviews* 53 (4): 568–626. https://doi.org/10.1080/15583724.2013.828750.

Wadajkar, Aniket S., Chul Ahn, Kytai T. Nguyen, Qiang Zhu, and Takashi Komabayashi. 2014. " In Vitro Cytotoxicity Evaluation of Four Vital Pulp Therapy Materials on L929 Fibroblasts ." *ISRN Dentistry* 2014: 1–4. https://doi.org/10.1155/2014/191068.

Wang, Lijun, Xiuling You, Lingli Zhang, Changqing Zhang, and Weiguo Zou. 2022. "Mechanical Regulation of Bone Remodeling." *Bone Research* 10 (1): 16. https://doi.org/10.1038/s41413-022-00190-4.

Wang, Lixia, Dongfang Wang, Yiping Zhou, Yantao Zhang, Qian Li, and Changyu Shen. 2019. "Fabrication of Open-porous PCL/PLA Tissue Engineering Scaffolds and the Relationship of Foaming Process, Morphology, and Mechanical Behavior." *Polymers for Advanced Technologies* 30 (10): 2539–48. https://doi.org/10.1002/pat.4701.

Wang, Weiguang, Guilherme Caetano, William Stephen Ambler, Jonny James Blaker, Marco Andrey Frade, Parthasarathi Mandal, Carl Diver, and Paulo Bártolo. 2016. "Enhancing the Hydrophilicity and Cell Attachment of 3D Printed PCL/Graphene Scaffolds for Bone Tissue Engineering." *Materials* 9 (12): 992. https://doi.org/10.3390/ma9120992.

Wang, Xianggang, Zuhao Li, Jiaqi Liu, Chenyu Wang, Haotian Bai, Xiujie Zhu, Hui Wang, Zhonghan Wang, He Liu, and Jincheng Wang. 2023. "3D-Printed PCL Scaffolds with Anatomy-Inspired Bionic Stratified Structures for the Treatment of Growth Plate Injuries." *Materials Today Bio* 23: 100833. https://doi.org/10.1016/j.mtbio.2023.100833.

Welle, Alexander, Mario Kröger, Manfred Döring, Kerstin Niederer, Elvira Pindel, and Ioannis S. Chronakis. 2007. "Electrospun Aliphatic Polycarbonates as Tailored Tissue Scaffold Materials." *Biomaterials* 28 (13): 2211–19. https://doi.org/10.1016/j.biomaterials.2007.01.024.

Whitfield, Richard, Nghia P. Truong, Daniel Messmer, Kostas Parkatzidis, Manon Rolland, and Athina Anastasaki. 2019. "Tailoring Polymer Dispersity and Shape of Molecular Weight Distributions: Methods and Applications." *Chemical Science* 10 (38): 8724–34. https://doi.org/10.1039/c9sc03546j.

Wickramasinghe, Maduni L., George J. Dias, and Kariyawasam Majuwana Gamage Prasanna Premadasa. 2022. "A Novel Classification of Bone Graft Materials." *Journal of Biomedical Materials Research - Part B Applied Biomaterials* 110 (7): 1724–49. https://doi.org/10.1002/jbm.b.35029.

Woodruff, Maria Ann, and Dietmar Werner Hutmacher. 2010. "The Return of a Forgotten Polymer - Polycaprolactone in the 21st Century." *Progress in Polymer Science (Oxford)* 35 (10): 1217–56. https://doi.org/10.1016/j.progpolymsci.2010.04.002.

Wu, Ai Min, Catherine Bisignano, Spencer L. James, Gdiom Gebreheat Abady, Aidin

Abedi, Eman Abu-Gharbieh, Robert Kaba Alhassan, et al. 2021. “Global, Regional, and National Burden of Bone Fractures in 204 Countries and Territories, 1990–2019: A Systematic Analysis from the Global Burden of Disease Study 2019.” *The Lancet Healthy Longevity* 2 (9): 580–92. https://doi.org/10.1016/S2666-7568(21)00172-0.

Wu, Chin San, and Hsin Tzu Liao. 2012. “Polycaprolactone-Based Green Renewable Ecocomposites Made from Rice Straw Fiber: Characterization and Assessment of Mechanical and Thermal Properties.” *Industrial and Engineering Chemistry Research* 51 (8): 3329–37. https://doi.org/10.1021/ie202002p.

Wu, Yibo, Yong X. Chen, Jiahan Yan, Shihao Yang, Ping Dong, and Pranav Soman. 2015. “Fabrication of Conductive Polyaniline Hydrogel Using Porogen Leaching and Projection Microstereolithography.” *Journal of Materials Chemistry B* 3 (26): 5352–60. https://doi.org/10.1039/C5TB00629E.

Xu Chris, and Yu Liu. 2023. “Osteosarcoma Cells/Cell Lines Are Not Appropriate for Studies on Bone Regeneration in Vitro.” *Bone and Joint Research* 12 (5): 311–12. https://doi.org/10.1302/2046-3758.125.BJR-2023-0088.R1.

Yaseri, Raziye, Milad Fadaie, Esmaeil Mirzaei, Hadi Samadian, and Alireza Ebrahiminezhad. 2023. “Surface Modification of Polycaprolactone Nanofibers through Hydrolysis and Aminolysis: A Comparative Study on Structural Characteristics, Mechanical Properties, and Cellular Performance.” *Scientific Reports* 13 (1): 9434. https://doi.org/10.1038/s41598-023-36563-w.

Yazdanpanah, Zahra, James D. Johnston, David M.L. Cooper, and Xiongbiao Chen. 2022. “3D Bioprinted Scaffolds for Bone Tissue Engineering: State-Of-The-Art and Emerging Technologies.” *Frontiers in Bioengineering and Biotechnology* 10. 1-25. https://doi.org/10.3389/fbioe.2022.824156.

Yeo, Alvin, Wah Jie Wong, and Swee Hin Teoh. 2010. “Surface Modification of PCL-TCP Scaffolds in Rabbit Calvaria Defects: Evaluation of Scaffold Degradation Profile, Biomechanical Properties and Bone Healing Patterns.” *Journal of Biomedical Materials Research - Part A* 93 (4): 1358–67. https://doi.org/10.1002/jbm.a.32633.

Zamani, Yasaman, Javad Mohammadi, Ghassem Amoabediny, Dafydd O. Visscher, Marco N. Helder, Behrouz Zandieh-Doulabi, and Jenneke Klein-Nulend. 2019. “Enhanced Osteogenic Activity by MC3T3-E1 Pre-Osteoblasts on Chemically Surface-Modified Poly(ϵ-Caprolactone) 3D-Printed Scaffolds Compared to RGD Immobilized Scaffolds.” *Biomedical Materials (Bristol)* 14 (1): 015008. https://doi.org/10.1088/1748-605X/aaeb82.

Zhang, Dajun, Uday Chippada, and Kenneth Jordan. 2007. “Effect of the Structural Water on the Mechanical Properties of Collagen-like Microfibrils: A Molecular Dynamics Study.” *Annals of Biomedical Engineering* 35 (7): 1216–30. https://doi.org/10.1007/s10439-007-9296-8.

Zhang, Nianli, and David H. Kohn. 2012. “Using Polymeric Materials to Control Stem Cell Behavior for Tissue Regeneration.” *Birth Defects Research Part C - Embryo Today: Reviews* 96 (1): 63–81. https://doi.org/10.1002/bdrc.21003.

Zhang, Qiliang, Jian Zhou, Peixuan Zhi, Leixin Liu, Chaozong Liu, Ao Fang, and Qidong Zhang. 2023. “3D Printing Method for Bone Tissue Engineering Scaffold.” *Medicine in Novel Technology and Devices* 17: 100205. https://doi.org/10.1016/j.medntd.2022.100205.

Zhang, Tao, Rajashekharayya A. Sanguramath, Sima Israel, and Michael S. Silverstein. 2019. “Emulsion Templating: Porous Polymers and Beyond.” *Macromolecules* 52 (15): 5445–79. https://doi.org/10.1021/acs.macromol.8b02576.

Zhang, Wenshuo, Ziying He, Ying Han, Qinyuan Jiang, Chenhao Zhan, Kaiji Zhang, Zekun Li, and Rufan Zhang. 2020. “Structural Design and Environmental Applications of Electrospun Nanofibers.” *Composites Part A: Applied Science and Manufacturing* 137: 106009. https://doi.org/10.1016/j.compositesa.2020.106009.

Zhang, Wentao, Naiguo Wang, Ming Yang, Tianze Sun, Jing Zhang, Yantao Zhao, Na Huo, and Zhonghai Li. 2022. “Periosteum and Development of the Tissue-Engineered Periosteum for Guided Bone Regeneration.” *Journal of Orthopaedic Translation* 33: 41–54. https://doi.org/10.1016/j.jot.2022.01.002.

Zhao, Rusin, Ruijia Yang, Paul R. Cooper, Zohaib Khurshid, Amin Shavandi, and Jithendra Ratnayake. 2021. “Bone Grafts and Substitutes in Dentistry: A Review of Current Trends and Developments.” *Molecules* 26 (10): 1–27. https://doi.org/10.3390/molecules26103007.

Zhou, Shengzhong, Alexander Bismarck, and Joachim H.G. Steinke. 2012. “Thermoresponsive Macroporous Scaffolds Prepared by Emulsion Templating.” *Macromolecular Rapid Communications* 33 (21): 1833–39. https://doi.org/10.1002/marc.201200336.

Zhou, Zhu-Xing, You-Rong Chen, Ji-Ying Zhang, Dong Jiang, Fu-Zhen Yuan, Zi-Mu Mao, Fei Yang, Wen-Bo Jiang, Xing Wang, and Jia-Kuo Yu. 2020. “Facile Strategy on Hydrophilic Modification of Poly(ε-Caprolactone) Scaffolds for

Assisting Tissue-Engineered Meniscus Constructs In Vitro." *Frontiers in Pharmacology* 11. 1-11. https://doi.org/10.3389/fphar.2020.00471.

Zhu, Hailin, Jinyu Shen, Xinxing Feng, Huapeng Zhang, Yuhai Guo, and Jianyong Chen. 2010. "Fabrication and Characterization of Bioactive Silk Fibroin/Wollastonite Composite Scaffolds." *Materials Science and Engineering: C* 30 (1): 132–40. https://doi.org/10.1016/j.msec.2009.09.009.

Zhu, Kun, and Richard L. Prince. 2015. "Lifestyle and Osteoporosis." *Current Osteoporosis Reports* 13 (1): 52–59. https://doi.org/10.1007/s11914-014-0248-6.

Zuo, Shuchun, and Yueguang Wei. 2007. "Effective Elastic Modulus of Bone-like Hierarchical Materials." *Acta Mechanica Solida Sinica* 20 (3): 198–205. https://doi.org/10.1007/s10338-007-0723-z.

APPENDIX A

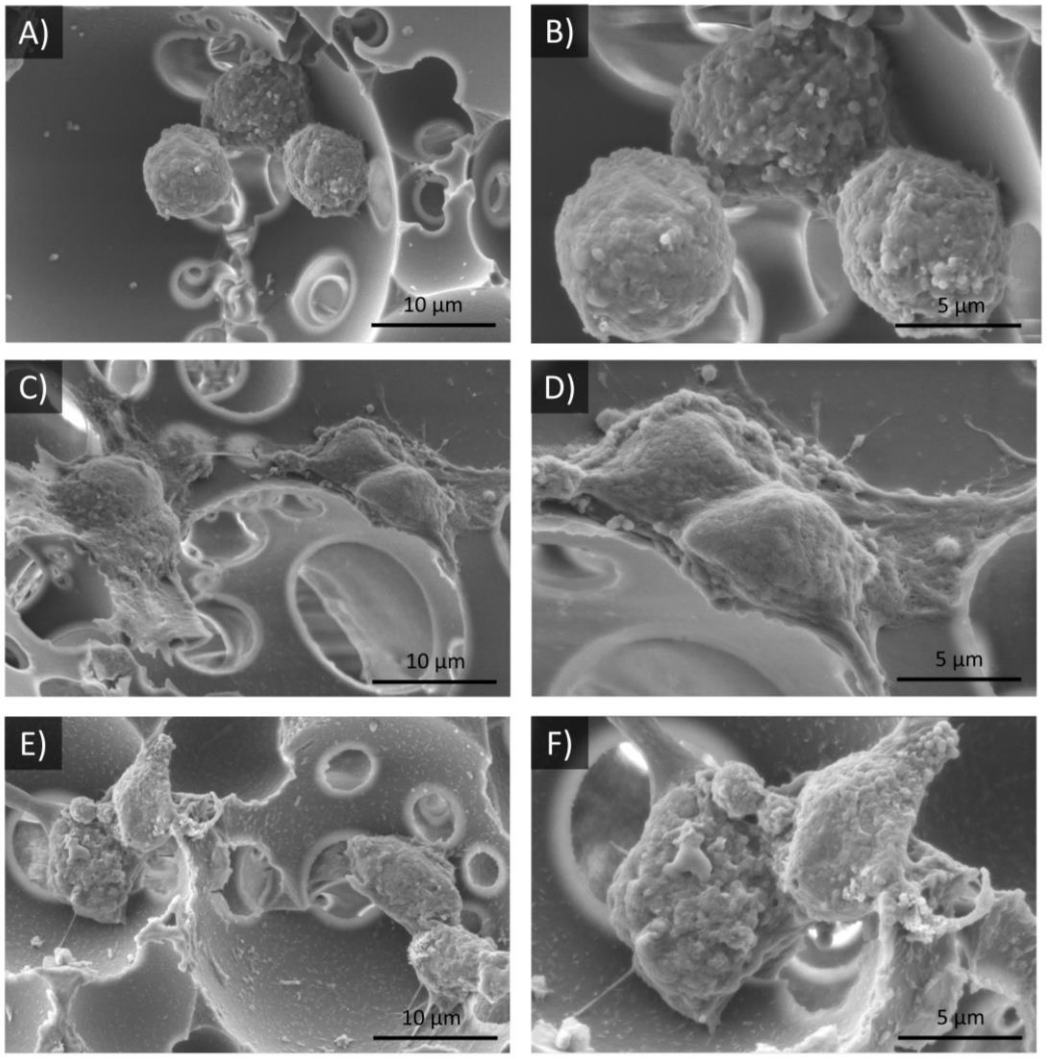

Figure 37. Uncoloured biological SEM images of PolyHIPE scaffolds *(Original images of Figure 33)*. Morphological images of Saos-2 cells cultured on A-B) N0, C-D) N1M24h and E-F) 5M24h PolyHIPE scaffolds after 4h incubation.